

# WEAK RELATIVE CALABI-YAU STRUCTURES FOR LEGENDRIAN CONTACT HOMOLOGY

JIAJIE MA AND JOSHUA M. SABLOFF

**ABSTRACT.** Legendrian Contact Homology (LCH) and its augmentations are important invariants of Legendrian submanifolds, and for Legendrian knots in the standard contact 3-space in particular. We increase understanding of the algebraic structure of LCH by generalizing the duality isomorphism and long exact sequence for linearized LCH for Legendrian knots to a weak relative Calabi-Yau structure for  $A_\infty$  bimodules over the positive augmentation category.

## CONTENTS

1. Introduction	1
2. DGAs and Legendrian Contact Homology	5
3. $A_\infty$ Background	11
4. Weak Relative Calabi-Yau Structures	19
5. Pushoffs, Reeb Chords, and Disks	23
6. Augmentation Categories, Bimodules, and Isomorphisms	42
7. Proof of the Main Theorem	56
References	66

## 1. INTRODUCTION

**1.1. Context and Goals.** Invariants built from  $J$ -holomorphic curves play a central role in both symplectic and smooth topology. In the study of Legendrian knots, the fundamental  $J$ -holomorphic invariant is the Legendrian Contact Homology (LCH), which is derived from the Chekanov-Eliashberg differential graded algebra (DGA). First defined almost thirty years ago [6, 17, 18], LCH has yielded essential insights into the topology of the space of Legendrian submanifolds and Lagrangian cobordisms between them. The goal of this paper is to better understand the structure of LCH by extending a type of duality on linearized LCH [15, 47] to the non-linear setting of augmentation categories of a Legendrian knot.

---

*Date:* September 3, 2025.

*2020 Mathematics Subject Classification.* 53D42; 53D37, 57K10, 57K33.

*Key words and phrases.* Legendrian knot, Legendrian Contact Homology, Calabi-Yau structure.

Structural results are particularly important for understanding the nature and applications of LCH. Among the first of these results was the existence of a Poincaré-Lefschetz-like duality and a fundamental class for the LCH, linearized with respect to an augmentation [15, 47]. This duality eased computations (see, for example, [4, 38]), connected the linearized LCH to the Poincaré-Lefschetz duality of Lagrangian fillings [5, 10, 12, 16], provided a framework for capacities that measure the length [49] and relative Gromov width [50] of Lagrangian cobordisms, and even inspired duality results for related invariants such as those based on generating families [48] and microlocal sheaves [36].

The linearized LCH of a Legendrian knot  $\Lambda$  ignores a wealth of non-linear information contained in the differential of the full DGA. In order to reintroduce that non-linear information, it has proven useful to use  $A_\infty$  structures. The starting point was to define  $A_\infty$  algebras for a fixed augmentation [9]; this idea was then generalized to the  $A_\infty$  categories  $\mathcal{A}\text{ug}_-(\Lambda)$  [2] and  $\mathcal{A}\text{ug}_+(\Lambda)$  [43], whose objects are augmentations and whose structure maps capture the (dual of) the LCH differential. The augmentation categories are designed to connect the LCH framework to wrapped Fukaya categories and to sheaf invariants [43]. As frameworks for understanding LCH have grown more sophisticated, linearized versions of duality have followed. In [9], the original linearized duality was interpreted in terms of cup and cap products. In [2], the duality long exact sequence of [15] was extended and reinterpreted in terms of “bi-linearized” LCH. Finally, in [43], the duality long exact sequence was recast in terms of a relationship between the (linear) morphism spaces of  $\mathcal{A}\text{ug}_-(\Lambda)$  and of  $\mathcal{A}\text{ug}_+(\Lambda)$ .

The next step in this development, embodied in this paper, is to incorporate non-linear information into the duality structure, i.e. to upgrade the duality relationship between the morphism spaces of  $\mathcal{A}\text{ug}_\pm(\Lambda)$  to a relationship on the full  $A_\infty$  structure. The main difficulty is in figuring out the proper algebraic setting for this upgrade. We frame our results using Brav and Dyckerhoff’s relative Calabi-Yau structures [3]. Calabi-Yau (CY) structures on  $A_\infty$  algebras first appeared in Kontsevich and Soibelman’s work [33]. Since then, they have arisen naturally in the geometry of CY manifolds and in various formulations of mirror symmetry; see, for example, [24, 25, 54] and, in particular, Seidel’s notion of a boundary  $A_\infty$  algebra [53] that motivated earlier work on this paper. See [34] for a more comprehensive survey of the recent wave of discoveries of CY and relative CY structures.

**1.2. Results.** The main theorem of this paper is a generalization of the linearized duality to a weak right relative CY structure. The precise definition of a relative Calabi-Yau structure appears in Section 4.

To state the theorem, we need an additional  $A_\infty$  category beyond the augmentation categories  $\mathcal{A}\text{ug}_\pm(\Lambda)$ . The circle category  $\mathcal{C}(\Lambda)$  is based on the Morse theory of the Legendrian  $\Lambda$  and comes equipped with a projection functor  $\pi_{\mathcal{C}}$  from  $\mathcal{A}\text{ug}_+(\Lambda)$ . From these categories, we will derive three

$\mathcal{A}\text{ug}_+(\Lambda)$ -bimodules:  $\mathcal{M}_+$  is the diagonal bimodule of  $\mathcal{A}\text{ug}_+(\Lambda)$ ,  $\mathcal{M}_-$  is a submodule of  $\mathcal{M}_+$  related to the diagonal bimodule of  $\mathcal{A}\text{ug}_-(\Lambda)$ , and  $\mathcal{N}$  is the pullback of the diagonal bimodule of  $\mathcal{C}$  over the projection  $\pi_{\mathcal{C}}$ . Precise definitions of all of these categories and bimodules will be presented in Section 6.

For simplicity, we work with coefficients in  $\mathbb{F}_2 = \mathbb{Z}/2\mathbb{Z}$ , though there should be no mathematical obstruction to lifting the coefficients to  $\mathbb{Q}$  or even to any commutative ring. We say that  $\mathcal{A}\text{ug}_+(\Lambda)$  is **simply perturbed** if it is defined using a Morse function  $f : \Lambda \rightarrow \mathbb{R}$  having one maximum and one minimum that are adjacent in the Lagrangian diagram of  $\Lambda$ , with a unique basepoint just before the maximum with respect to the orientation of  $\Lambda$ .

**Theorem 1.1.** *Let  $\Lambda$  be a Legendrian knot in the standard contact  $\mathbb{R}^3$ . For a simply perturbed augmentation category  $\mathcal{A}\text{ug}_+(\Lambda)$  over  $\mathbb{F}_2$ , the projection functor  $\pi_{\mathcal{C}} : \mathcal{A}\text{ug}_+(\Lambda) \rightarrow \mathcal{C}(\Lambda)$  admits a weak right relative Calabi-Yau structure of dimension 2.*

Again, the full definition of a weak right relative CY structure will appear below, but briefly, the theorem tells us that there is an isomorphism of exact triangles of  $\mathcal{A}\text{ug}_+(\Lambda)$ -bimodules of the following form in the derived category:

$$(1.1) \quad \begin{array}{ccccccc} \cdots & \longrightarrow & \mathcal{M}_+[1] & \xrightarrow{\pi_{\mathcal{N}}} & \mathcal{N}[1] & \xrightarrow{I_{\mathcal{N}}} & \mathcal{M}_-[2] \longrightarrow \cdots \\ & & \downarrow & & \downarrow & & \downarrow \\ \cdots & \longrightarrow & \mathcal{M}_-^\vee[-1] & \xrightarrow{I_{\mathcal{N}}^\vee} & \mathcal{N}^\vee & \xrightarrow{\pi_{\mathcal{N}}^\vee} & \mathcal{M}_+^\vee \longrightarrow \cdots \end{array}$$

*Remark 1.2.* By reducing Diagram (1.1) to the linear level (i.e. to the level of morphisms), using the first vertical quasi-isomorphism to replace  $\text{Hom}_+(\varepsilon, \varepsilon)$  with  $\text{Hom}_-(\varepsilon, \varepsilon)^\vee[-2]$ , and translating between the language of [43, §5] and [15], we recover the original duality long exact sequence in [15] from the top line of the diagram. See Remark 7.11 for more details.

We make several comments on the relationship between our main theorem and other past and recent work. First and foremost, we note that Chen [7] has proven a closely related result. Chen constructs  $\mathcal{M}_-$ , proves that the top line in (1.1) is an exact sequence of  $\mathcal{A}\text{ug}_+$ -bimodules, and shows that the first and third vertical maps in (1.1) are  $A_\infty$  quasi-isomorphisms (cf. Proposition 6.25, below). Chen's results hold over an arbitrary commutative ring. Chen uses a different framework for the proof, namely Ng's Legendrian Symplectic Field Theory [41] rather than the close analysis of the DGAs of  $n$ -copies of the Legendrian used in this paper. Both groups of authors view their results as independent, and virtually simultaneous, discoveries.

Other recent related work includes Légout's generalization of the linear duality map to a CY structure on the full Chekanov-Eliashberg DGA for horizontally displaceable Legendrian spheres [35]. Dimitroglou Rizell and

Légout have a further generalization of the duality long exact sequence in [15] to a weak relative CY structure for general dg-bimodules using LCH over chains in the based loop space of  $\Lambda$ ; see [11] for a preliminary report. Relatedly, Gorsky and Haiden [29] constructed a weak relative CY structure on a dg-category quasi-equivalent to  $\mathcal{A}\text{ug}_+(\Lambda)$  by gluing together “2CY structures” defined on simple Legendrian tangles. Asplund [1] constructs a *strong* relative smooth CY structure involving the full Chekanov-Eliashberg DGA for a class of higher-dimensional singular links of Legendrian unknots by using a relation to relative Ginzburg algebras. Finally, Kuo and Li construct a *strong* relative CY structure for microlocal sheaf invariants [34]; this structure was predicted in [36, Remark 1.10].

Next, the main theorem should generalize to higher-dimensional Legendrian submanifolds in the standard contact  $\mathbb{R}^{2n+1}$ , or any “horizontally displaceable” Legendrian in a 1-jet space; see [37] for the necessary machinery. As noted in [43, Remark 1.4], however, in higher dimensions there are issues with ensuring that the augmentation category is well-defined with respect to choices of perturbation of the  $n$ -copy. A generalization of [15, Theorem 3.6] to multiple mixed punctures would also be necessary. Alternatively, the aforementioned work of Dimitroglou Rizell and Légout [11] paves the way for an approach to duality in higher dimensions using DGAs with coefficients in chains on the based loop space of  $\Lambda$  rather than using augmentation categories and  $n$ -copies.

Finally, there is evidence that the weak relative CY structure in the main theorem generalizes to a strong relative CY structure, which we plan to return to in future work. The evidence comes from observations about symmetries of the inverse to the leftmost quasi-isomorphism in (1.1), from Asplund’s aforementioned work [1], from the existence of such a strong structure in the closely related microlocal sheaf invariants [34], and from computations on examples such as those in [9].

**1.3. Plan of the Paper.** We review the construction of Legendrian Contact Homology in Section 2, with an eye towards reviewing older duality results and setting notation that will be used in future sections. In Section 3, we set the language of  $A_\infty$  categories and bimodules. We complete the necessary algebraic background in Section 4 by defining weak relative CY structures and proving a key algebraic lemma that lets us construct such a structure from even weaker information.

We begin to construct the geometric framework for the proof of Theorem 1.1 with a careful discussion of pushoffs of Legendrian knots, especially the Reeb chords and immersed disks in those pushoffs, in Section 5. In Section 6, we use this geometric framework to review the definition of the augmentation categories  $\mathcal{A}\text{ug}_\pm(\Lambda)$  from [43], and then proceed to define the  $\mathcal{A}\text{ug}_+(\Lambda)$ -bimodules that appear in the statement of the main theorem. Finally, we prove the main theorem in Proposition 6.25, where we prove that

the first and last vertical maps in Diagram (1.1) are quasi-isomorphisms, and in Section 7, where we prove the homotopy commutativity of Diagram (1.1).

**Acknowledgements.** We thank Zhenyi Chen for the open dialogue and sharing of ideas as both teams worked to complete their approaches to weak relative CY structures for augmentation categories. We also thank Johan Asplund, Georgios Dimitroglou Rizell, Sheel Ganatra, Christopher Kuo, Noémie Legout, Wenyuan Li, Aaron Lowe, Lenny Ng, Paul Seidel, and Yiyang Xu for stimulating conversations about the material in this paper. We are also grateful to the participants of the Philadelphia Area Contact / Topology seminar for their early feedback on this work. JM was partially supported by NSF grant DMS-2003404 and JMS was partially supported by NSF grant DMS-1406093 during the research leading to this paper. Part of the research was done while JMS was hosted by the Institute for Advanced Study; in particular, this paper is partly based on work supported by the Institute for Advanced Study.

## 2. DGAs AND LEGENDRIAN CONTACT HOMOLOGY

The goal of this section is to briefly review the foundational ideas of Legendrian Contact Homology (LCH) for Legendrian knots in  $\mathbb{R}^3$ : the Chekanov-Eliashberg algebra in Section 2.1, the idea of an augmentation in Section 2.2, duality for linearized Legendrian Contact Homology in Section 2.3, and Mishachev's link grading in Section 2.4. These sections serve mostly to set notation and perspective. For more depth for all of this material, see the recent survey [19] or the original papers [6, 17, 20]; we follow the notation developed in [43] as much as reasonable.

**2.1. The Chekanov-Eliashberg Algebra.** Our first task is to sketch the definition of the Chekanov-Eliashberg differential graded algebra (DGA) of an oriented Legendrian link  $\Lambda$ . We emphasize that we only define the DGA over the field  $\mathbb{F}_2$ ; see the references above for more general coefficients. First, label the crossings of the Lagrangian projection  $\pi_{xy}(\Lambda)$  — that is, label the Reeb chords of  $\Lambda$  — with natural numbers from 1 to  $n$ . Further, choose base points  $\circ_1, \dots, \circ_M$  on  $\Lambda$  so that the complement of the base points is contractible; in particular, there must be at least one base point on every component of  $\Lambda$ . Let  $\mathcal{R} = \{a_1, \dots, a_n\}$  be labels corresponding to the Reeb chords, let  $\mathcal{T} = \{t_1, t_1^{-1}, \dots, t_M, t_M^{-1}\}$  be labels corresponding to the base points with  $\mathcal{T}_{\pm} = \{t_1^{\pm 1}, \dots, t_M^{\pm 1}\}$ , and let  $\mathcal{S} = \mathcal{R} \cup \mathcal{T}$ .

Define the algebra  $\mathcal{A}$  to be the unital algebra freely generated by  $\mathcal{S}$  over the field  $\mathbb{F}_2$ , quotiented by the relations  $t_i t_i^{-1} = 1$  and  $t_i^{-1} t_i = 1$ ; such an algebra is called **semi-free** on  $\mathcal{S}$ . The algebra  $\mathcal{A}$  has a grading in  $\mathbb{Z}/2r(\Lambda)\mathbb{Z}$  derived from the Conley-Zehnder index, where  $r(\Lambda)$  is the greatest common divisor of the rotation numbers of the components of  $\Lambda$ ; see [6, 20] for details when  $\Lambda$  is a knot and [40] in the case of a link. Denote the grading of a generator  $a_i$  by  $|a_i|$ ; we specify that the gradings of  $t_i^{\pm 1}$  are all zero.

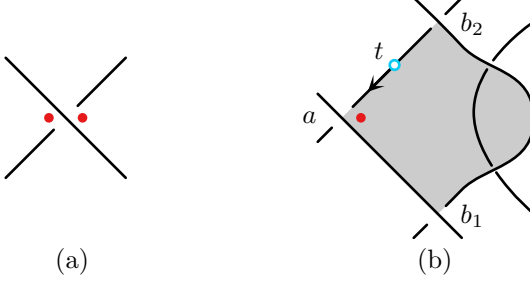


FIGURE 1. (a) Reeb signs at a crossing of the Lagrangian diagram of a Legendrian knot  $\Lambda$ , with dots denoting positive corners and a lack of decoration denoting a negative corner. (b) A schematic picture of a disk in  $\Delta_\Lambda(a, b_1b_2t)$ .

The differential  $\partial$  on  $\mathcal{A}$  is defined by counting immersed disks in the Lagrangian diagram  $\pi_{xy}(\Lambda)$ , which stand in for pseudo-holomorphic disks in the symplectization  $\mathbb{R} \times \mathbb{R}^3$ ; see [14, 20] for more on the latter perspective. More specifically, begin by decorating the quadrants of the Lagrangian diagram near each crossing with positive or negative **Reeb signs** as in Figure 1(a). To find the differential of a generator  $a \in \mathcal{R}$ , let  $\mathbf{b} = b_1 \cdots b_n$  be a word in  $\mathcal{A}$ . Define  $\Delta(a, \mathbf{b})$  to be the set of immersions  $u : D^2 \rightarrow \mathbb{R}^2$  (up to smooth reparametrization) that extend continuously to the closed disk, whose boundaries lie in the Lagrangian projection  $\pi_{xy}(\Lambda)$ , and whose boundaries encounter the letters of  $\mathbf{b}$  in counterclockwise order. Additionally, each immersed disk must satisfy the following:

- (1) The disk has only *convex* corners at the crossings,
- (2) The disk must have a corner covering a positive Reeb sign at  $a$ ,
- (3) If  $b_i \in \mathcal{R}$ , the disk has a corner covering a negative Reeb sign at  $b_i$ , and
- (4) If  $b_i \in \mathcal{T}_+$  (resp.  $\mathcal{T}_-$ ), then the orientation of  $\Lambda$  and the counterclockwise orientation of the boundary of  $u$  agree (resp. disagree).

See Figure 1(b). The differential is then defined on generators in  $\mathcal{R}$  by

$$(2.1) \quad \partial a = \sum_{u \in \Delta(a, \mathbf{b})} \mathbf{b}.$$

Additionally, define the differential to vanish on the base point generators  $t_i^{\pm 1}$ . Extend the differential over all of  $\mathcal{A}$  by linearity and the Leibniz rule.

**Theorem 2.1** ([6]; see also [20, 40]). *The differential  $\partial$  is well-defined, has degree  $-1$ , and squares to zero. The homology  $H_*(\mathcal{A}, \partial)$  is invariant under Legendrian isotopy.*

*Example 2.2.* The knot in Figure 2 has seven crossings and a single base point. The generators  $t, a_4, a_5$  have grading 0;  $a_1, a_6, a_7$  have grading 1; and

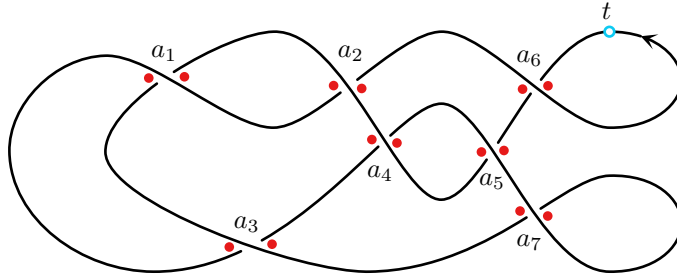


FIGURE 2. The Lagrangian diagram of a Legendrian figure eight knot.

$a_2, a_3$  have grading  $-1$ . The differential is given by:

$$\begin{aligned}\partial a_1 &= \partial a_2 = \partial a_3 = \partial a_5 = \partial t^{\pm 1} = 0 \\ \partial a_4 &= a_2 + a_3 + a_2 a_1 a_3 \\ \partial a_6 &= t + a_5 + a_1 a_3 a_5 \\ \partial a_7 &= 1 + a_5 + a_5 a_2 a_1.\end{aligned}$$

The Chekanov-Eliashberg DGA is filtered by the length of the Reeb chords. This follows from an application of Stokes' Theorem. Stated precisely, we have:

**Lemma 2.3** ([6, Lemma 6.1]). *Let  $\ell(x)$  represent the length of the Reeb chord  $x$ . If the set  $\Delta(a, b_1 \cdots b_n)$  is nonempty, then*

$$(2.2) \quad \ell(a) > \sum_i \ell(b_i).$$

*In particular, if  $\mathcal{B} \subset \mathcal{A}$  is a subalgebra freely generated by all chords below a given height, then it is a sub-DGA.*

**2.2. Augmentations.** The Chekanov-Eliashberg DGA is difficult to use directly for practical computations, so we use Chekanov's idea of an **augmentation** to linearize the differential. An augmentation is a DGA map  $\varepsilon : (\mathcal{A}, \partial) \rightarrow (\mathbb{F}_2, 0)$ , where  $(\mathbb{F}_2, 0)$  is the trivial DGA in grading 0. Note that  $\varepsilon(t_i^{\pm 1})$  must be 1. Such augmentations do not always exist [21, 22, 46], and further, ever more sophisticated “counts” of augmentations are interesting Legendrian invariants [30, 42, 44].

An augmentation induces further structures on a semi-free DGA. We define the  $\mathbb{F}_2$ -algebra  $\mathcal{A}^\varepsilon = \mathcal{A}/(t_i = \varepsilon(t_i))$ ; since  $\partial t_i^{\pm 1} = 0$ , the differential descends to  $\mathcal{A}^\varepsilon$ . Setting  $A$  to be the graded vector space generated by  $\mathcal{R}$ , we write  $\mathcal{A}^\varepsilon$  as a unital tensor algebra:

$$\mathcal{A}^\varepsilon = TA = \bigoplus_{k \geq 0} A^{\otimes k}.$$

This, in turn, leads us to define the truncated tensor algebra, or **bar algebra**

$$\bar{T}A = \bigoplus_{k \geq 1} A^{\otimes k}.$$

By changing coordinates using the automorphism  $\Phi_\varepsilon : \mathcal{A}^\varepsilon \rightarrow \mathcal{A}^\varepsilon$  defined by  $\Phi_\varepsilon(a_i) = a_i + \varepsilon(a_i)$ , we have a new **twisted differential**

$$\partial^\varepsilon = \Phi_\varepsilon \partial \Phi_\varepsilon^{-1}$$

on  $\mathcal{A}^\varepsilon$ . The following proposition is well-known (see [6], for example) and straightforward to check.

**Proposition 2.4.** *The differential  $\partial^\varepsilon$  descends to a differential on the bar algebra  $\bar{T}A$ , i.e.  $(\bar{T}A, \partial^\varepsilon)$  is itself a DGA.*

The DGA  $(\bar{T}A, \partial^\varepsilon)$  is the **augmented DGA** of  $(\mathcal{A}, \partial)$  with respect to  $\varepsilon$ . Observe that, by the Leibniz rule, the differential  $\partial^\varepsilon$  on  $\bar{T}A$  is determined by its components  $\partial_k^\varepsilon : A \rightarrow A^{\otimes k}$ . We call the homology of the chain complex  $(A, \partial_1^\varepsilon)$  the **linearized Legendrian contact homology**, which we also denote by  $LCH_*(\varepsilon)$ . The linear differential  $\partial_1^\varepsilon$  comes from disks with one positive corner, one negative corner, and perhaps other “augmented” negative corners on which  $\varepsilon$  is nonzero; see Figure 3.

*Example 2.5.* Referring back to Example 2.2, it can easily be checked that there are exactly two augmentations  $\varepsilon_1, \varepsilon_2$  over  $\mathbb{F}_2$ . Both send the degree 0 generators  $t$  and  $a_5$  to 1, but differ on  $a_4$ , with  $\varepsilon_1(a_4) = 0$  and  $\varepsilon_2(a_4) = 1$ . Since  $a_4$  does not contribute to terms in the differential, the resulting twisted differentials are the same:

$$\begin{aligned}\partial^{\varepsilon_i} a_1 &= \partial^{\varepsilon_i} a_2 = \partial_1^{\varepsilon_i} a_3 = \partial^{\varepsilon_i} a_5 = 0 \\ \partial^{\varepsilon_i} a_4 &= a_2 + a_3 + a_2 a_1 a_3 \\ \partial^{\varepsilon_i} a_6 &= a_5 + a_1 a_3 + a_1 a_3 a_5 \\ \partial^{\varepsilon_i} a_7 &= a_5 + a_2 a_1 + a_5 a_2 a_1,\end{aligned}$$

for  $i = 1, 2$ . The only nontrivial linear terms are  $\partial_1^{\varepsilon_i} a_4 = a_2 + a_3$ ,  $\partial_1^{\varepsilon_i} a_6 = a_5$ , and  $\partial^{\varepsilon_i} a_7 = a_5$ . It follows that the linearized Legendrian contact homology induced by either augmentation is generated by  $[a_1]$ ,  $[a_2]$ , and  $[a_6 + a_7]$ . In particular,  $LCH_1(\varepsilon_i) \simeq \mathbb{F}_2^2$ ,  $LCH_{-1}(\varepsilon_i) \simeq \mathbb{F}_2$ , and the homology in all other degrees is 0.

It will prove useful to consider the duals of augmented DGAs. Denote by  $A^*$  the dual vector space  $\text{hom}(A, \mathbb{F}_2)$ . The dual space has a dual basis  $\{a_i^*\}$  — that is,  $\langle a_i^*, a_j \rangle = \delta_{ij}$  — whose gradings are defined by  $|a_i^*| = |a_i|$ . Extend the pairing between the dual bases to a pairing between  $\bar{T}A$  and  $\bar{T}A^*$  so that

$$\langle a_{i_k}^* \cdots a_{i_1}^*, a_{i_1} \cdots a_{i_k} \rangle = 1,$$

with all other pairings going to 0. As  $\bar{T}A$  is a (graded) algebra, we see that  $\bar{T}A^*$  is naturally a (graded) co-algebra called the **cobar coalgebra**.

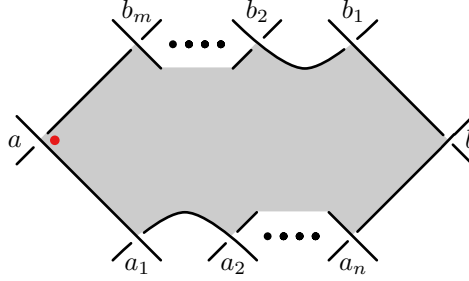


FIGURE 3. A term  $b$  in the linearized differential  $\partial_1^\varepsilon(a)$  arises from a disk in  $\Delta_\Lambda(a, a_1, \dots, a_n, b, b_1, \dots, b_m)$  with  $\varepsilon(a_i) = 1 = \varepsilon(b_i)$ .

To turn  $\bar{T}A^*$  into a DG co-algebra (DGCA), we take the adjoint  $\delta_\varepsilon$  of  $\partial^\varepsilon$  with respect to the pairing  $\langle , \rangle$ :

$$\langle \delta_\varepsilon x^*, y \rangle = \langle x^*, \partial^\varepsilon y \rangle.$$

See [28, §1] for a concise introduction to DG co-algebras (DGCA). Using Proposition 2.4, we obtain the following.

**Proposition 2.6.** *The map  $\delta_\varepsilon : \bar{T}A^* \rightarrow \bar{T}A^*$  is a codifferential, i.e. it is a coderivation of degree 1 with  $\delta_\varepsilon^2 = 0$ , and hence  $(\bar{T}A^*, \delta_\varepsilon)$  is a DGCA.*

As with the differential  $\partial^\varepsilon$ , the codifferential  $\delta_\varepsilon$  is determined by its components  $\delta_\varepsilon^k : (A^*)^{\otimes k} \rightarrow A^*$ . Further, observe that  $(A^*, \delta_\varepsilon^1)$  forms the cochain complex dual to  $(A, \partial_1^\varepsilon)$ , whose homology we term the **linearized contact cohomology** and denote by  $LCH^*(\varepsilon)$ .

*Example 2.7.* For either augmentation  $\varepsilon_i$  in Example 2.5, the codifferential of the induced DGCA is given by:

$$\begin{array}{ll} \delta_{\varepsilon_i}^1(a_2^*) = \delta_{\varepsilon_i}^1(a_3^*) = a_4^* & \delta_{\varepsilon_i}^3(a_3^*, a_1^*, a_2^*) = a_4^* \\ \delta_{\varepsilon_i}^1(a_5^*) = a_6^* + a_7^* & \delta_{\varepsilon_i}^3(a_5^*, a_3^*, a_1^*) = a_6^* \\ \delta_{\varepsilon_i}^2(a_1^*, a_2^*) = a_7^* & \delta_{\varepsilon_i}^3(a_1^*, a_2^*, a_5^*) = a_7^* \\ \delta_{\varepsilon_i}^2(a_3^*, a_1^*) = a_6^* & \end{array}$$

and vanishes otherwise. It follows that the linearized contact cohomology induced by  $\varepsilon_i$  is generated by  $[a_1^*]$ ,  $[a_6^*]$ , and  $[a_2^* + a_3^*]$ , with  $LCH^1(\varepsilon_i) \simeq \mathbb{F}_2^2$ ,  $LCH^{-1}(\varepsilon_i) \simeq \mathbb{F}_2$ , and the cohomology vanishes in all other degrees.

**2.3. Duality.** The linearized Legendrian contact (co)homology groups obey a duality reminiscent of Poincaré-Lefschetz duality for manifolds with boundary. We state the duality exact sequence for Legendrian knots in  $\mathbb{R}^3$ , though the theorem works in more general settings.

**Theorem 2.8** (Duality [15, 47]). *Suppose  $\varepsilon$  is an augmentation for a Legendrian knot  $\Lambda$ . There is a long exact sequence*

$$\cdots \longrightarrow H^k(\Lambda) \xrightarrow{\sigma} LCH^k(\varepsilon) \xrightarrow{\eta} LCH_{-k}(\varepsilon) \xrightarrow{\rho} H^{k+1}(\Lambda) \longrightarrow \cdots$$

When  $\Lambda$  is connected, the map  $\sigma$  is injective in degree 1 and zero in degree 0.

The exact sequence in the theorem above parallels the long exact sequence of a pair  $(M, \partial M)$  together with Poincaré-Lefschetz duality, with  $LCH_*(\varepsilon)$  playing the role of the cohomology of the manifold  $M$  and  $H^*(\Lambda)$  playing the role of the cohomology of the boundary. Indeed, the Seidel isomorphism [10, 13] makes this parallel precise.

The central aim of this paper is to generalize the (linear) duality in Theorem 2.8 to the (non-linear)  $A_\infty$  category setting.

**2.4. Link Gradings.** Before formulating the  $A_\infty$  category framework used to generalize duality, we need to introduce one more technical tool. When  $\Lambda$  is a link (or, more generally, a decomposition of  $\Lambda$  into sets of connected components), Mishachev [39] defined an additional structure on the Chekanov-Eliashberg DGA; see also [40]. The algebraic underpinning of this structure is a pair of maps called a link grading.

**Definition 2.9.** Let  $(\mathcal{A}, \partial)$  be a semi-free DGA generated by  $\mathcal{S} = \mathcal{R} \sqcup \mathcal{T}$ . An  $m$ -component **link grading** on  $(\mathcal{A}, \partial)$  is a pair of maps

$$o, v : \mathcal{S} \rightarrow \{1, \dots, m\}.$$

A word  $a_1 \cdots a_k$  in  $\mathcal{A}$  is **composable** if  $o(a_{i+1}) = v(a_i)$  for  $i = 1, \dots, k-1$ . The link grading maps must satisfy:

- (1) For any  $a \in \mathcal{R}$  with  $o(a) \neq v(a)$ , each term  $a_1 \cdots a_k$  in  $\partial a$  is composable with  $o(a_1) = o(a)$  and  $v(a_k) = v(a)$ .
- (2) For any  $a \in \mathcal{R}$  with  $o(a) = v(a)$ , each term  $a_1 \cdots a_k$  in  $\partial a$  is composable with  $o(a_1) = o(a)$  and  $v(a_k) = v(a)$  or is a constant.
- (3) For any  $j$ ,  $o(t_j) = v(t_j) = o(t_j^{-1}) = v(t_j^{-1})$ .

We write  $\mathcal{S}^{ij} = (o \times v)^{-1}(i, j)$ ; the sets  $\mathcal{R}^{ij}$  is defined similarly. A generator in  $\mathcal{S}^{ii}$  is **diagonal** and a generator in  $\mathcal{S}^{ij}$  with  $i \neq j$  is **off-diagonal**. All elements of  $\mathcal{T}$  are diagonal by definition, and we write  $\mathcal{T}^i = (o \times v)^{-1}(i, i)$ . An augmentation **respects the link grading** if it vanishes on off-diagonal generators.

The geometry underlying this algebraic definition is that given a Legendrian link  $\Lambda$  whose components have been decomposed into  $\Lambda = \Lambda_1 \sqcup \cdots \sqcup \Lambda_m$ , the link grading function  $o$  (resp.  $v$ ) sends a crossing to the index of the component of its overcrossing (resp. its undercrossing); both functions send a base point to its component. Thus,  $\mathcal{R}^{ij}$  can be thought of as the set of Reeb chords that start on  $\Lambda_j$  and end on  $\Lambda_i$ .

### 3. $A_\infty$ BACKGROUND

In order to bring non-linear information from the Chekanov-Eliashberg DGA back to the linearized Legendrian contact cohomology, we use  $A_\infty$  structures. In this section, we briefly overview of the  $A_\infty$  structures that we will need to generalize the duality expressed in Theorem 2.8:  $A_\infty$  algebras,  $A_\infty$  categories, and  $A_\infty$  bimodules, as well as mapping cones and mapping cylinders.

Our notation for  $A_\infty$  algebras and categories is designed to be consistent, for the most part, with that of [43] which, in turn, follows [32]; when we turn to  $A_\infty$  bimodules, we follow [24, 52]. For simplicity, we work over  $\mathbb{F}_2$  and assume, when necessary, that the morphism spaces are finite dimensional; see [24, 32, 43] for more general constructions.

**3.1.  $A_\infty$  Algebras.** One may think of an  $A_\infty$  algebra as a DGA that is associative up to homotopy, with those homotopies encoded in higher product structures. Later on, we will use  $A_\infty$  algebras to encode information dual to that of augmented DGAs.

**Definition 3.1.** An  $A_\infty$  algebra  $A$  is a graded  $\mathbb{F}_2$  vector space  $A$  together with a sequence of maps

$$m^k : A^{\otimes k} \rightarrow A$$

for  $k \geq 1$  of degree  $2 - k$  such that the following quadratic relation holds for each  $k$ :

$$(3.1) \quad \sum_{\substack{0 < r \leq k \\ 0 \leq s \leq k-r}} m^{k-s+1}(\mathbb{1}^{\otimes k-r} \otimes m^s \otimes \mathbb{1}^{\otimes r}) = 0.$$

The first of the  $A_\infty$  relations implies that  $m^1$  is a codifferential, while the second shows that  $m^2$  descends to a product on cohomology. The third relation is

$$\begin{aligned} m^2(m^2(\cdot, \cdot), \cdot) + m^2(\cdot, m^2(\cdot, \cdot)) &= m^1(m^3(\cdot, \cdot, \cdot)) + m^3(m^1(\cdot), \cdot, \cdot) \\ &\quad + m^3(\cdot, m^1(\cdot), \cdot) + m^3(\cdot, \cdot, m^1(\cdot)), \end{aligned}$$

which shows that the product is associative on cohomology.

To connect with the Chekanov-Eliashberg DGA, we re-characterize  $A_\infty$  algebras using the cobar construction as in [28, 31, 55]. Given an augmented DGA  $(\bar{T}A, \partial^\varepsilon)$ , construct its dual DGCA  $(\bar{T}A^*, \delta_\varepsilon)$  as in Section 2.2. Recall that  $\delta_\varepsilon$  is determined by a sequence of maps  $\delta_\varepsilon^k : (A^*)^{\otimes k} \rightarrow A^*$ . Let  $s : A \rightarrow A[1]$  be the canonical degree  $-1$  shift map, and denote  $A^*[-1]$  by  $A^\vee$ ; further, if  $a$  is a generator of  $A$ , then we denote its dual in  $A^\vee$  by  $a^\vee$ . We define a sequence of maps  $m_\varepsilon^k : (A^\vee)^{\otimes k} \rightarrow A^\vee$  by

$$s \circ m_\varepsilon^k = \delta_\varepsilon^k \circ s^{\otimes k}.$$

This construction has a geometric characterization in the context of the Chekanov-Eliashberg DGA. A disk contributes  $a^\vee$  to  $m_\varepsilon^k(a_{i_k}^\vee, \dots, a_{i_1}^\vee)$  if it has a positive corner at  $a$ , negative corners at  $a_{i_1}, \dots, a_{i_k}$  (in counter-clockwise

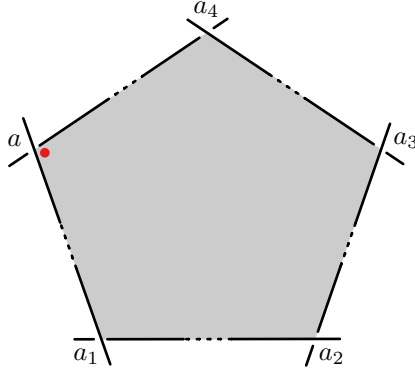


FIGURE 4. When all of the corners in the dotted parts of the boundary are mapped to 1 by  $\varepsilon$ , this disk contributes  $a^\vee$  to  $m_\varepsilon^k(a_4^\vee, \dots, a_1^\vee)$ .

order), and possibly other negative corners that the augmentation  $\varepsilon$  maps to 1; see Figure 4.

It is straightforward to check that the defining equation  $(\partial^\varepsilon)^2 = 0$  implies the following:

**Proposition 3.2.** *A semi-free DGA  $(\mathcal{A}, \partial)$  with augmentation  $\varepsilon$  determines an  $A_\infty$  algebra  $(A^\vee, \{m_\varepsilon^k\})$ .*

This construction first appeared in the context of the Chekanov-Eliashberg DGA in [9], though without the correct gradings.

*Example 3.3.* The  $A_\infty$  algebra induced by either augmentation  $\varepsilon_i$  of Example 2.5 is generated by the duals of the generators of the Chekanov-Eliashberg DGA with grading  $|a_2^\vee| = |a_3^\vee| = 0$ ,  $|a_4^\vee| = |a_5^\vee| = 1$ , and  $|a_1^\vee| = |a_6^\vee| = |a_7^\vee| = 2$  (note the grading shift compared to Example 2.7). The  $A_\infty$  operations match those in Example 2.7 with suitable changes in notation. We see that  $H^0(A, m_1) \simeq \mathbb{F}_2$  and  $H^2(A, m_1) \simeq \mathbb{F}_2^2$ .

In the presence of an  $m$ -component link grading  $o \times v : \mathcal{S} \rightarrow \{1, \dots, m\}^2$ , we may refine the associated  $A_\infty$  algebra structure  $(A^\vee, \{m_\varepsilon^k\})$  further. Following [43, §3.2], we write  $A^{ij}$  for the subspace of  $A$  generated by  $\mathcal{R}^{ij}$ , splitting  $A$  as  $\bigoplus_{i,j} A^{ij}$  and  $A^\vee$  as  $\bigoplus_{i,j} A_{ij}^\vee$ . If the augmentation  $\varepsilon$  respects the link grading, then the products in the  $A_\infty$  algebra  $(A^\vee, \{m_\varepsilon^k\})$  split, with the only non-vanishing products being the following:

$$(3.2) \quad m_\varepsilon^k : A_{i_k i_{k+1}}^\vee \otimes \cdots \otimes A_{i_1 i_2}^\vee \rightarrow A_{i_1 i_{k+1}}^\vee.$$

**3.2.  $A_\infty$  Categories.** The next step in our generalization is to move from an  $A_\infty$  algebra up to an  $A_\infty$  category. In Section 6, we shall define several  $A_\infty$  categories for a Legendrian  $\Lambda$ , whose objects will be augmentations and whose morphisms will be generalizations of the linearized Legendrian

contact homology complex. In this section, we set down basic notions and notations for  $A_\infty$  categories, following [24, 52].

**3.2.1. Definition of an  $A_\infty$  Category.** Just as an algebra may be understood as a category with a single object, an  $A_\infty$  algebra may be thought of as an  $A_\infty$  category with a single object.

**Definition 3.4.** An  $A_\infty$  category  $\mathcal{C}$  (over  $\mathbb{F}_2$ ) consists of the following data:

- a collection of objects  $\text{ob } \mathcal{C}$ ,
- for every pair  $X, X'$  of objects, a graded vector space  $\text{Hom}_{\mathcal{C}}(X, X')$  over  $\mathbb{F}_2$ , and
- for any set of  $k + 1$  objects  $X_1, \dots, X_{k+1}$ , structure maps

$$m_{\mathcal{C}}^k : \text{Hom}_{\mathcal{C}}(X_k, X_{k+1}) \otimes \dots \otimes \text{Hom}_{\mathcal{C}}(X_1, X_2) \rightarrow \text{Hom}_{\mathcal{C}}(X_1, X_{k+1})$$

of degree  $2 - k$  that satisfy the relation (3.1), with appropriate changes of notation.

For convenience, we shall henceforth denote by  $\text{Hom}_{\mathcal{C}}(X_{k+1}, \dots, X_1)$  the tensor product  $\text{Hom}_{\mathcal{C}}(X_k, X_{k+1}) \otimes \dots \otimes \text{Hom}_{\mathcal{C}}(X_1, X_2)$ .

As for  $A_\infty$  algebra, the  $k = 1$  instance of the relations for an  $A_\infty$  category  $\mathcal{C}$  says that  $m_{\mathcal{C}}^1$  is a differential on each graded vector space  $\text{Hom}_{\mathcal{C}}(X, X')$ . Thus, we may define the **cohomology category**  $H(\mathcal{C})$  of  $\mathcal{C}$  whose objects are the same as  $\mathcal{C}$  and whose morphisms are given by the cohomology  $H^*(\text{Hom}_{\mathcal{C}}(X, X'))$ . That the cohomology category is actually a category stems from the  $k = 2$  and  $k = 3$  instances of the  $A_\infty$  relations for  $\mathcal{C}$ , which yield composition of morphisms and associativity for that composition, respectively.

Given an  $A_\infty$  category  $\mathcal{C}$ , a natural construction is a **wide subcategory**  $\mathcal{D}$  of  $\mathcal{C}$ , which is an  $A_\infty$  category that has the same objects as  $\mathcal{C}$ , whose morphisms are subspaces  $\text{Hom}_{\mathcal{D}}(X, X') \subset \text{Hom}_{\mathcal{C}}(X, X')$ , and whose structure maps are restrictions of those on  $\mathcal{C}$ , assuming the latter have image in the appropriate  $\text{Hom}_{\mathcal{D}}$  spaces. A wide subcategory  $\mathcal{D}$  of  $\mathcal{C}$  induces a **quotient category**  $\mathcal{C}/\mathcal{D}$  that has the same objects as  $\mathcal{C}$ , whose morphisms are defined by  $\text{Hom}_{\mathcal{C}/\mathcal{D}}(X, X') = \text{Hom}_{\mathcal{C}}(X, X') / \text{Hom}_{\mathcal{D}}(X, X')$ , and whose structure maps are defined by  $m_{\mathcal{C}}^k$  modulo elements in  $\text{Hom}_{\mathcal{D}}(X_i, X_{i+1})$ .

The theory of  $A_\infty$  categories requires a notion of unitality for  $A_\infty$  equivalence to make sense. The most relevant notion of unitality for this paper is the following.

**Definition 3.5.** An  $A_\infty$  category  $\mathcal{C}$  is **strictly unital** if for any object  $X$ , there is an element  $e_X \in \text{Hom}_{\mathcal{C}}(X, X)$  of grading 0 such that

- $m_{\mathcal{C}}^1(e_X) = 0$ ,
  - for any objects  $X, X'$  and  $a \in \text{Hom}_{\mathcal{C}}(X, X')$ ,
- $$m_{\mathcal{C}}^2(e_{X'}, a) = m_{\mathcal{C}}^2(a, e_X) = a,$$
- $m_{\mathcal{C}}^k(\dots, e_X, \dots) = 0$  for all  $k \geq 3$ .

**3.2.2. Definition of an  $A_\infty$  Functor.** The definition of an  $A_\infty$  functor between  $A_\infty$  categories generalizes the standard definition of a functor as follows:

**Definition 3.6.** An  $A_\infty$  **functor**  $F : \mathcal{C} \rightarrow \mathcal{D}$  of degree  $d$  consists of the following data:

- A map  $F : \text{ob } \mathcal{C} \rightarrow \text{ob } \mathcal{D}$ ;
- For any  $k + 1$  objects  $X_1, \dots, X_{k+1} \in \text{ob } \mathcal{C}$ , a linear map

$$F^k : \text{Hom}_{\mathcal{C}}(X_{k+1}, \dots, X_1) \rightarrow \text{Hom}_{\mathcal{D}}(F(X_1), F(X_{k+1})),$$

of degree  $1 - k + d$  that satisfies the relations

$$\sum_{j, i_1 + \dots + i_j = k} m_{\mathcal{D}}^j(F^{i_j} \otimes \dots \otimes F^{i_1}) = \sum_{\substack{0 < s \leq k \\ 0 \leq r \leq k-s}} F^{k-s+1}(\mathbb{1}^{\otimes k-r-s} \otimes m_{\mathcal{C}}^s \otimes \mathbb{1}^{\otimes r}).$$

The first two relations show that an  $A_\infty$  functor  $F : \mathcal{C} \rightarrow \mathcal{D}$  induces an ordinary functor  $[F]$  between the corresponding cohomology categories.

Note that if  $\mathcal{D}$  is a subcategory of  $\mathcal{C}$ , there is a canonical inclusion functor  $i : \mathcal{D} \rightarrow \mathcal{C}$  where  $i^1$  is the inclusion of linear subspace and  $i^k = 0$  for  $k > 1$ . Similarly, there is a canonical projection functor  $\pi : \mathcal{C} \rightarrow \mathcal{C}/\mathcal{D}$  where  $\pi^1$  is the projection of vector spaces and  $\pi^k = 0$  for  $k > 1$ . Functors such as these, whose higher order terms vanish, are termed **naïve functors**.

Strict unitality for functors follows a similar pattern as for strictly unital categories.

**Definition 3.7.** An  $A_\infty$  functor  $F : \mathcal{C} \rightarrow \mathcal{D}$  between strictly unital categories is **strictly unital** if for all objects  $X \in \text{ob } \mathcal{C}$ ,  $F^1(e_X) = e_{F(X)}$  and  $F^k(\dots, e_{X_i}, \dots) = 0$  for any  $1 \leq i \leq k$  and  $k \geq 2$ .

Again, it is straightforward to check that a strictly unital  $A_\infty$  functor induces a unital functor on the cohomology categories. An  $A_\infty$  functor between two strictly unital  $A_\infty$  categories is an  $A_\infty$  **equivalence** between if the induced functor on cohomology categories is an equivalence of categories in the usual sense, in particular preserving units.  $A_\infty$  equivalence is indeed an equivalence relation; see [52, Theorem 2.9].

**3.3.  $A_\infty$  Bimodules.** Theorem 1.1 sets up a duality relationship between  $A_\infty$  bimodules over augmentation categories. In this section, we lay out the basic definitions and constructions of  $A_\infty$  bimodules that we will need to describe and prove that relationship. We will not develop the most general theory in this section, as we work in a setting where all of the underlying vector spaces are finite dimensional.

**3.3.1. The Definition of an  $A_\infty$  Bimodule.** We begin with the definition of an  $A_\infty$  bimodule over two  $A_\infty$  categories.

**Definition 3.8.** Given  $A_\infty$  categories  $\mathcal{C}$  and  $\mathcal{D}$  over  $\mathbb{F}_2$ , an  $\mathcal{C}$ - $\mathcal{D}$  **bimodule**  $\mathcal{M}$  consists of the following data:

- for  $X \in \text{ob } \mathcal{C}$  and  $Y \in \text{ob } \mathcal{D}$ , a graded vector space  $\mathcal{M}(X, Y)$ ;
- for  $r, s \geq 0$ , objects  $X_1, \dots, X_{r+1} \in \text{ob } \mathcal{C}$ , and  $Y_1, \dots, Y_{s+1} \in \text{ob } \mathcal{D}$ , bimodule structure maps

$$\begin{aligned} n_{\mathcal{M}}^{r|s} : \text{Hom}_{\mathcal{C}}(X_{r+1}, \dots, X_1) \otimes \mathcal{M}(X_1, Y_1) \otimes \text{Hom}_{\mathcal{D}}(Y_1, \dots, Y_{s+1}) \\ \rightarrow \mathcal{M}(X_{r+1}, Y_{s+1}), \end{aligned}$$

of degree  $1 - r - s$ , satisfying the relations

$$(3.3) \quad \begin{aligned} 0 = & \sum n_{\mathcal{M}}^{r-i|s-j} (\mathbb{1}_{\mathcal{C}}^{\otimes r-i} \otimes n_{\mathcal{M}}^{i|j} \otimes \mathbb{1}_{\mathcal{D}}^{\otimes s-j}) \\ & + \sum n_{\mathcal{M}}^{r-i+1|s} (\mathbb{1}_{\mathcal{C}}^{\otimes r-i-j} \otimes m_{\mathcal{C}}^i \otimes \mathbb{1}_{\mathcal{C}}^{\otimes j} \otimes \mathbb{1}_{\mathcal{M}} \otimes \mathbb{1}_{\mathcal{D}}^{\otimes s}) \\ & + \sum n_{\mathcal{M}}^{r|s-j+1} (\mathbb{1}_{\mathcal{C}}^{\otimes r} \otimes \mathbb{1}_{\mathcal{M}} \otimes \mathbb{1}^{\otimes i} \otimes m_{\mathcal{D}}^j \otimes \mathbb{1}^{\otimes s-i-j}) \end{aligned}$$

In the case when the base categories  $\mathcal{C} = \mathcal{D}$  are the same, we simply refer such a bimodule as a  $\mathcal{C}$ -bimodule. Further, an  $A_{\infty}$  bimodule may come with a **grading shift**, denoted by  $\mathcal{M}[n]$ , meaning that its graded vector spaces are the shifted spaces  $\mathcal{M}[n](X, Y) = \mathcal{M}(X, Y)[n]$ , where  $[n]$  means shifting the grading of a vector space down by  $n \in \mathbb{Z}$ . Since we work over  $\mathbb{F}_2$ , the structure maps are unchanged.

If  $\mathcal{C}$  and  $\mathcal{D}$  are strictly unital, then, following [23, §3.7] or [51], we say that an  $\mathcal{C}$ - $\mathcal{D}$  bimodule  $\mathcal{M}$  is **strictly unital** if for any objects  $X \in \text{ob } \mathcal{C}$  and  $Y \in \text{ob } \mathcal{D}$ , the units  $e_X \in \text{Hom}_{\mathcal{C}}(X, X)$  and  $e_Y \in \text{Hom}_{\mathcal{D}}(Y, Y)$  satisfy the following relations for any  $\mathbf{z} \in \mathcal{M}(X, Y)$ :

- $n_{\mathcal{M}}^{1|0}(e_X, \mathbf{z}) = \mathbf{z} = n_{\mathcal{M}}^{0|1}(\underline{\mathbf{z}}, e_Y)$ , and
- $n_{\mathcal{M}}^{r|s}(\dots, e_X, \dots, \underline{\mathbf{z}}, \dots) = 0 = n_{\mathcal{M}}^{r|s}(\dots, \underline{\mathbf{z}}, \dots, e_Y, \dots)$  for  $r + s \geq 2$ .

**3.3.2. Fundamental Constructions of  $A_{\infty}$  Bimodules.** We review some general constructions of  $A_{\infty}$  bimodules, including submodules, linear duals, pullbacks, diagonal bimodules, and Serre bimodules, which combine to give the language necessary for the relative Calabi-Yau structure promised in Theorem 1.1.

A **submodule**  $\mathcal{N}$  of an  $A_{\infty}$   $\mathcal{C}$ - $\mathcal{D}$  bimodule  $\mathcal{M}$  is simply an assignment, for each  $X \in \text{ob } \mathcal{C}$  and  $Y \in \text{ob } \mathcal{D}$ , of a subspace  $\mathcal{N}(X, Y) \subset \mathcal{M}(X, Y)$  that is preserved under the bimodule action.

The **linear dual**  $\mathcal{M}^{\vee}$  of an  $A_{\infty}$   $\mathcal{C}$ - $\mathcal{D}$  bimodule  $\mathcal{M}$  is a  $\mathcal{D}$ - $\mathcal{C}$  bimodule whose underlying vector spaces are defined by

$$\mathcal{M}^{\vee}(X, Y) = \text{hom}(\mathcal{M}(Y, X), \mathbb{F}_2).$$

Note the reversal of the order of the actions of  $\mathcal{C}$  and  $\mathcal{D}$ . Further, the grading of  $\mathcal{M}^{\vee}(X, Y)$  should also be carefully noted: the base field is assumed to lie in grading zero and the linear functionals in  $\text{hom}(\mathcal{M}(Y, X), \mathbb{F}_2)$  are meant to have degree 0. Thus, if  $\{b_i\}$  is a basis for  $\mathcal{M}(X, Y)$  with dual basis  $\{b_i^{\vee}\}$ , then  $|b_i^{\vee}| = -|b_i|$ . The  $A_{\infty}$  operations on  $\mathcal{M}^{\vee}$  are defined by

$$(3.4) \quad n_{\mathcal{M}^{\vee}}^{s|r}(b_s, \dots, b_1, \underline{\beta}, a_1, \dots, a_r)(\mathbf{z}) = \beta(n_{\mathcal{M}}^{r|s}(a_1, \dots, a_r, \underline{\mathbf{z}}, b_s, \dots, b_1)).$$

We will also need to change the base categories for an  $A_\infty$  bimodule by pulling back along a pair of functors. Let  $F : \mathcal{C} \rightarrow \mathcal{C}'$  and  $G : \mathcal{D} \rightarrow \mathcal{D}'$  be two functors of  $A_\infty$  categories of degree 0. For a  $\mathcal{C}'\text{-}\mathcal{D}'$  bimodule  $\mathcal{M}$ , the **pullback**  $(F \otimes G)^*\mathcal{M}$  of  $\mathcal{M}$  along  $F$  and  $G$  is an  $\mathcal{C}\text{-}\mathcal{D}$  bimodule with graded vector spaces  $(F \otimes G)^*\mathcal{M}(X, Y) = \mathcal{M}(F(X), G(Y))$  and structure maps

$$(3.5) \quad n_{(F \otimes G)^*\mathcal{M}}^{r|s} = \sum_{\substack{i, p_1 + \dots + p_i \leq r \\ j, q_1 + \dots + q_j \leq s}} n_{\mathcal{M}}^{i|j}(F^{p_i} \otimes \dots \otimes F^{p_1} \otimes \mathbb{1}_{\mathcal{M}} \otimes G^{q_1} \otimes \dots \otimes G^{q_j}).$$

If  $F = G$ , we use the shorthand  $F^*\mathcal{M} = (F \otimes F)^*\mathcal{M}$ . It follows directly from the definition that the pullback construction commutes with the linear dual.

Finally, every  $A_\infty$  category  $\mathcal{C}$  induces a  $\mathcal{C}$ -bimodule  $\mathcal{C}_\Delta$  — called the **diagonal bimodule** of  $\mathcal{C}$  — with underlying vector spaces  $\mathcal{C}_\Delta(X, Y) = \text{Hom}_{\mathcal{C}}(X, Y)$  and structure maps given by  $n_{\mathcal{C}_\Delta}^{r|s} = m_{\mathcal{C}}^{r+s+1}$ . The linear dual of a diagonal bimodule of  $\mathcal{C}_\Delta$  is also a  $\mathcal{C}\text{-}\mathcal{C}$  bimodule, called the **Serre bimodule** of  $\mathcal{C}$  and denoted by  $\mathcal{C}^\vee$ .

**3.3.3. Morphisms of  $A_\infty$  Bimodules.** We finish our recollection of  $A_\infty$  bimodule concepts by considering morphisms between  $A_\infty$  bimodules. A key step in generalizing duality in [15, 47] will be promoting the duality map  $\eta$  in Theorem 2.8 to an  $A_\infty$  bimodule quasi-isomorphism. To get there, we need to first define a weaker notion.

**Definition 3.9.** A **pre-morphism** of  $\mathcal{C}\text{-}\mathcal{D}$  bimodules  $f : \mathcal{M} \rightarrow \mathcal{N}$  of degree  $k$  consists of a collection of linear maps

$$\begin{aligned} f^{r|s} : \text{Hom}_{\mathcal{C}}(X_{r+1}, \dots, X_1) &\otimes \mathcal{M}(X_1, Y_1) \otimes \text{Hom}_{\mathcal{D}}(Y_1, \dots, Y_{s+1}) \\ &\rightarrow \mathcal{N}(X_{r+1}, Y_{s+1}), \end{aligned}$$

of degree  $k - r - s$  for all  $r, s \geq 0$ , and objects  $X_1, \dots, X_{r+1} \in \text{ob } \mathcal{C}$  and  $Y_1, \dots, Y_{s+1} \in \text{ob } \mathcal{D}$ .

For two pre-morphisms  $f : \mathcal{M} \rightarrow \mathcal{N}$  and  $g : \mathcal{N} \rightarrow \mathcal{P}$  of degrees  $k$  and  $l$ , their **composition**  $gf : \mathcal{M}_0 \rightarrow \mathcal{M}_2$  is a pre-morphism of degree  $k + l$  consisting of maps

$$(3.6) \quad (gf)^{r|s} := \sum_{i,j} g^{r-i|s-j}(\mathbb{1}_{\mathcal{C}}^{\otimes r-i} \otimes f^{i|j} \otimes \mathbb{1}_{\mathcal{D}}^{\otimes s-j}).$$

We will use three special types of pre-morphisms. First, a bimodule structure map is a degree 1 pre-morphism.

To define the second type, let the **differential**  $\delta(f)$  of a pre-morphism  $f$  be the pre-morphism of degree  $k + 1$  consisting of maps given by

$$\begin{aligned} (\delta(f))^{r|s} &= \sum_{i,j} n_{\mathcal{M}}^{r-i|s-j} (\mathbb{1}_{\mathcal{C}}^{\otimes r-i} \otimes f^{i|j} \otimes \mathbb{1}_{\mathcal{D}}^{\otimes s-j}) \\ &\quad + \sum_{i,j} f^{r-i|s-j} (\mathbb{1}_{\mathcal{C}}^{\otimes r-i} \otimes n_{\mathcal{M}}^{i|j} \otimes \mathbb{1}_{\mathcal{D}}^{\otimes s-j}) \\ &\quad + \sum_{i,j} f^{r-i+1|s} (\mathbb{1}_{\mathcal{C}}^{\otimes j} \otimes m_{\mathcal{C}}^i \otimes \mathbb{1}_{\mathcal{C}}^{\otimes r-i-j} \otimes \mathbb{1}_{\mathcal{M}} \otimes \mathbb{1}_{\mathcal{D}}^{\otimes s}) \\ &\quad + \sum_{i,j} f^{r|s-j+1} (\mathbb{1}_{\mathcal{C}}^{\otimes r} \otimes \mathbb{1}_{\mathcal{M}} \otimes \mathbb{1}_{\mathcal{D}}^{\otimes j} \otimes m_{\mathcal{D}}^i \otimes \mathbb{1}_{\mathcal{D}}^{\otimes s-i-j}), \end{aligned}$$

for all  $r, s \geq 0$  and objects  $X_1, \dots, X_{r+1} \in \text{ob } \mathcal{M}$ ,  $Y_1, \dots, Y_{s+1} \in \text{ob } \mathcal{N}$ .

Note that if  $\delta(f) = 0$ , then  $f^{0|0}$  is a chain map, which leads us to the following definition:

**Definition 3.10.** A pre-morphism of  $\mathcal{C}$ - $\mathcal{D}$  bimodules  $f : \mathcal{M} \rightarrow \mathcal{N}$  is a **bimodule morphism** if  $\delta(f) = 0$ .

A simple, but useful, example of a bimodule morphism arises from a family of chain maps  $f_{X,Y} : \mathcal{M}(X, Y) \rightarrow \mathcal{N}(X, Y)$ . In this case, we may define a bimodule morphism  $f : \mathcal{M} \rightarrow \mathcal{N}$  by setting  $f^{0|0}$  to be  $f_{X,Y}$  on  $\mathcal{M}(X, Y)$  and all higher maps vanish; this is called a **naïve morphism**. In particular, for a  $\mathcal{C}$ - $\mathcal{D}$  bimodule  $\mathcal{M}$ , the **identity morphism** is a naïve morphism obtained by extending the identity maps on  $\mathcal{M}(X, Y)$ .

Other useful examples of bimodule morphisms arise from the constructions in Section 3.3.2. First, for an  $A_\infty$  functor  $F : \mathcal{C} \rightarrow \mathcal{D}$  of degree 0, the **induced bimodule morphism**  $f : \mathcal{C}_\Delta \rightarrow F^* \mathcal{D}_\Delta$  of  $F$  is a  $\mathcal{C}$ -bimodule morphism of degree 0 defined by  $f^{r|s} = F^{r+s+1}$ . In general, if  $f : \mathcal{M} \rightarrow \mathcal{N}$  is a  $\mathcal{D}$ -bimodule morphism, its **pullback morphism**  $F^* f : F^* \mathcal{M} \rightarrow F^* \mathcal{N}$  is a  $\mathcal{C}$ -bimodule morphism defined using a formula analogous to Equation (3.5). Further, we may form the **adjoint**  $f^\vee : \mathcal{N}^\vee \rightarrow \mathcal{M}^\vee$  using a formula analogous to Equation (3.4).

The final type of pre-morphism we will use generalizes the notion of a chain homotopy.

**Definition 3.11.** Let  $f : \mathcal{M} \rightarrow \mathcal{N}$  and  $g : \mathcal{M} \rightarrow \mathcal{N}$  be two  $\mathcal{C}$ - $\mathcal{D}$  bimodule morphisms of degree  $k$ . An  $A_\infty$  **homotopy** between  $f$  and  $g$  is a pre-morphism  $H : \mathcal{M} \rightarrow \mathcal{N}$  of degree  $k - 1$  such that

$$(3.7) \quad f + g = \delta(H).$$

In this case,  $f$  is homotopic to  $g$  and we write  $f \sim g$ .

The following lemma, which will be useful in proving Proposition 4.4, is straightforward to check.

**Lemma 3.12.** *The  $A_\infty$  homotopy relation is an equivalence relation. Further, if  $f, f' : \mathcal{M} \rightarrow \mathcal{N}$  are homotopic and if  $j : \mathcal{N} \rightarrow \mathcal{P}$  and  $g : \mathcal{L} \rightarrow \mathcal{M}$  are  $A_\infty$  morphisms, then  $jf$  and  $jf'$  are homotopic, as are  $fg$  and  $f'g$ .*

A key ingredient in the generalization of duality is the invertibility of morphisms. First, a bimodule morphism  $f$  is a **quasi-isomorphism** if  $f^{0|0}$  is a chain quasi-isomorphism (i.e.  $[f^{0|0}]$  is an isomorphism on homology). A bimodule morphism  $f : \mathcal{M} \rightarrow \mathcal{N}$  is an  $A_\infty$  **homotopy equivalence** if there is an  $A_\infty$  **homotopy inverse**  $g : \mathcal{N} \rightarrow \mathcal{M}$  such that

$$fg \sim 1_{\mathcal{N}} \text{ and } gf \sim 1_{\mathcal{M}}.$$

By noting that  $A_\infty$  homotopy equivalence implies ordinary homotopy equivalence at the linear level, we see that an  $A_\infty$  homotopy equivalence is automatically a quasi-isomorphism. Conversely, if  $f : \mathcal{M} \rightarrow \mathcal{N}$  is a quasi-isomorphism and all  $\mathcal{M}(X, Y)$  and  $\mathcal{N}(X, Y)$  are finite-dimensional as graded vector spaces, then we can explicitly construct a quasi-inverse to  $f^{0|0}$  and bootstrap up to the following proposition. The bootstrapping proof appears in a variety of sources, but the source closest to the our setting of modules over  $A_\infty$  categories is [26, Lemma 8.1].

**Proposition 3.13.** *If  $f : \mathcal{M} \rightarrow \mathcal{N}$  is a quasi-isomorphism of  $A_\infty$  bimodules with all  $\mathcal{M}(X, Y)$  and  $\mathcal{N}(X, Y)$  finite-dimensional as graded vector spaces, then  $f$  is an  $A_\infty$  homotopy equivalence.*

This proposition is a key feature of the  $A_\infty$  bimodules, and we will use it repeatedly in our work to come.

**3.4. Mapping Cones and Cylinders.** The proof of Theorem 2.8 in [47] identifies the linearized LCH of a “separated 2-copy” as the mapping cone of the duality map  $\eta$  to deduce the duality exact sequence. The proof of the main theorem in this paper will generalize this structure to an  $A_\infty$  mapping cone of an  $A_\infty$  bimodule morphism. Following [52, §3s], we recall the definition of these objects here, beginning with the mapping cone.

**Definition 3.14.** Given a degree 0  $\mathcal{C}$ - $\mathcal{D}$  bimodule morphism  $f : \mathcal{M} \rightarrow \mathcal{N}$ , the  $A_\infty$  **mapping cone**  $\text{Cone}(f)$  of  $f$  is the  $\mathcal{C}$ - $\mathcal{D}$  bimodule consisting of the following data:

- for  $X \in \text{ob } \mathcal{C}$  and  $Y \in \text{ob } \mathcal{D}$ , a graded vector space

$$\text{Cone}(f)(X, Y) = \mathcal{M}(X, Y)[1] \oplus \mathcal{N}(X, Y).$$

- For  $r, s \geq 0$ , the structure map of degree  $1 - r - s$  is defined by

$$\begin{aligned} n_{\text{Cone}(f)}^{r|s}(\dots, (\underline{\mathbf{x}}, \mathbf{y}), \dots) &= (n_{\mathcal{M}}^{r|s}(\dots, \underline{\mathbf{x}}, \dots), \\ &\quad n_{\mathcal{N}}^{r|s}(\dots, \underline{\mathbf{y}}, \dots) + f^{r|s}(\dots, \underline{\mathbf{x}}, \dots)). \end{aligned}$$

Note that  $\mathcal{N}$  is a submodule of  $\text{Cone}(f)$ . Further,  $\text{Cone}(f)$  comes with two degree 0 bimodule morphisms, the inclusion  $i_{\mathcal{N}} : \mathcal{N} \rightarrow \text{Cone}(f)$  and

the projection  $\pi_{\mathcal{M}} : \text{Cone}(f) \rightarrow \mathcal{M}[1]$ , both defined as the naïve morphisms extending the corresponding linear map.

The **mapping cocone** of  $f$  is given by  $\text{Cocone}(f) = \text{Cone}(f^{\vee})[-1]$ . The cocone is also equipped with two degree 0 bimodule morphisms  $i_{\mathcal{N}}^{\vee} : \text{Cocone}(f) \rightarrow \mathcal{N}^{\vee}$  and  $\pi_{\mathcal{M}}^{\vee} : \mathcal{M}^{\vee}[-1] \rightarrow \text{Cocone}(f)$  corresponding to the duals of  $i_{\mathcal{N}}$  and  $\pi_{\mathcal{M}}$  respectively.

As stated in [51, §2], a mapping cone structure naturally arises when a bimodule contains a submodule. In particular, suppose  $\mathcal{Q}$  is a submodule of an  $\mathcal{C}$ -bimodule  $\mathcal{M}$ . Let  $\mathcal{P}$  be the quotient  $\mathcal{M}/\mathcal{Q}$ . We get a naïve short exact sequence of  $\mathcal{C}$ -bimodules

$$0 \longrightarrow \mathcal{Q} \xrightarrow{i} \mathcal{M} \xrightarrow{\pi} \mathcal{P} \longrightarrow 0$$

From this data, we may define a morphism  $\varphi : \mathcal{P}[-1] \rightarrow \mathcal{Q}$ . For any choice of a naïve pre-morphism  $\sigma : \mathcal{P} \rightarrow \mathcal{M}$  whose underlying vector space maps split  $\pi$ , define  $\varphi$  by  $(id - \sigma\pi) \circ n_{\mathcal{M}} \circ \sigma$ .

**Lemma 3.15.** *In the setting above,  $\varphi : \mathcal{P}[-1] \rightarrow \mathcal{Q}$  is a bimodule morphism and  $\mathcal{M}$  is quasi-isomorphic to  $\text{Cone}(\varphi)$ .*

Finally, we recall the relevant concepts of the mapping cylinder in the  $A_{\infty}$  bimodule setting.

**Definition 3.16.** The  $A_{\infty}$  **mapping cylinder**  $\text{Cyl}(f)$  of a  $\mathcal{C}$ - $\mathcal{D}$  bimodule morphism  $f : \mathcal{M} \rightarrow \mathcal{N}$  is the shifted cone  $\text{Cone}(\pi_{\mathcal{M}})[-1]$  of the canonical projection  $\pi_{\mathcal{M}} : \text{Cone}(f) \rightarrow \mathcal{M}[1]$ . The  $A_{\infty}$  **mapping cocylinder**  $\text{Cocyl}(f)$  of a  $\mathcal{C}$ - $\mathcal{D}$  bimodule morphism  $f : \mathcal{M} \rightarrow \mathcal{N}$  is the shifted cocone  $\text{Cocone}(\pi_{\mathcal{M}})[1]$ .

A useful fact about these constructions is encapsulated in the following lemma, whose proof follows from the fact that the naïve inclusion  $I_{\mathcal{N}} : \mathcal{N} \rightarrow \text{Cyl}(f)$  and naïve projection  $\Pi_{\mathcal{N}} : \text{Cyl}(f) \rightarrow \mathcal{N}$  are homotopy inverses.

**Lemma 3.17.** *The mapping cylinder  $\text{Cyl}(f)$  of a  $\mathcal{C}$ - $\mathcal{D}$  bimodule morphism  $f : \mathcal{M} \rightarrow \mathcal{N}$  is homotopy equivalent to  $\mathcal{N}$  and the mapping cocylinder  $\text{Cocyl}(f)$  is homotopy equivalent to  $\mathcal{N}^{\vee}$ .*

#### 4. WEAK RELATIVE CALABI-YAU STRUCTURES

The goal of this section is to introduce the algebraic structures used to generalize duality. As above, we will not develop the most general theory, but rather work over  $\mathbb{F}_2$  and under the assumption that the morphism spaces of the  $A_{\infty}$  categories and bimodules are finite-dimensional. We first define the notions of weak and very weak relative Calabi-Yau (CY) structures, basing the definitions on work of Brav and Dyckerhoff [3] and Chen [7]. We then show that, under mild assumptions, a very weak relative CY structure gives rise to a weak one; this transition from very weak to weak structures will be the algebraic key to the proof of the main theorem.

The following definition of a weak relative CY structure is adapted from Chen's transcription of Brav and Dyckerhoff's original definition in terms of  $A_\infty$  bimodules, which aligns more closely with our setup.

**Definition 4.1** ([3],[7]). Let  $\mathcal{A}$  and  $\mathcal{C}$  be strictly unital  $A_\infty$  categories and let  $F : \mathcal{A} \rightarrow \mathcal{C}$  be an  $A_\infty$  functor. A **weak right relative Calabi-Yau structure of dimension  $n$**  on  $F$  consists of

- An  $A_\infty$  morphism  $\kappa : \mathcal{C}_\Delta[n-1] \rightarrow \mathcal{C}^\vee$  and
- An  $A_\infty$  pre-morphism  $\phi : \mathcal{A}_\Delta[n] \rightarrow \mathcal{A}^\vee$

so that

- (1)  $\phi$  is a null-homotopy for the composition

$$\mathcal{A}_\Delta[n-1] \xrightarrow{f} F^*\mathcal{C}_\Delta[n-1] \xrightarrow{F^*\kappa} F^*\mathcal{C}^\vee \xrightarrow{f^\vee} \mathcal{A}^\vee,$$

where  $f : \mathcal{A}_\Delta \rightarrow F^*\mathcal{C}_\Delta$  is the bimodule morphism induced by  $F$ ;

- (2) Let the morphisms  $\zeta$  and  $\zeta'$  be induced by  $\phi$  via the universal properties of  $\text{Cone}(f)$  and  $\text{Cocone}(f)$  that make the following diagram coherent in the derived category  $D(\mathcal{A}\text{-bimod})$ :

$$(4.1) \quad \begin{array}{ccccccc} \cdots & \longrightarrow & \mathcal{A}_\Delta[n-1] & \xrightarrow{f} & F^*\mathcal{C}_\Delta[n-1] & \xrightarrow{i} & \text{Cone}(f)[n-1] \longrightarrow \cdots \\ & & \downarrow \zeta & & \downarrow F^*\kappa & & \downarrow \zeta' \\ \cdots & \longrightarrow & \text{Cocone}(f) & \xrightarrow{i^\vee} & F^*\mathcal{C}^\vee & \xrightarrow{f^\vee} & \mathcal{A}^\vee \longrightarrow \cdots \end{array}$$

The morphisms  $\kappa$ ,  $\zeta$ , and  $\zeta'$  are all quasi-isomorphisms.

Several comments are in order to clarify the definition above and to connect it to other notions in the literature. First, the diagram in the definition above mirrors the Poincaré-Lefschetz Duality for a manifold with boundary  $(M, \partial M)$ , where  $\text{Cone}(f)$  plays the role of  $H^*(M)$ ,  $F^*\mathcal{C}_\Delta$  plays the role of  $H^*(\partial M)$ , and  $\mathcal{A}_\Delta$  plays the role of  $H^*(M, \partial M)$ .

Second, weak relative right CY structures of dimension  $n$  were originally defined in [3] to be morphisms from relative Hochschild homology  $HH_{*+n}(\mathcal{C}, \mathcal{A})$  of the functor  $F$  to the base field satisfying a non-degeneracy condition. Definition 4.1 is a translation of the Hochschild homology definition to  $A_\infty$  language. The idea behind the translation builds on the correspondence between non-degenerate morphisms in  $\text{hom}(HH_*(\mathcal{A}), \mathbb{F}_2)$  and bimodule quasi-isomorphisms  $\mathcal{A}_\Delta[n] \rightarrow \mathcal{A}^\vee$ , which both define weak right (absolute) CY structures of dimension  $n$  on a proper category  $\mathcal{A}$ ; see [54, Appendix A] or [27, Definition 6.3]. In the relative case, morphisms in  $\text{hom}(HH_{*+n}(\mathcal{C}, \mathcal{A}), \mathbb{F}_2)$  correspond (cohomologically) to the pair  $(\kappa, \phi)$  in Definition 4.1. The non-degeneracy condition can be translated to condition (2) of Definition 4.1.

Next, a weak CY structure is a weaker notion than a strong CY structure, which puts extra conditions on the functor  $F$ . While a weak CY structure is a condition on the relative Hochschild homology, a strong structure is a condition on the relative cyclic homology. As noted in Cho [8], the weak

CY condition on a bimodule requires many fewer relations to hold than a strong CY condition on an  $A_\infty$  category.

Finally, a “right” CY structure is also called a “proper” CY structure in the literature; see [25, 27, 54]. Our terminology agrees with [3]. There is a parallel notion of a left or smooth CY structure defined using the inverse dualizing bimodule, but we will not discuss these structures in this paper.

We will not extract a weak relative CY structure directly from the geometry under our consideration. Rather, we will use an even weaker structure as an intermediate step.

**Definition 4.2.** Let  $\mathcal{A}$  be a (strictly) unital  $A_\infty$  category, let  $\mathcal{M}, \mathcal{N}$  be  $\mathcal{A}$ -bimodules, and let  $f : \mathcal{N} \rightarrow \mathcal{M}$  be an  $A_\infty$  morphism. A **very weak relative Calabi-Yau structure of dimension  $n$**  on  $f$  consists of  $A_\infty$  quasi-isomorphisms  $\eta : \mathcal{M}^\vee[n] \rightarrow \text{Cone}(f)$ ,  $\theta : \mathcal{N}^\vee[n] \rightarrow \mathcal{N}[1]$ , and  $\eta' : \text{Cone}(f)[n+1] \rightarrow \mathcal{M}[1]$  so that the diagram

$$(4.2) \quad \begin{array}{ccccccc} \cdots & \longrightarrow & \mathcal{M}^\vee[n] & \xrightarrow{f^\vee} & \mathcal{N}^\vee[n] & \xrightarrow{\pi_N^\vee} & \text{Cocone}(f)[n+1] \longrightarrow \cdots \\ & & \downarrow \eta & & \downarrow \theta & & \downarrow \eta' \\ \cdots & \longrightarrow & \text{Cone}(f) & \xrightarrow{\pi_N} & \mathcal{N}[1] & \xrightarrow{f} & \mathcal{M}[1] \longrightarrow \cdots \end{array}$$

commutes up to homotopy.

It turns out that the existence of the leftmost coherent square in Diagram (4.2) is sufficient for constructing a very weak relative CY structure.

**Lemma 4.3.** *Given a morphism  $f : \mathcal{N} \rightarrow \mathcal{M}$  and quasi-isomorphisms  $\eta : \mathcal{M}^\vee[n] \rightarrow \text{Cone}(f)$  and  $\theta : \mathcal{N}^\vee[n] \rightarrow \mathcal{N}[1]$  such that  $\pi_N \eta \sim \theta f^\vee$ , there exists a quasi-isomorphism  $\eta' : \text{Cocone}(f)[n+1] \rightarrow \mathcal{M}[1]$  such that  $(\eta, \theta, \eta')$  constitutes a very weak relative Calabi-Yau structure on  $f$ .*

*Proof.* Let  $H : \mathcal{M}^\vee[n] \rightarrow \mathcal{N}[1]$  be the homotopy between  $\pi_N \eta$  and  $\theta f^\vee$ . Define  $\eta' = (\pi_M \eta + fH)i_M^\vee + f\theta i_N^\vee$ . That  $\eta'$  is a bimodule morphism follows from  $\delta$  being a derivation on the category of pre-morphisms together with the facts that  $\eta, i_M^\vee, f$ , and  $\theta$  are morphisms, that  $\delta(\pi_M) = f\pi_N$ , and that  $\delta(i_N^\vee) = f^\vee i_M^\vee$ .

With  $\eta'$  defined above, it is immediate that the second square in Diagram (4.2) commutes strictly. That the next (unseen) square commutes up to homotopy follows a similar idea as [56, Lemma 4.9]. Define a pre-morphism  $K : \text{Cocone}(f)[n+1] \rightarrow \text{Cone}[1]$  by

$$K = (\eta', (\theta f^\vee + H)i_M^\vee + \theta i_N^\vee).$$

Since

$$\eta i_M^\vee + i_M \eta' = (\pi_M \eta i_M^\vee + \eta', \pi_N \eta i_M^\vee),$$

the equation  $\eta i_M^\vee + i_M \eta' = \delta(K)$  holds in the first component due to the definition of  $\eta'$  and the fact that  $\eta'$  is a bimodule morphism. It holds in the second component since  $\theta, \theta f^\vee$  are bimodule morphisms and  $H$  is a

homotopy between  $\pi_{\mathcal{N}}\eta$  and  $\theta f^{\vee}$ . Thus,  $K$  is a homotopy between  $\eta i_{\mathcal{M}}^{\vee}$  and  $i_{\mathcal{M}}\eta'$  as desired.

Finally, the Five Lemma guarantees that  $\eta'$  is a quasi-isomorphism.  $\square$

We end this section by introducing an algebraic tool to produce a weak right relative CY structure from a very weak relative CY structure. In Section 7, we will use geometric considerations to construct a very weak relative CY structure on  $A_{\infty}$  bimodules associated to a Legendrian link. The algebraic tool described in this section will then exploit the extra structure in this relationship to derive the main theorem. We emphasize that the form and proof of the algebraic tool rely on the assumption that the underlying vector spaces of all  $A_{\infty}$  structures involved are finite-dimensional, though a more general statement may hold.

In order to state the algebraic tool, we first specify the extra information needed to pass from very weak to weak relative CY structures. Begin with strictly unital  $A_{\infty}$  categories  $\mathcal{A}$  and  $\mathcal{C}$ , an  $\mathcal{A}$ -bimodule  $\mathcal{M}$ , a functor  $\pi : \mathcal{A} \rightarrow \mathcal{C}$ , and a morphism  $\rho : \pi^*\mathcal{C}_{\Delta}[-1] \rightarrow \mathcal{M}$ . For convenience, we set  $\mathcal{N} = \pi^*\mathcal{C}_{\Delta}$ . We say that the data  $(\mathcal{A} \xrightarrow{\pi} \mathcal{C}, \mathcal{N}[-1] \xrightarrow{\rho} \mathcal{M})$  is a **conical pair** if the diagonal bimodule  $\mathcal{A}_{\Delta}$  is  $\text{Cone}(\rho)$  and if the functor  $\pi$  induces the canonical projection  $\pi_{\mathcal{N}} : \mathcal{A}_{\Delta} \rightarrow \mathcal{N}$  of  $\text{Cone}(\rho)$ .

**Proposition 4.4.** *Let  $(\mathcal{A} \xrightarrow{\pi} \mathcal{C}, \mathcal{N}[-1] \xrightarrow{\rho} \mathcal{M})$  be a conical pair. If there is a very weak relative Calabi-Yau structure of dimension  $-n$  on  $\rho$  then there exists a weak right relative Calabi-Yau structure of dimension  $n$  on  $\pi$ .*

*Proof.* To set notation, suppose that the given very weak CY structure on  $\rho$  is captured by the following homotopy commutative diagram:

$$(4.3) \quad \begin{array}{ccccccc} \dots & \longrightarrow & \mathcal{M}^{\vee} & \xrightarrow{\rho^{\vee}} & \mathcal{N}^{\vee}[1] & \xrightarrow{\pi_{\mathcal{N}}^{\vee}} & \mathcal{A}_{\Delta}^{\vee}[1] \longrightarrow \dots \\ & & \downarrow \eta & & \downarrow \theta & & \downarrow \eta' \\ \dots & \longrightarrow & \mathcal{A}_{\Delta}[n] & \xrightarrow{\pi_{\mathcal{N}}} & \mathcal{N}[n] & \xrightarrow{\rho} & \mathcal{M}[n+1] \longrightarrow \dots \end{array}$$

Compare with Diagram 4.2 and note that the degree shifts result from the assumptions of dimension  $-n$  and that  $\mathcal{A}_{\Delta} \simeq \text{Cone}(\rho)$  for  $\rho : \mathcal{N}[-1] \rightarrow \mathcal{M}$ .

Our goal is to construct  $\kappa$  and  $\phi$  that satisfy the requirements of a weak right relative CY structure. As a first step, the fact that  $\eta$  and  $\theta$  are quasi-isomorphisms means that Proposition 3.13 yields  $A_{\infty}$  homotopy inverses  $\xi : \mathcal{A}_{\Delta}[n] \rightarrow \mathcal{M}^{\vee}$  and  $\kappa : \mathcal{N}[n] \rightarrow \mathcal{N}^{\vee}[1]$ , respectively. Further, we use coherence of the left square of Diagram (4.3) and Lemma 3.12 to see that

$$\kappa\pi_{\mathcal{N}} \sim \kappa\pi_{\mathcal{N}}\eta\xi \sim \kappa\theta\rho^{\vee}\xi \sim \rho^{\vee}\xi.$$

In particular, we obtain a homotopy  $H : \mathcal{A}_{\Delta}[n] \rightarrow \mathcal{N}^{\vee}$  between  $\rho^{\vee}\xi$  and  $\kappa\pi_{\mathcal{N}}$ . Define a pre-morphism of  $\mathcal{A}$ -bimodules  $\phi : \mathcal{A}_{\Delta}[n] \rightarrow \mathcal{A}_{\Delta}^{\vee} = \mathcal{M}^{\vee} \oplus \mathcal{N}^{\vee}$  by

$$\phi = (\xi, H).$$

We claim that the bimodule morphism  $\kappa$  and the pre-morphism  $\phi$  induce a weak right relative Calabi-Yau structure of dimension  $n$  on the functor  $\pi : \mathcal{A} \rightarrow \mathcal{C}$ . By Lemma 4.3, it suffices to show that the choice of explicit chain model  $\zeta = (\kappa\pi_{\mathcal{N}}, \phi)$  is a bimodule quasi-isomorphism in the following commutative diagram:

$$(4.4) \quad \begin{array}{ccccccc} \cdots & \longrightarrow & \mathcal{A}_{\Delta}[n-1] & \xrightarrow{\pi_{\mathcal{N}}} & \mathcal{N}[n-1] & \xrightarrow{I_{\mathcal{N}}} & \text{Cyl}(\rho)[n] \longrightarrow \cdots \\ & & \downarrow \zeta & & \downarrow \kappa & & \downarrow \zeta' \\ \cdots & \longrightarrow & \text{Cocyl}(\rho)[-1] & \xrightarrow{I_{\mathcal{N}}^{\vee}} & \mathcal{N}^{\vee} & \xrightarrow{\pi_{\mathcal{N}}^{\vee}} & \mathcal{A}_{\Delta}^{\vee} \longrightarrow \cdots \end{array}$$

Recall from Section 3.4 that we have  $\text{Cyl}(\rho) = \text{Cone}(\pi_{\mathcal{N}})[-1]$ ,  $\text{Cocyl}(\rho) = \text{Cocone}(\pi_{\mathcal{N}})[1]$ , and  $\mathcal{N} = \pi^*\mathcal{C}_{\Delta}$ .

We first verify that  $\zeta$  is, indeed, a bimodule morphism. Expanding the definition of the cocylinder and writing out  $\zeta : \mathcal{A}_{\Delta}[n-1] \rightarrow \mathcal{N}^{\vee} \oplus \mathcal{M}^{\vee}[-1] \oplus \mathcal{N}^{\vee}[-1]$  componentwise yields

$$\zeta = (\kappa\pi_{\mathcal{N}}, \xi, H)$$

Checking that  $\zeta$  is an  $A_{\infty}$  bimodule morphism comes down to the fact that  $\kappa\pi_{\mathcal{N}}$  is a bimodule morphism in the first component, that  $\xi$  is a bimodule morphism in the second component, and that  $H$  is a homotopy between  $\rho^{\vee}\xi$  and  $\kappa\pi_{\mathcal{N}}$  in the last component.

To finish the proof, we need to show that  $\zeta$  is a quasi-isomorphism. We already know that  $\kappa$  is a quasi-isomorphism, as it is the homotopy inverse of  $\theta$ . For  $\zeta : \mathcal{A}_{\Delta}[n-1] \rightarrow \text{Cocyl}(\rho)$ , we write  $I_{\mathcal{M}^{\vee}}\xi = I_{\mathcal{M}^{\vee}}\Pi_{\mathcal{M}^{\vee}}\zeta$ , where  $I_{\mathcal{M}^{\vee}}$  and  $\Pi_{\mathcal{M}^{\vee}}$  are the naïve inclusion and projection from Lemma 3.17. Since  $I_{\mathcal{M}^{\vee}}\Pi_{\mathcal{M}^{\vee}}$  is homotopic to the identity  $\mathbb{1}_{\text{Cocyl}(\rho)}$ , it follows that  $\zeta$  is homotopic to  $I_{\mathcal{M}^{\vee}}\xi$ . This further implies that  $\eta\Pi_{\mathcal{M}^{\vee}}$  is a homotopy inverse for  $\zeta$ . Hence,  $\zeta$  is a quasi-isomorphism.  $\square$

## 5. PUSHOFFS, REEB CHORDS, AND DISKS

In this section, we examine the geometric models that underlie the main algebraic objects in the paper. The  $n$ -copy of a Legendrian link, described in Section 5.1, will lead to the definition of the augmentation categories  $\mathcal{A}\text{ug}_{\pm}(\Lambda)$  and  $\mathcal{C}$  in Section 6.1. The  $(s, r)$ -copy of the 2-copy of a Legendrian knot, described in Sections 5.2 and 5.3, will lead to the definition of the augmentation bimodules  $\mathcal{M}_{\pm}$  and  $\mathcal{N}$  in Section 6.2. Finally, the  $(s, r)$ -copy of the separated 2-copy of a Legendrian knot, described in Section 5.4, will yield the structures that play a key role in the proof of the main theorem.

For each of these geometric models, we begin by examining the Reeb chords and immersed disks. We then discuss how to identify disks in the copied links with enrichments of disks in the original Lagrangian diagram. These “disk identification lemmas” will be important tools in the proof of the main theorem.

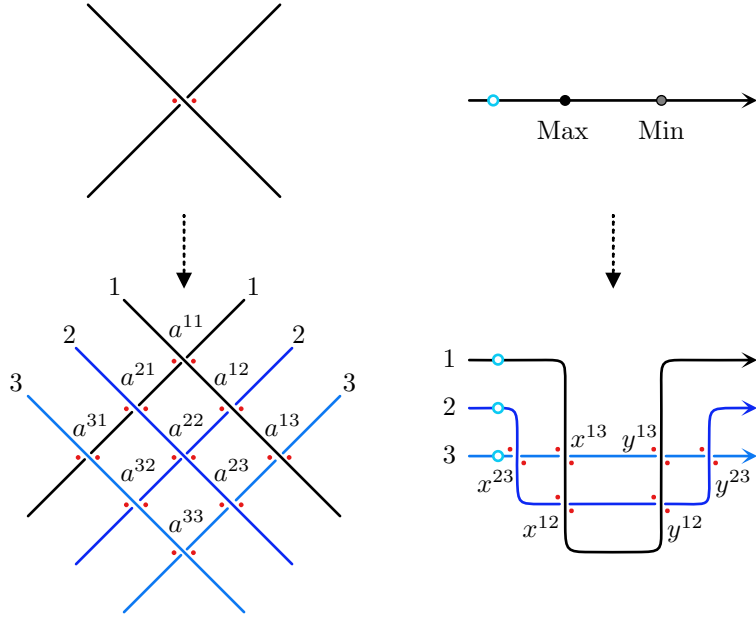


FIGURE 5. (a) For every crossing of  $\Lambda$ , there are  $n^2$  crossings of  $\Lambda^n$ . (b) For every critical point of the perturbing function  $f$ , there are  $\frac{1}{2}n(n - 1)$  crossings of  $\Lambda^n$ .

**5.1. The  $n$ -Copy of a Link.** We begin by setting notation for the Reeb chords of the  $n$ -copy of a Legendrian link, and analyze the behavior of immersed disks in the  $n$ -copy. These constructions will lead to the definition of the augmentation categories in Section 6.

**5.1.1. The  $n$ -Copy Construction.** Given a Legendrian link  $\Lambda$ , we form its  **$n$ -copy**  $\Lambda^n$  by taking  $n$  copies of  $\Lambda$ , pushing each successive copy in the negative Reeb ( $z$ ) direction by a small amount, and then perturbing the results by the 1-jet of a Morse function  $f : \Lambda \rightarrow \mathbb{R}$  in a small Weinstein neighborhood, with an additional perturbation near the critical points of  $f$ ; see Figure 5. The  $n$ -copy depends on the choice of  $f$ , though we do not explicitly include  $f$  in the notation for readability. We assume that  $f$  has a unique maximum and a unique minimum on each component, though the theory in this section may be developed for more general perturbations.

To set notation for the Reeb chords of  $\Lambda^n$ , we label the copies of  $\Lambda^n$  from top to bottom by  $\Lambda_1^n, \dots, \Lambda_n^n$ . There is a natural link grading on  $\Lambda^n$  in which the set of Reeb chords splits into the union of sets  $\mathcal{R}^{ij}$ , each of which consists of Reeb chords that begin on the (lower) component  $\Lambda_j^n$  and end on the (upper) component  $\Lambda_i^n$ , as in Section 2.4.

As shown in Figure 5(a), for every Reeb chord  $a_k$  of  $\Lambda$ , there are  $n^2$  Reeb chords of  $\Lambda^n$ , one in each of the sets  $\mathcal{R}^{ij}$ . We label these chords by  $a_k^{ij} \in \mathcal{R}^{ij}$ .

For every critical point of the perturbing function  $f$ , there are  $\frac{1}{2}n(n - 1)$  Reeb chords of  $\Lambda^n$ , one in each set  $\mathcal{R}^{ij}$  for  $i > j$ ; see Figure 5(b). We denote by  $x_l^{ij}$  the chord in  $\mathcal{R}^{ij}$  at a maximum of  $f$ , and by  $y_l^{ij}$  the chord in  $\mathcal{R}^{ij}$  at a minimum.

Since the  $n$  copies of  $\Lambda^n$  are separated by a small distance in the  $z$  direction, the lengths of the Reeb chords  $x_l^{ij}$  and  $y_l^{ij}$  are much smaller than the lengths of the Reeb chords  $a_k^{ij}$ . Thus, we call the former chords **short chords**, collected in the set  $\mathcal{R}_f$ , and the latter chords **long chords**, which comprise the set  $\mathcal{R}_\Lambda$ . We further divide the short chords into  $\mathcal{R}_x$ , which correspond to the maxima of  $f$ , and  $\mathcal{R}_y$ , which correspond to the minima of  $f$ .

We next place a base point on the original link  $\Lambda$  at each maximum of  $f$ . We then place base points on every copy  $\Lambda_i^n$  of  $\Lambda^n$  preceding (with respect to the orientation of  $\Lambda$ ) the corresponding half twist. Recall from Section 2.4 that these base points correspond to invertible symbols  $(t_l^i)^{\pm 1}$ , with  $\mathcal{T}^i$  denoting the collection of symbols  $(t_l^i)^{\pm 1}$  associated with base points on  $\Lambda_i^n$ . As in Section 2.4, let  $\mathcal{S}^{ij} = \mathcal{R}^{ij} \cup \mathcal{T}^{ij}$ , where  $\mathcal{T}^{ij} = \emptyset$  if  $i \neq j$  and  $\mathcal{T}^i$  otherwise.

The sets of Reeb chords and base points are all *graded* sets, with the gradings coming from [43]:

- invertible generators  $(t_k^i)^{\pm 1}$  have grading  $|t_k^i| = |(t_k^i)^{-1}| = 0$ ;
- long chords  $a_k^{ij}$  have grading  $|a_k^{ij}| = |a_k|$ ;
- maxima  $x_l^{ij}$  have grading  $|x_l^{ij}| = 0$ ; and
- minima  $y_l^{ij}$  have grading  $|y_l^{ij}| = -1$ .

As in Section 2.1, the Chekanov-Eliashberg DGA  $\mathcal{A}^n$  of the  $n$ -copy is generated by  $\bigcup_{i,j} \mathcal{S}^{ij}$ .

**5.1.2. Disks in the  $n$ -Copy.** The disks that define the differential of the Chekanov-Eliashberg DGA of an  $n$ -copy  $\Lambda^n$  may be identified with “thin” disks that collapse into  $\pi_{xy}(\Lambda)$  and “thick” disks that correspond to disks that define the Chekanov-Eliashberg differential of  $\Lambda$ . This idea goes back to [45] and the original proof of duality for linearized LCH [47], with further developments most relevant to this paper in [43]. The notation and work needed for this identification serves as a model for later, more subtle, disk identification lemmas that will be essential for the proof of the main theorem in Section 7.

To enable translation between chords in the  $n$ -copy and chords in the original Legendrian, we introduce the **stick-together map**  $s : \mathbb{R}^2 \rightarrow \mathbb{R}^2$ , which retracts the Lagrangian diagram of  $\Lambda^n$  onto the diagram of  $\Lambda$ . The stick-together map induces the **algebraic projection** map  $\check{\alpha} : \mathcal{A}^n \rightarrow \mathcal{A}$ , which is defined on the generators as follows:

- A Reeb chord in  $\mathcal{R}_\Lambda$  is mapped to the associated Reeb chord in  $\mathcal{R}$ .
- A Reeb chord in  $\mathcal{R}_f$  is mapped to 1.
- A base point in  $\mathcal{T}^i$  is mapped to the associated base point in  $\mathcal{T}$ .

See Figure 5 once again. For compactness of notation, we will, at times, denote the image of  $a \in \mathcal{A}^n$  under  $\check{\alpha}$  by  $\check{a}$ . In particular, we have  $\check{a}_k^{ij} = a_k$  and  $\check{x}_l^{ij} = 1 = \check{y}_l^{ij}$ .

The stick-together map divides the disks that define the differential in the  $n$ -copy into two types. A disk  $u \in \Delta_{\Lambda^n}(a, \mathbf{a})$  is **thick** if  $s \circ u$  is still immersed. In contrast, a disk  $u \in \Delta_{\Lambda^n}(a, \mathbf{a})$  is **thin** if the image of  $s \circ u$  lies entirely inside  $\pi_{xy}(\Lambda)$ . A geometric argument using the convexity of the corners of disks in  $\Delta_{\Lambda^n}$  and Figure 5, or an examination of the formulae of [43, Proposition 4.14] shows that thick and thin disks are the only two possibilities.

Before analyzing thick and thin disks more precisely, we need to introduce some notation. Given a choice of  $n - 1$  indices  $1 \leq i_1 < \dots < i_{n-1} \leq N$ , we write the word  $\mathbf{a} = a_1 \cdots a_N$  as

$$(5.1) \quad \mathbf{a} = \mathbf{a}_1 a_{i_1} \mathbf{a}_2 a_{i_2} \mathbf{a}_3 \cdots \mathbf{a}_{n-1} a_{i_{n-1}} \mathbf{a}_n.$$

This word could come from the generators for a single Legendrian, or could come from the generators for an  $n$ -copy. When working with words in  $\mathcal{A}^n$ , we say that a pair  $(a, \mathbf{a})$  is in **positive  $n$ -copy form** with respect to the indices  $\{i_1, \dots, i_{n-1}\}$  if

- $a \in \mathcal{R}^{1,n}$ ,
- $a_{i_k} \in \mathcal{R}^{k,k+1}$ , and
- $\mathbf{a}_k$  a word in the alphabet  $\mathcal{S}^{kk}$ .

Similarly, the pair  $(a, \mathbf{a})$  is in **negative  $n$ -copy form** if  $a \in \mathcal{R}^{n,1}$ ,  $a_{i_k} \in \mathcal{R}^{n-k+1,n-k}$ , and  $\mathbf{a}_k$  a word in the alphabet  $\mathcal{S}^{n-k+1,n-k+1}$ .

We turn to describing the thin disks. Propositions 4.14 and 4.26 of [43] or an examination of Figure 6 yield the following characterization of thin disks. Note that the formula is simplified — as in Proposition 4.26 of [43] — by the assumption that  $\Lambda^n$  is **simply perturbed**. Namely,  $\Lambda^n$  is perturbed by a Morse function  $f : \Lambda \rightarrow \mathbb{R}$  with one maximum and one minimum on each component that are adjacent in the Lagrangian diagram of  $\Lambda$ , preceded (with respect to the orientation of  $\Lambda$ ) by the unique base point on  $\Lambda$ .

**Lemma 5.1** ( $n$ -Copy Thin Disk Identification). *Suppose  $\Lambda^n$  is simply perturbed and that  $(a, \mathbf{a})$  is in positive  $n$ -copy form. The set  $\Delta_{\Lambda^n}(a, \mathbf{a})$  consists of thin disks precisely when  $(a, \mathbf{a})$  is in one of the following forms; see Figure 6. We suppress the indices of the  $x$ ,  $y$ , and  $t$  generators for readability.*

**Flowlines:**

$$\begin{array}{ll} (x^{12}, y^{12}) & (x^{12}, t^{-1}y^{12}t) \\ (x^{13}, x^{12}y^{23}) & (x^{13}, t^{-1}y^{12}tx^{23}) \end{array}$$

**Partial Flowlines:**

$$\begin{array}{ll} (a^{12}, y^{12}a^{22}) & (a^{13}, y^{12}a^{23}) \\ (a^{12}, a^{11}y^{12}) & (a^{13}, a^{12}y^{23}) \end{array}$$

**Constant Flowlines:**  $(y^{13}, y^{12}y^{23})$

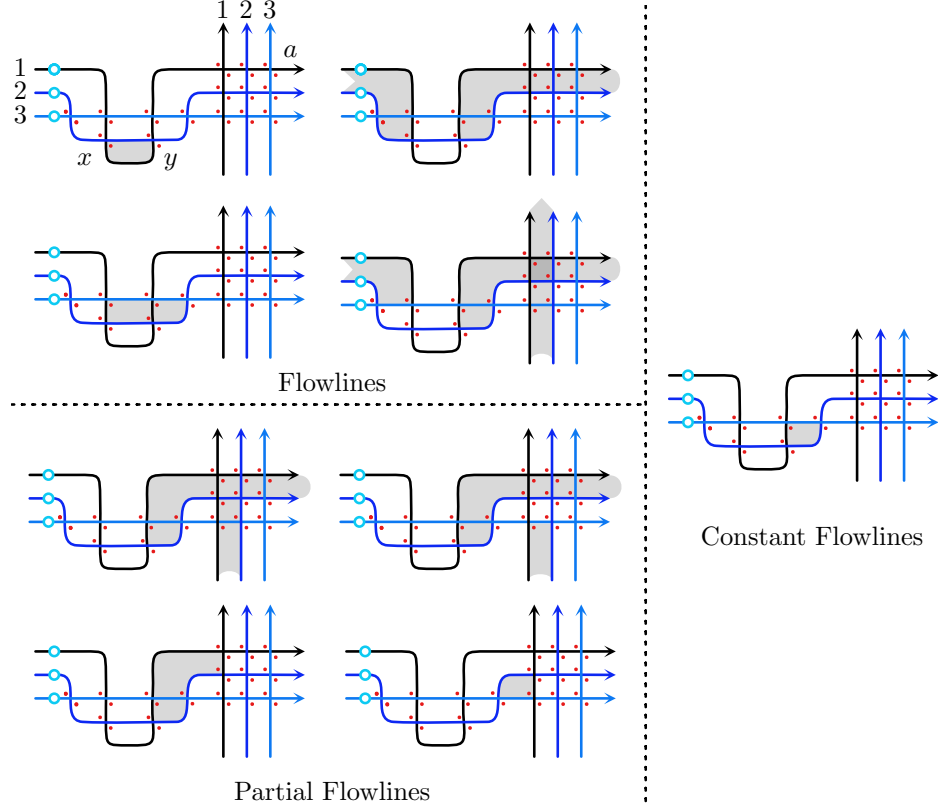


FIGURE 6. The thin disks in the  $n$ -copy of a Legendrian link take one of these forms, as listed in Lemma 5.1. We will use the red dots to indicate crossing information in this and subsequent figures that display disks in Lagrangian diagrams.

In particular, a disk in  $\Delta_{\Lambda^n}(a, \mathbf{a})$  is thin if and only if  $\mathbf{a}$  contains a  $y$  generator.

If  $(a, \mathbf{a})$  is in negative  $n$ -copy form, then no disk in  $\Delta_{\Lambda^n}(a, \mathbf{a})$  is thin.

We next describe thick disks, building on the definition of  $\Delta_{\Lambda}(a, \mathbf{a})$ .

**Definition 5.2.** An  $m$ -enriched disk is a pair  $(u, \mathbf{w})$  consisting of a disk  $u \in \Delta_{\Lambda}(a, \mathbf{a} = a_1 \cdots a_N)$  and a multiset of indices  $\mathbf{w}$  of total multiplicity  $m$  whose elements are from  $\{1, \dots, N\}$ , where an element  $i$  may have multiplicity greater than 1 only if  $a_i \in \mathcal{T}_-$ . The set of  $m$ -enriched disks with corners  $(a, \mathbf{a})$ , up to smooth reparametrization, is denoted  $\Delta_{\Lambda}^m(a, \mathbf{a})$ .

Enriched disks allow us to identify thick disks in the diagram of the  $n$ -copy with objects in the diagram of original knot, as shown in Figure 7. One direction of such an identification involves the stick-together map. Given  $u \in \Delta_{\Lambda^n}(a, \mathbf{a})$ , with  $(a, \mathbf{a})$  in positive  $n$ -copy form as in Equation (5.1), let  $s \circ u$  be the stick-together disk in the Lagrangian diagram of  $\Lambda$ . We describe

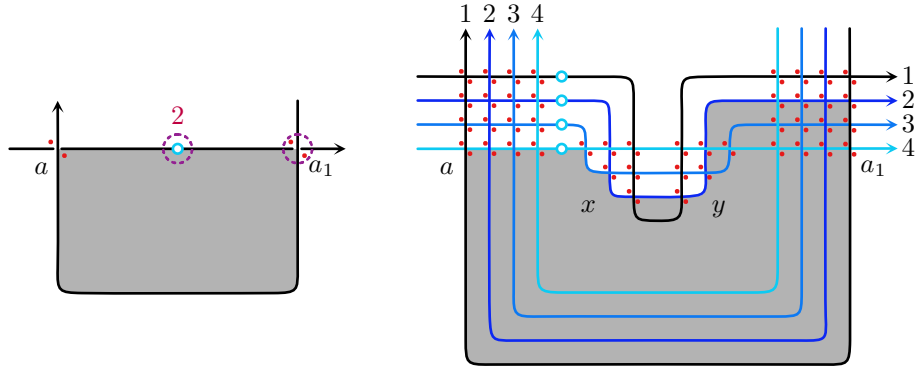


FIGURE 7. The disk at left is an enriched disk in  $\Delta_{\Lambda}^3(a, a_1 t^{-1})$  with  $\mathbf{w} = \{1, 2, 2\}$ . The disk at right is its lift to a disk in  $\Delta_{\Lambda^4}(a^{14}, a_1^{12} x^{23} x^{34}(t^4)^{-1})$ , following Lemma 5.3.

how  $s \circ u$  induces an enriched disk  $(\check{u}, \mathbf{w}(u))$  in  $\Delta_{\Lambda}^{n-1}(\check{a}, \check{\mathbf{a}})$ , with enrichment  $\mathbf{w}(u)$  to be determined, called the **projection** of  $u$ .

If a convex corner of  $u$  is labeled with  $a \in \mathcal{R}_{\Lambda}$ , then an examination of the configuration of crossings in Figure 5 shows that  $s \circ u$  has a convex corner labeled by  $\check{a} \in \mathcal{R}$  decorated with the same sign as  $a \in \mathcal{R}_{\Lambda}$ ; we enrich  $\check{u}$  by adding the position of  $\check{a}$  in  $\check{\mathbf{a}}$  to  $\mathbf{w}(u)$  if  $a$  is one of the  $a_{i_k}$ , but not if  $a$  is in one of the  $\mathbf{a}_i$ . Similarly, if the boundary of  $u$  passes through a basepoint  $t^{\pm 1} \in \mathcal{T}^i$ , then  $s \circ u$  passes through the corresponding basepoint  $\check{t}^{\pm 1}$ ; we do not yet enrich these marked points.

We are left to understand the relationship between  $u$  and  $s \circ u$  near negative corners of  $u$  at maxima  $x \in \mathcal{R}_x^{i,i+1}$ . Since  $\check{x} = 1$ , we record the corner of  $u$  at  $x$  in  $\check{u}$  by enriching the position in  $\check{\mathbf{a}}$  of the associated basepoint (which necessarily appears in  $\mathbf{a}$ ). As can be seen in Figure 5, if the orientations of  $\Lambda^n$  and the boundary of  $u$  agree at  $x$ , then at most one  $x$  can serve as a negative corner; this corresponds to the associated marked point being enriched once. On the other hand, if the orientations disagree, then multiple generators  $x$  can serve as negative corners, and the position of the marked point may be enriched multiple times. See Figure 7 for an example. This completes the description of the enriched disk  $\check{u}$ .

Conversely, we may also describe a (**geometric**) **lift** of an enriched disk  $(v, \{m_1 i_1, \dots, m_l i_l\}) \in \Delta_{\Lambda}^{n-1}(a, \mathbf{a})$  to a thick disk in the  $n$ -copy. It suffices to specify the corners of the lift  $\hat{v}$  of  $v$  in  $\Lambda^n$ , as this will also specify the lift of the boundary. We start by lifting  $a$  to  $a^{1n}$ . For each  $k \in \{1, \dots, l\}$ , let  $r_k = \sum_{j=1}^k m_j$ . We lift an enriched Reeb chord  $a_{i_k}$  to  $a_{i_k}^{r_k, r_k+1}$ . Similarly, we lift an enriched marked point  $t_{i_k}^{\pm 1}$  with multiplicity  $m_k$  to  $m_k$  corners between strands  $r_{k-1} + 1$  and  $r_{k-1} + 2$  up to corners between strands  $r_k$  and  $r_k + 1$  at the nearby maxima, preceded by the marked point  $t_{i_k}^{r_{k-1}+1}$  or

succeeded by  $\left(t_{i_k}^{r_k+1}\right)^{-1}$ . Note that these additional corners at the maxima add  $m_k$  to the strand number, and hence the instructions for non-enriched generators and subsequent enriched corners or marked points are consistent. Further, we add corners for all non-enriched generators in  $\mathbf{a}_i$  to the corresponding self-crossings (or marked points) in  $\mathcal{S}^{r_{i-1}r_i-1}$ . An examination of the configuration of crossings in Figure 5 shows that the lifted corners yield an immersed disk in  $\pi_{xy}(\Lambda^{n+1})$  with one positive corner at  $a^{1^n}$ . Again, see Figure 7 for an example of this process.

It is straightforward to check that the lifting process  $v \mapsto \hat{v}$  inverts the projection process  $u \mapsto \check{u}$  and vice versa. A similar projection / lifting framework works for disks in negative  $n$ -copy form, though this time, there are no corners at maxima in the  $n$ -copy, and no enrichments at the marked points for the enriched disks. We summarize these findings in the following lemma.

**Lemma 5.3** ( $n$ -Copy Thick Disk Identification). *Suppose  $(a, \mathbf{a})$  is in positive  $n$ -copy form with no generators at the minima of  $f$ . There is a bijective correspondence between thick disks  $u \in \Delta_{\Lambda^n}(a, \mathbf{a})$  and  $(n-1)$ -enriched disks  $(s \circ u, \mathbf{w}(u))$  in  $\Delta_{\Lambda}^{n-1}(\check{a}, \check{\mathbf{a}})$ . An identical statement holds when  $(a, \mathbf{a})$  is in negative  $n$ -copy form.*

*Remark 5.4.* The strands of the  $n$ -copy traversed by the boundary of the disk need not be consecutive. That is, the lemma holds for indices  $1 \leq j_1 < \dots < j_{k+1} \leq n$ , with  $a \in \mathcal{R}_{\Lambda}^{j_1, j_{k+1}}$  and  $\mathbf{a}$  a word in the alphabet  $\mathcal{S}^n$  with  $a_{i_k} \in \mathcal{R}^{j_k, j_{k+1}}$  and  $\mathbf{a}_k$  a word in the alphabet  $\mathcal{S}^{j_k, j_k}$  with no generators at the minima of  $f$ . The proof is the same as the one above, with somewhat more work when taking care of indices. Such a characterization is useful for directly checking  $A_\infty$  relations, but will not be discussed further in this paper.

**5.2. The  $(s,r)$ -Copy of a Link.** Our next step in setting the geometric underpinnings of the augmentation categories and their associated bimodules is to understand the  $(s, r)$ -copy of an ordered two-component Legendrian link. This construction involves taking the  $s$ -copy of one component and the  $r$ -copy of the other. Of particular interest are the  $(s, r)$ -copies of the 2-copy of a Legendrian knot and of the separated 2-copy of a Legendrian knot, both of which will be examined in greater detail in subsequent subsections.

**5.2.1. The  $(s,r)$ -Copy Construction.** We begin by refining the link grading notation of Section 2.4 in the presence of a pair of link gradings. Given an ordered 2-component Legendrian link  $\Lambda = \Lambda_1 \sqcup \Lambda_2$  with the canonical 2-component link grading  $O \times \Upsilon$ , we denote the  $(s, r)$ -**copy** link formed by the  $s$ -copy of the first component (with perturbation function  $f_1$ ) and the  $r$ -copy of the second component (with perturbation function  $f_2$ ) by  $\Lambda^{s,r}$ . Note that the ordering of the components of  $\Lambda$  matters.

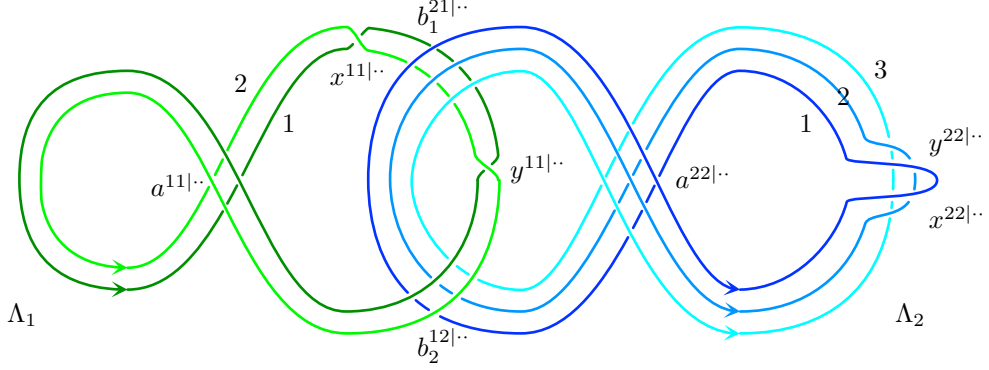


FIGURE 8. A Lagrangian diagram of the  $(2,3)$ -copy  $\Lambda^{2,3}$  of a 2-component link  $\Lambda$ .

Label the components of the  $s$ -copy from bottom to top and those of the  $r$ -copy from top to bottom. Finally, place base points on  $\Lambda^{s,r}$  just before the maxima of the functions  $f_i$ , as in the case of an  $n$ -copy. Note that there could be crossings between copies of  $\Lambda_1$  and  $\Lambda_2$  between the maximum and minimum of the perturbation functions. See Figure 8.

There is a  $\max(s,r)$ -component link grading  $o \times v$  on  $\Lambda^{s,r}$  so that, along with  $O \times \Upsilon$ , the Reeb chords of  $\Lambda^{s,r}$  split into the union of the sets  $\mathcal{R}^{ij|kl}$  which consists of Reeb chords that start on the  $l^{\text{th}}$  component of the  $r$ -copy of the  $j^{\text{th}}$  component of  $\Lambda$  and end on the  $k^{\text{th}}$  component of the  $s$ -copy of the  $i^{\text{th}}$  component of  $\Lambda$ . We denote generators in  $\mathcal{R}^{ij|kl}$  by  $a^{ij|kl}$  when convenient. Similarly, the link gradings  $O \times \Upsilon$  and  $o \times v$  also split the marked points of  $\Lambda^{s,r}$  into sets  $\mathcal{T}^{i|k}$ , and we denote a generator therein by  $t^{i|k}$ . As usual, we also define  $\mathcal{S}^{ij|kl} = \mathcal{R}^{ij|kl} \cup \mathcal{T}^{ij|kl}$ , with  $\mathcal{T}^{ij|kl} = \emptyset$  if  $i \neq j$  or  $k \neq l$ . Call the elements of  $\mathcal{R}^{ij|kl}$  with  $i \neq j$  **mixed**, and those with  $i = j$  **pure**.

We extend the algebraic projection map  $\check{\alpha}$  to the  $(s,r)$ -copy setting as a map the Chekanov-Eliashberg DGA of  $\Lambda^{s,r}$  to that of  $\Lambda$  induced from the stick-together map. On the generators, we define

$$\begin{aligned}\check{\alpha}(a^{ij|kl}) &= \check{a}^{ij|kl} = a^{ij} \\ \check{\alpha}(t^{i|k}) &= \check{t}^{i|k} = t^i\end{aligned}$$

Thick and thin disks in  $\Lambda^{s,r}$  are defined as in Section 5.1.

**5.2.2. Disks in the  $(s,r)$ -Copy.** The analysis of thin and thick disks for the  $(s,r)$ -copy of a Legendrian link is similar to that for the  $n$ -copy, though the notation is more involved. Given a choice of  $s-1$  indices  $1 \leq i_1 < \dots < i_{s-1} \leq M$  and  $r-1$  indices  $1 \leq j_1 < \dots < j_{r-1} \leq N$ , we write the word  $\underline{\mathbf{a}}w\underline{\mathbf{b}} = a_M \dots a_1 w b_1 \dots b_N$  as

$$(5.2) \quad \underline{\mathbf{a}}w\underline{\mathbf{b}} = \mathbf{a}_s a_{i_{s-1}} \mathbf{a}_{s-1} \dots \mathbf{a}_2 a_{i_1} \mathbf{a}_1 w \mathbf{b}_1 b_{j_1} \mathbf{b}_2 \dots \mathbf{b}_{r-1} b_{j_{r-1}} \mathbf{b}_r.$$

We say that the position index of  $w$  is 0. As before, the word could come from the generators for a single Legendrian link, or from the generators for

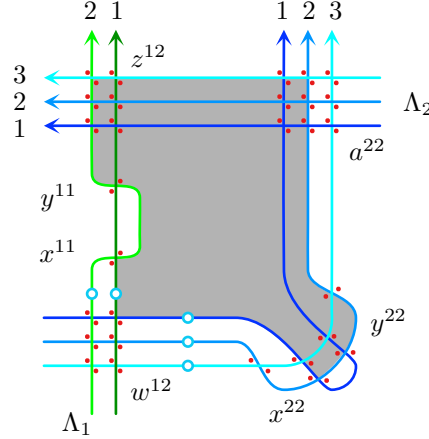


FIGURE 9. A thick disk in  $(s, r)$ -copy form in the set  $\Delta_{\Lambda}(\underline{z}^{12|23}, x^{11|21}(t^{1|1})^{-1}\underline{w}^{12|11}t^{2|1}x^{22|22}a^{22|23})$ .

the  $(s, r)$ -copy. When working with the  $(s, r)$ -copy, we say a pair  $(\underline{z}, \mathbf{awb})$  is in **(s,r)-copy form** if

- $z \in \mathcal{R}^{12|sr}$ ,
- $w \in \mathcal{R}^{12|11}$ ,
- $a_{ik} \in \mathcal{R}^{11|k+1,k}$  and  $\mathbf{a}_k$  are words in the alphabet  $\mathcal{S}^{11|kk}$ , and
- $b_{jk} \in \mathcal{R}^{22|k,k+1}$  and  $\mathbf{b}_k$  are words in the alphabet  $\mathcal{S}^{22|kk}$ .

We underline  $z$  and  $w$  in the pair to emphasize the location of the mixed chords, i.e. chords in  $\mathcal{S}^{ij|kl}$  for  $i \neq j$ . Note that all generators in  $\mathbf{a}$  come from chords or basepoints of  $\Lambda_1$ , while all generators in  $\mathbf{b}$  come from  $\Lambda_2$ . As can be seen in Figure 9, disks in  $\Delta_{\Lambda^{s,r}}(\underline{z}, \mathbf{awb})$  have a positive corner at a mixed chord  $z$ , a negative corner at a mixed chord  $w$  sandwiched by a collection of negative corners lying in  $\Lambda_1^s$ ,  $s - 1$  of which are mixed relative to  $\Lambda_1^r$ , and a similar collection for  $\Lambda_2^r$ .

Rather than identifying thin and thick disks at this stage using flowlines and enriched disks, we shall describe the process in detail only when the link in question is the 2-copy and separated 2-copy of a Legendrian knot. That said, there is no obstruction to working with enriched disks for Legendrian links.

**5.3. The 2-Copy.** Two special cases of the  $(s, r)$ -copy construction will be important for the definition and analysis of the “augmentation bimodules” in Section 6. The first arises when the underlying link is the 2-copy of a Legendrian knot  $\Lambda$ , ordered either from top to bottom (we call this the **2-copy**  $\bar{\Lambda}$ ) or bottom to top (the **opposite 2-copy**  $\underline{\Lambda}$ ). The second special case, which we will encounter in the next subsection, involves separating the two copies by a large distance in the  $z$  direction. In both cases, there is an additional “stick-together” map from the two-component link to a

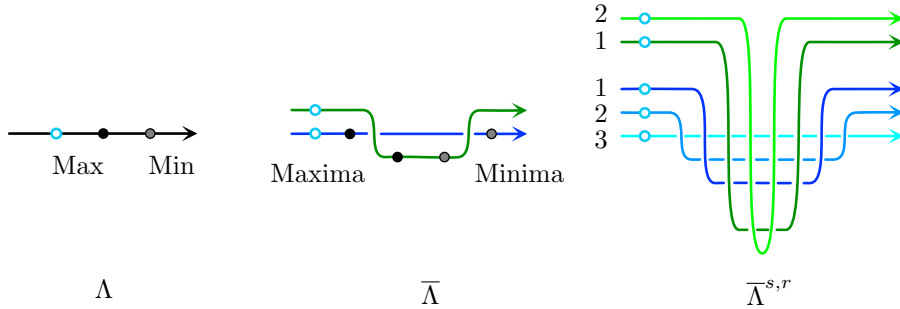


FIGURE 10. The construction of a simply perturbed  $(s, r)$ -copy of the 2-copy near the critical points.

Legendrian knot, allowing us to identify disks in the  $(s, r)$ -copy with disks in the *knot*, not just the 2-copy *link*.

**5.3.1. The 2-Copy Construction.** For each crossing  $a$  of  $\Lambda$ , there are four types of crossings in the  $(s, r)$ -copy of the 2-copy  $\bar{\Lambda} = \bar{\Lambda}_1 \sqcup \bar{\Lambda}_2$ : those of the form  $a^{12|kl}$  (which, again, we call mixed chords), those of the form  $a^{21|kl}$  (which we will ignore), those of the form  $a^{11|kl}$ , and those of the form  $a^{22|kl}$  (both of which we refer to as pure chords). Similarly, there are two kinds of crossings induced by critical points: those produced by perturbing the original 2-copy of  $\Lambda$  and those produced by perturbing the  $(s, r)$ -copy of  $\bar{\Lambda}$ . The former type yields mixed Reeb chords in  $\bar{\mathcal{R}}^{12|kl}$  (for any  $i, j$ ) and the latter type yields pure Reeb chords in  $\bar{\mathcal{R}}^{11|kl}$  (for  $l < k$ ) and  $\bar{\mathcal{R}}^{22|kl}$  (for  $k < l$ ). We denote both types by  $x$  and  $y$ .

From this point on, we assume that  $\bar{\Lambda}$  is simply perturbed and its  $(s, r)$ -copy is perturbed by a pair of Morse functions with the maxima and minima placed as shown in Figure 10. We call this a **simply perturbed  $(s, r)$ -copy of  $\bar{\Lambda}$** . In this configuration, the combinatorics of the Lagrangian diagram of  $\bar{\Lambda}^{s,r}$  matches that of the diagram of a simply perturbed  $\Lambda^{s+r}$ , up to relabeling.

The description of the Reeb chords for the opposite 2-copy  $\underline{\Lambda}$  is similar, though the critical points of the perturbing function induce generators in  $\underline{\mathcal{R}}^{21|kl}$  rather than  $\mathcal{R}^{12|kl}$ . This is because in the opposite 2-copy, the bottom copy is labeled 1, and there are no Reeb chords that go from the top to the bottom copy at a critical point.

**5.3.2. Disks in the 2-Copy.** Since either 2-copy can be further retracted onto the original knot, disks in  $\bar{\Lambda}^{s,r}$  and  $\underline{\Lambda}^{s,r}$  can be classified thin or thick with respect to the original Legendrian  $\Lambda$ . As before, we can classify thin and thick disks in the  $(s, r)$ -copy of the two 2-copies.

**Lemma 5.5** (2-copy Thin Disk Identification). *Suppose  $(\underline{z}, \mathbf{awb})$  is in  $(s, r)$ -copy form for  $\bar{\Lambda}$ . The set of disks  $\Delta_{\bar{\Lambda}^{s,r}}(\underline{z}, \mathbf{awb})$  consists of thin disks precisely when  $(\underline{z}, \mathbf{awb})$  is in one of the following forms:*

**Flowlines:**

$$\begin{aligned}
 (5.3a) \quad & (\underline{x}^{12|11}, t^{-1}\underline{y}^{12|11}t) & (\underline{x}^{12|11}, \underline{y}^{12|11}) \\
 (5.3b) \quad & (\underline{x}^{12|21}, t^{-1}y^{11|21}t\underline{x}^{12|11}) & (\underline{x}^{12|12}, \underline{x}^{12|11}y^{22|12}) \\
 (5.3c) \quad & (\underline{x}^{12|12}, t^{-1}\underline{y}^{12|11}x^{12|11}) & (\underline{x}^{12|21}, x^{11|21}\underline{y}^{12|11}).
 \end{aligned}$$

**Partial Flowlines:**

$$\begin{aligned}
 (5.4a) \quad & (\underline{a}^{12|12}, \underline{a}^{12|11}y^{22|12}) & (\underline{a}^{12|21}, y^{11|21}\underline{a}^{12|11}) \\
 (5.4b) \quad & (\underline{a}^{12|11}, a^{11|11}\underline{y}^{12|11}) & (\underline{a}^{12|11}, \underline{y}^{12|11}a^{22|11}) \\
 (5.4c) \quad & (\underline{a}^{12|21}, a^{11|21}\underline{y}^{12|11}) & (\underline{a}^{12|12}, \underline{y}^{12|11}a^{22|12}).
 \end{aligned}$$

**Constant Flowlines:**  $(\underline{y}^{12|21}, y^{11|21}\underline{y}^{12|11})$  or  $(\underline{y}^{12|12}, \underline{y}^{12|11}y^{22|12})$ .

In particular, a disk in  $\Delta_{\bar{\Lambda}^{s,r}}(\underline{z}, \mathbf{awb})$  is thin with respect to  $\Lambda$  if and only if  $\mathbf{a}$ ,  $w$ , or  $\mathbf{b}$  contains a  $y$  generator.

Similarly, the moduli spaces consist of thin disks in one of the following forms, both of which are partial flowlines:

$$(\underline{a}^{12|12}, \underline{a}^{12|11}y^{22|12}), \quad (\underline{a}^{12|21}, y^{11|21}\underline{a}^{12|11}).$$

In particular, if  $(\underline{z}, \mathbf{awb})$  is in  $(s, r)$ -copy form for  $\Lambda$ , a disk in  $\Delta_{\bar{\Lambda}^{s,r}}(\underline{z}, \mathbf{awb})$  is thin with respect to  $\Lambda$  if and only if  $\mathbf{a}$  or  $\mathbf{b}$  contains a  $y$  generator.

The proof of the lemma comes down to direct combinatorial enumeration, half of which is carried out in Figure 11.

*Remark 5.6.* Notice that there are more thin disks for the  $(s, r)$ -copy of  $\bar{\Lambda}$  than for the  $n$ -copy. A thin disk in the  $n$ -copy with more than one negative corner corresponds to two thin disks in the  $(s, r)$ -copy of  $\bar{\Lambda}$ , depending on which of the two corners are pure and which are mixed. These will contribute to the  $A_\infty$  bimodule maps in different ways in Section 6.

Next, we use enriched disks to identify the thick disks in an  $(s, r)$ -copy of the 2-copy with disks in the original Legendrian. First, we need to slightly generalize the notion of an enriched disk to incorporate enrichments on each component. Recall the notation in Equation (5.2) for  $\mathbf{awb}$ .

**Definition 5.7.** An  $(m, n)$ -doubly enriched disk is a triple  $(u, \mathbf{w}_1, \mathbf{w}_2)$  consisting of a disk  $u \in \Delta_\Lambda(\underline{z}, \mathbf{awb})$  with  $w \in \mathcal{R} \cup \mathcal{T}$  and two multisets of indices  $\mathbf{w}_1$  and  $\mathbf{w}_2$ , termed the **pure enrichments**, so that

- $\mathbf{w}_1$  has total multiplicity  $m$  and draws elements from  $\{0, \dots, M\}$ , while
- $\mathbf{w}_2$  has total multiplicity  $n$  and draws elements from  $\{0, \dots, N\}$ .

The index 0 of  $\underline{w}$  carries an additional enrichment with multiplicity 1; we term this the **mixed enrichment**. An index  $i$  may have multiplicity greater than 1 in  $\mathbf{w}_j$  only if the corresponding generator is  $t^{-1}$ .

The set of  $(m, n)$ -enriched disks with corners  $(\underline{z}, \mathbf{awb})$  is denoted by  $\Delta_\Lambda^{m,n}(\underline{z}, \mathbf{awb})$ .

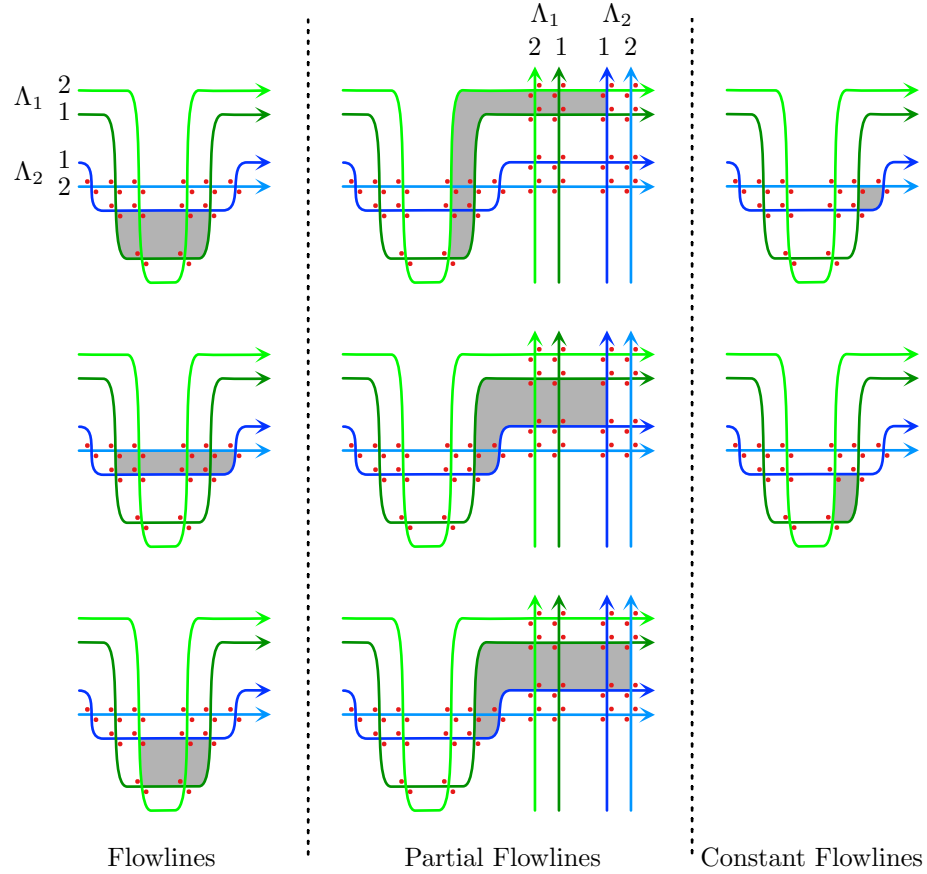


FIGURE 11. The thin disks in the 2-copy listed in the second column of Lemma 5.5. The disks listed in the first column are similar, but pass around larger portions of the knot as in Figure 6.

Before describing the projection and lifting operations, we modify how the algebraic projection map on a word in  $(s, r)$ -copy form for the 2-copy interacts with the splitting of the word into **a**, w, and **b**. Examining the word  $\check{\mathbf{a}}\check{w}\check{\mathbf{b}}$ , we see that if  $w$  arises from a Reeb chord of  $\Lambda$ , then the stuck-together word has the same tripartite structure as the original word. On the other hand, if  $w = x^{12|11}$ , then  $\check{\mathbf{a}}\check{w}\check{\mathbf{b}}$  no longer appears to have an underlined generator. In this case, a word arising from an immersed disk in  $(s, r)$ -copy form must either have a  $t$  at the end of  $\mathbf{a}$  or  $t^{-1}$  at the beginning of  $\mathbf{b}$ . We simply remove that  $t^{\pm 1}$  from one of the side words and underline it.

In parallel to Section 5.1.2, we describe how to project a thick disk  $u$  in  $(s, r)$ -copy form for  $\bar{\Lambda}$  to a doubly enriched disk for  $\Lambda$ . We first apply the stick-together map twice, once to pass from  $\bar{\Lambda}^{s,r}$  to  $\bar{\Lambda}$ , and again to reach  $\Lambda$ . Composition with this double stick-together map yields an immersed disk with convex corners in  $\Lambda$ . As before, we need only understand the

enrichment process. The pure enrichments  $\mathbf{w}_1(u)$  and  $\mathbf{w}_2(u)$  come from the positions of the  $a_{i_k}$  in  $\mathbf{a}$  and  $b_{j_l}$  in  $\mathbf{b}$ , while the mixed enrichment is at the central position 0; see Figure 12. One further adjustment may be necessary: if the underlined generator of  $\check{\alpha}(\underline{\mathbf{a}}\underline{\mathbf{w}}\mathbf{b})$  is  $t^{-1}$ , as in Figure 13, then we also enrich the position 0 in  $\mathbf{w}_1$  with the number of  $x^{11|\cdot}$  generators that precede  $\underline{w}$  in  $\underline{\mathbf{a}}\underline{\mathbf{w}}\mathbf{b}$  and enrich the position 0 in  $\mathbf{w}_2$  with the number of  $x^{22|\cdot}$  generators that succeed  $\underline{w}$ .

Lifting a doubly enriched disk  $(u, \mathbf{w}_1, \mathbf{w}_2)$  to the  $(s, r)$ -copy of  $\bar{\Lambda}$  is a straightforward generalization of lifting an enriched disk to the  $n$ -copy. As before, positions that are purely enriched in  $\mathbf{w}_i$  lift to Reeb chords of the  $s$ - or  $r$ -copy of  $\bar{\Lambda}_i$ . The mixed enriched position lifts to  $w^{12|11}$  if  $w \in \mathcal{R}$ , and to  $x^{12|11}$  if  $w = t^{\pm 1}$ . Note that if 0 is enriched in either  $\mathbf{w}_1$  or  $\mathbf{w}_2$ , then the lifting process will yield  $x$  chords on either side of  $x^{12|11}$ .

As before, it is straightforward to check that the projection and enrichment processes are inverses of each other, and we obtain the following lemma.

**Lemma 5.8** (2-copy Thick Disk Identification). *Suppose  $(\underline{z}, \underline{\mathbf{a}}\underline{\mathbf{w}}\mathbf{b})$  is in  $(s, r)$ -copy form for either  $\bar{\Lambda}$  or  $\underline{\Lambda}$  without any generator at a minimum of a perturbing function. There is a bijective correspondence between thick disks  $u \in \Delta_{\bar{\Lambda}^{s,r}}(\underline{z}, \underline{\mathbf{a}}\underline{\mathbf{w}}\mathbf{b})$  and doubly enriched disks  $(s \circ u, \mathbf{w}_1(u), \mathbf{w}_2(u)) \in \Delta_{\Lambda}^{s,r}(\check{z}, \check{\mathbf{a}}\check{\mathbf{w}}\check{\mathbf{b}})$ , where 0 has pure enrichments only if the mixed enrichment is at  $t^{-1}$ . The same holds true for the opposite 2-copy, though without any complications coming from  $w = x^{12|11}$ .*

We emphasize that for the 2-copy, the Reeb chords  $z$  and  $w$  start at the bottom copy and end at the top copy, while the opposite holds for the opposite 2-copy, even though the notation for the chords is forced to be identical.

**5.4. The Separated 2-Copy.** The second important special case of the  $(s, r)$ -copy construction occurs when the underlying link is the the *separated* 2-copy of a Legendrian knot  $\Lambda$ .

**5.4.1. The Separated 2-Copy Construction.** Given a Legendrian link  $\Lambda$ , we form its **separated 2-copy**  $\hat{\Lambda}$  by taking the 2-copy  $\bar{\Lambda}$  and pushing the bottom copy in the negative Reeb ( $z$ ) direction by a distance  $Z$  larger than the maximum length of the Reeb chords of  $\Lambda$ . See Figure 14, which should be compared and contrasted with the standard 2-copy in Figure 5. We distinguish the Chekanov-Eliashberg DGA of  $\hat{\Lambda}$  with that of the standard 2-copy  $\bar{\Lambda}$  by decorating related notation with a hat.

For  $i = 1, 2$ , pure chords and base points in  $\hat{\mathcal{S}}^{ii}$  are in bijection with Reeb chords and base points of the original Legendrian  $\Lambda$ , and thus in bijection with pure chords and base points  $\bar{\mathcal{S}}^{ii}$  of  $\bar{\Lambda}$ . We label such chords by  $a^{ii|kl}$  or  $t^{i|k}$ . All mixed chords in the separated 2-copy begin on the component  $\hat{\Lambda}_2$  and end on  $\hat{\Lambda}_1$ . That is, all mixed chords lie in  $\hat{\mathcal{R}}^{12}$ , and  $\hat{\mathcal{R}}^{21} = \emptyset$ . Following [47], we split chords of the separated 2-copy into two classes based

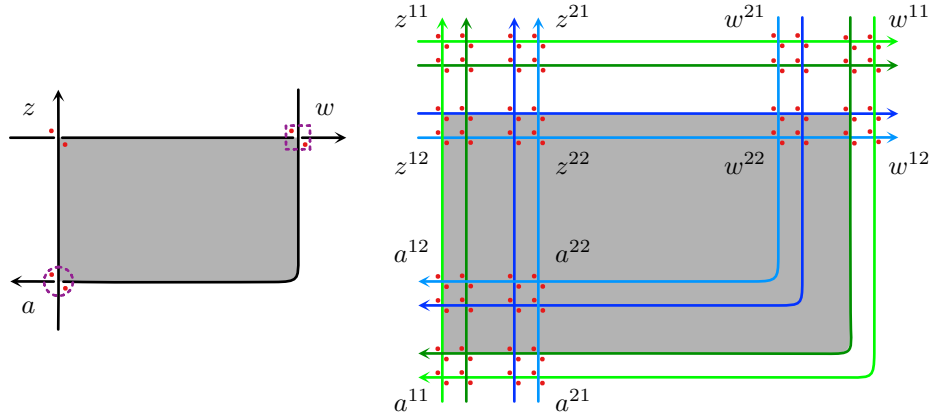


FIGURE 12. The disk at left is an enriched disk in  $\Delta_{\Lambda}^2(z, aw)$  with pure enrichments  $w_1 = \{1\}$  and  $w_2 = \emptyset$ . The disk at right is its lift to a disk in  $\Delta_{\bar{\Lambda}^{2,2}}(\underline{z}^{12|21}, a^{11|21}\underline{w}^{12|11})$ , following Lemma 5.8.

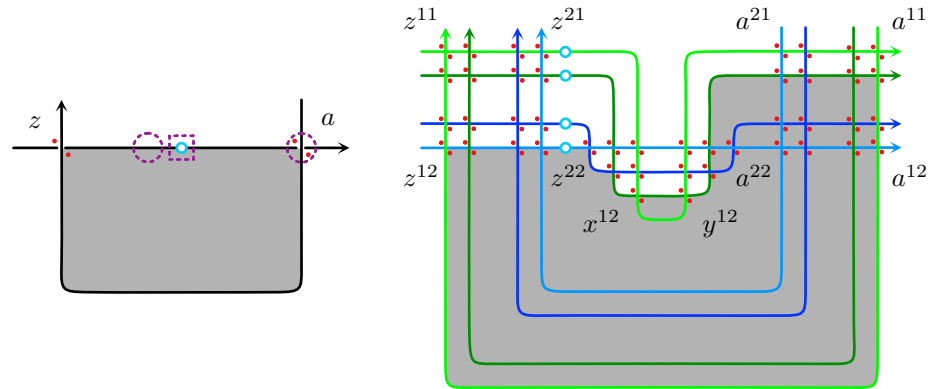


FIGURE 13. The disk at left is an enriched disk in  $\Delta_{\Lambda}^2(z, at^{-1})$  with pure enrichments  $w_1 = \{1\}$  and  $w_2 = \{0\}$ . The disk at right is its lift to a disk in  $\Delta_{\bar{\Lambda}^{2,2}}(\underline{z}^{12|22}, a^{11|21}\underline{x}^{12|11}\underline{x}^{22|12}(t^{2|2})^{-1})$ .

on a correspondence with chords of  $\bar{\Lambda}$ ; our formulation matches that in [43, Proposition 5.4].

**Proposition 5.9.** *There is a bijective correspondence between Reeb chords of  $\widehat{\mathcal{R}}^{12}$  (resp.  $\widehat{\mathcal{S}}^{ii}$ , for  $i = 1, 2$ ) and those of  $\overline{\mathcal{R}}^{12} \cup \overline{\mathcal{R}}^{21}$  (resp.  $\overline{\mathcal{S}}^{ii}$ ).*

Under this correspondence, Reeb chords in  $\overline{\mathcal{R}}^{21}$  are mapped to those in  $\widehat{\mathcal{R}}^{12}$  with length smaller than  $Z$  and chords in  $\overline{\mathcal{R}}^{12}$  are mapped to those in  $\widehat{\mathcal{R}}^{12}$  with length larger than  $Z$ . Following [47], we call the former type

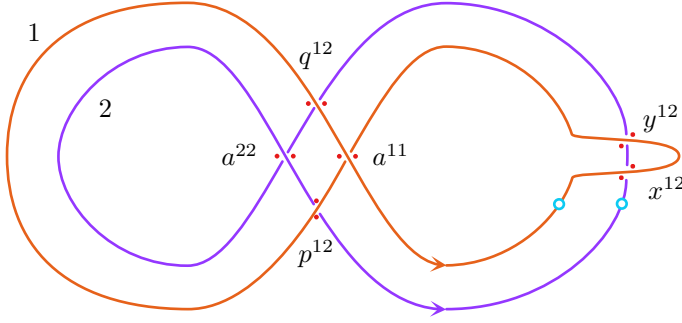


FIGURE 14. The separated 2-copy of a Legendrian knot.

of chords  $p$  **chords** and the latter type  $q$  **chords**, denoted by  $\widehat{\mathcal{R}}_p$  and  $\widehat{\mathcal{R}}_q$ , respectively. Note that the chords arising from the critical points of the perturbation are  $q$  chords. We also use these letters to distinguish these two kinds of chords when necessary, though we continue to label the  $q$  chords at critical points by  $x$  and  $y$ . The gradings of elements in  $\widehat{\mathcal{S}}^{ij}$  align with those in  $\overline{\mathcal{S}}^{ij}$  of the standard 2-copy except that  $|p_k| = -|a_k^{21}| - 1$ ; again, see [47].

**5.4.2. Disks in the Separated 2-Copy.** When analyzing immersed disks in  $\widehat{\Lambda}$ , we extend concepts such as the stick-together map, thin and thick disks, and enriched disks from the standard  $n$ -copy to the separated 2-copy. The set of immersed disks in the separated 2-copy is noticeably more complicated than in the settings above. Again, we shall always assume that the separated 2-copy and its  $(s, r)$ -copy are simply perturbed in the same sense as before. We begin by identifying thin disks of three different types.

**Lemma 5.10** (Separated 2-Copy Thin Disk Identification I). *Suppose that  $(\underline{z}, \underline{\mathbf{a}}w\underline{\mathbf{b}})$  is in  $(s, r)$ -copy form for  $\widehat{\Lambda}$ . A disk in the set  $\Delta_{\widehat{\Lambda}^{s,r}}(\underline{z}, \underline{\mathbf{a}}w\underline{\mathbf{b}})$  with both  $z$  and  $w$  in  $\widehat{\mathcal{R}}_q$  is thin with respect to  $\Lambda$  if and only if  $(\underline{z}, \underline{\mathbf{a}}w\underline{\mathbf{b}})$  is one of the following types:*

**Flowlines:**

$$\begin{aligned} & (\underline{x}^{12|11}, t^{-1}\underline{y}^{12|11}t), \quad (\underline{x}^{12|11}, \underline{y}^{12|11}), \\ & (\underline{x}^{12|21}, t^{-1}\underline{y}^{11|21}t\underline{x}^{12|11}), \quad (\underline{x}^{12|12}, \underline{x}^{12|11}\underline{y}^{22|12}), \\ & (\underline{x}^{12|12}, t^{-1}\underline{y}^{12|11}\underline{x}^{12|11}), \quad (\underline{x}^{12|21}, \underline{x}^{11|21}\underline{y}^{12|11}), \end{aligned}$$

**Partial Flowlines:**

$$\begin{aligned} & (\underline{q}^{12|12}, \underline{q}^{12|11}\underline{y}^{22|12}), \quad (\underline{q}^{12|21}, \underline{y}^{11|21}\underline{q}^{12|11}), \\ & (\underline{q}^{12|11}, \underline{a}^{11|11}\underline{y}^{12|11}), \quad (\underline{q}^{12|11}, \underline{y}^{12|11}\underline{a}^{22|11}), \\ & (\underline{q}^{12|21}, \underline{a}^{11|21}\underline{y}^{12|11}), \quad (\underline{q}^{12|12}, \underline{y}^{12|11}\underline{a}^{22|12}), \end{aligned}$$

**Constant Flowlines:**  $(\underline{y}^{12|21}, \underline{y}^{11|21}\underline{y}^{12|11})$  or  $(\underline{y}^{12|12}, \underline{y}^{12|11}\underline{y}^{22|12})$ .

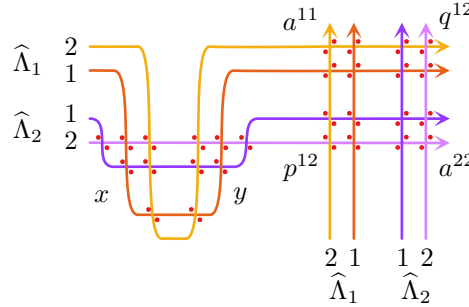


FIGURE 15. In Lemma 5.10, the configuration of the crossing signs for the  $x$ ,  $y$ , and  $q$  generators is the same as those for the  $x$ ,  $y$ , and  $a^{ij}$  ( $i \geq j$ ) generators in Figure 11.

*Proof.* The thin disks for the separated 2-copy with both  $z$  and  $w$  in  $\widehat{\mathcal{R}}_q$  are combinatorially identical to those in the ordinary 2-copy. To see this, first note that the configuration of the crossing signs for the flowlines and constant flowlines in Figure 10 is identical for the separated 2-copy; see Figure 15. Next, the partial flowlines in Figure 10 only have corners at the  $a^{12}$  crossings, which are configured identically to the  $q^{12}$  crossings in the separated 2-copy. Thus, the combinatorial count in the proof of Lemma 5.5 applies here with appropriate changes in notation.  $\square$

**Lemma 5.11** (Separated 2-Copy Thin Disk Identification II). *Suppose that  $(\underline{z}, \underline{awb})$  is in  $(s, r)$ -copy form for  $\widehat{\Lambda}$ . A disk in the set  $\Delta_{\widehat{\Lambda}^{s,r}}(\underline{z}, \underline{awb})$  with both  $z$  and  $w$  in  $\widehat{\mathcal{R}}_p$  is thin with respect to  $\Lambda$  if and only if  $(\underline{z}, \underline{awb})$  is one of the following types:*

$$(\underline{p}^{12|21}, y^{11|21} \underline{p}^{12|11}) \text{ or } (\underline{p}^{12|12}, \underline{p}^{12|11} y^{22|12}).$$

*Proof.* As shown in Figure 15, the thin disks for the separated 2-copy with both  $z$  and  $w$  in  $\widehat{\mathcal{R}}_p$  are combinatorially identical to those in the  $(s, r)$ -copy of an opposite 2-copy in Lemma 5.5.  $\square$

The final set of thin disks for the separated 2-copy that we will need are those that have a positive corner at an  $x$  generator and a negative corner at a  $p$  generator.

**Lemma 5.12** (Separated 2-Copy Thin Disk Identification III). *Suppose that  $(\underline{z}, \underline{awb})$  is in  $(s, r)$ -copy form for  $\widehat{\Lambda}$ . All disks in the set  $\Delta_{\widehat{\Lambda}^{s,r}}(\underline{z}, \underline{awb})$  with  $z \in \widehat{\mathcal{R}}_x$  and  $w$  in  $\widehat{\mathcal{R}}_p$  are thin with respect to  $\Lambda$ . In particular,  $(\underline{z}, \underline{awb})$  is one of the following half-flowlines.*

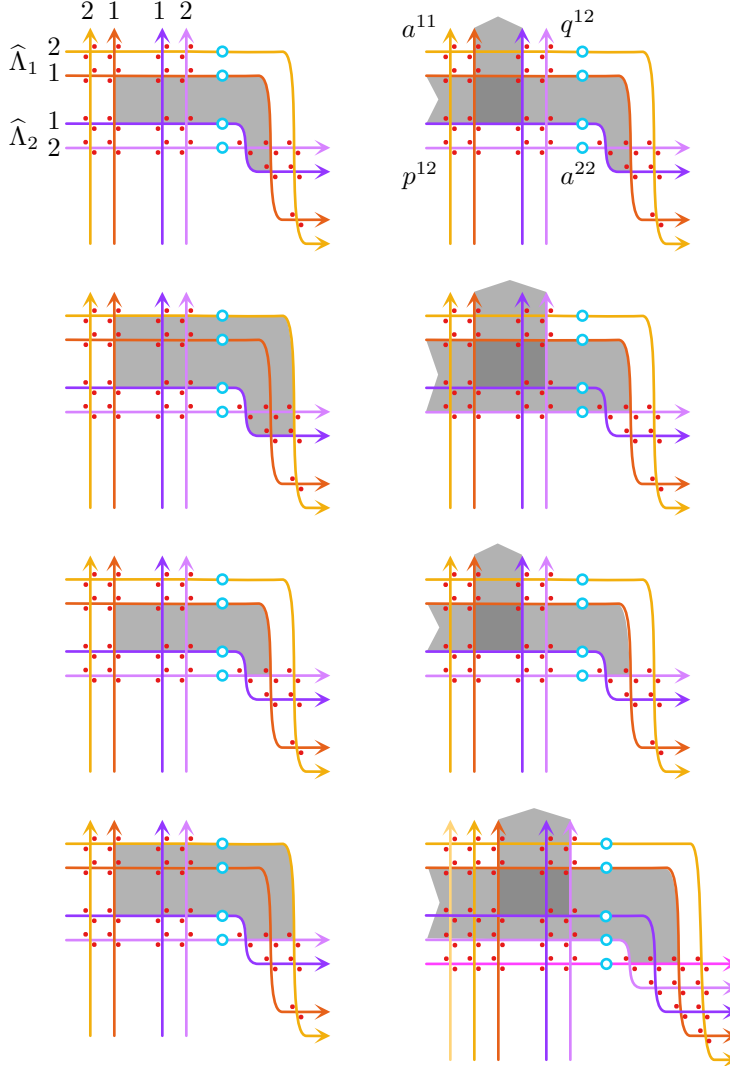


FIGURE 16. The thin disks in the 2-copy listed in Lemma 5.12.

- |        |  |  |
|--------|--|--|
| (5.5a) | $(\underline{x}^{12 11}, t^{-1}a^{11 11}\underline{p}^{12 11}t)$ | $(\underline{x}^{12 11}, t^{-1}\underline{p}^{12 11}a^{22 11}t)$ |
| (5.5b) | $(\underline{x}^{12 21}, t^{-1}a^{11 21}\underline{p}^{12 11}t)$ | $(\underline{x}^{12 12}, t^{-1}\underline{p}^{12 11}a^{22 12}t)$ |
| (5.5c) | $(x^{12 12}, t^{-1}a^{11 11}\underline{p}^{12 11}tx^{22 12})$    | $(x^{12 12}, t^{-1}\underline{p}^{12 11}a^{22 11}tx^{22 12})$    |
| (5.5d) | $(x^{12 22}, t^{-1}a^{11 21}\underline{p}^{12 11}tx^{22 12})$    | $(x^{12 13}, t^{-1}\underline{p}^{12 11}a^{22 12}tx^{22 23}).$   |

The proof is, once again, a straightforward combinatorial enumeration, which is carried out in Figure 16.

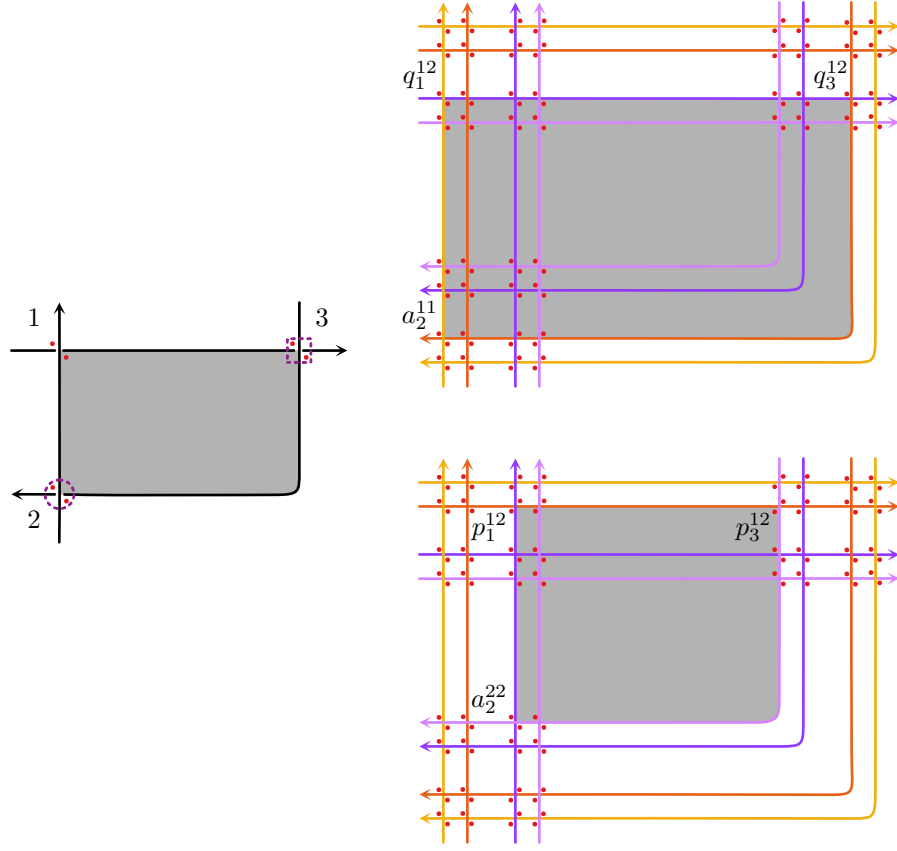


FIGURE 17. The thick disks captured by Lemma 5.14(1) on the top and (2) on the bottom come from the same underlying enriched disk in  $\Delta_{\Lambda}^{1,0}(\underline{a}_1, \underline{a}_2 \underline{a}_3)$  with pure enrichment  $\mathbf{w}_1 = \{1\}$  and  $\mathbf{w}_2 = \emptyset$ . At top, the enriched disk corresponds to a disk in  $\Delta_{\widehat{\Lambda}^{2,2}}(\underline{q}_1^{12|21}, \underline{a}_2^{12|21} \underline{q}_3^{12|11})$ . At bottom, the enriched disk corresponds to a disk in  $\Delta_{\widehat{\Lambda}^{2,2}}(\underline{p}_3^{12|12}, \underline{p}_1^{12|11} \underline{a}_2^{22|12})$ .

There are many more thin disks with  $z \in \widehat{\mathcal{R}}_q$  and  $w \in \widehat{\mathcal{R}}_p$ , including new configurations that lie between two crossings, or even lie inside a single crossing, but these will not need to be explicitly enumerated for the main proofs in Section 7.

We are now ready to describe the thick disks. The precise details of the projection and lifting operations depend on the nature of the  $z$  and  $w$  generators in  $(\underline{z}, \underline{a} \underline{w} \underline{\mathbf{b}})$ , divided into the following three cases.

$z, w \in \widehat{\mathcal{R}}_q$ : The projection and lifting operations are identical to those for the ordinary 2-copy. See Figure 17.

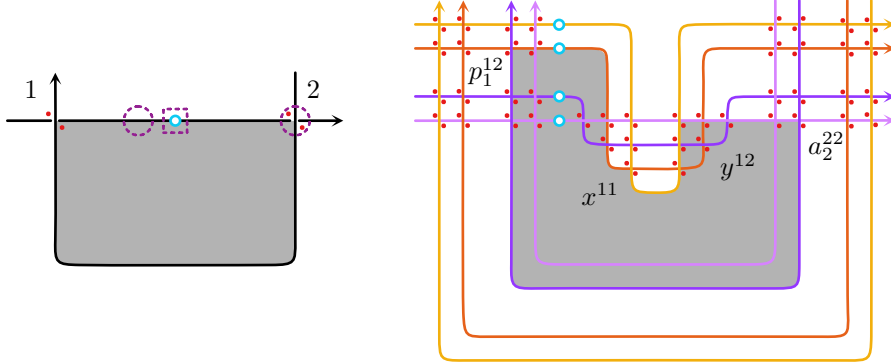


FIGURE 18. The thick disks captured by Lemma 5.14(3). The enriched disk at left lies in  $\Delta_{\Lambda}^{1,0}(a_1, a_2 t^{-1})$  with pure enrichments  $\mathbf{w}_1 = \{1\}$  and  $\mathbf{w}_2 = \{0\}$  corresponds to the disk at right in  $\Delta_{\widehat{\Lambda}^{2,2}}(\underline{y}^{12|22}, x^{11|21}(t^{1|1})^{-1} \underline{p}_1^{12|11} \underline{a}_2^{22|12})$ .

$z \in \widehat{\mathcal{R}}_p, w \in \widehat{\mathcal{R}}_p$ : The stick-together map sends a corner of a disk in the diagram of  $\widehat{\Lambda}^{s,r}$  at a  $p$  chord to a corner of a disk in the diagram of  $\Lambda$  with the opposite sign. Thus, a disk in  $\Delta_{\Lambda^{s,r}}(\underline{z}, \mathbf{a} \underline{w} \mathbf{b})$ , which has a positive  $p$ -corner at  $\check{z}$  and a negative  $p$ -corner at  $\check{w}$ , projects to a doubly enriched disk in  $\Delta_{\Lambda}^{r,s}(\underline{w}, \mathbf{b} \check{z} \mathbf{a})$ . The pure enrichments follow the cyclic movement of  $\mathbf{a}$  and  $\mathbf{b}$ , and the mixed enrichment lies at  $\underline{z}$ . See Figure 17 once again.

Once we specify that the target lifts of  $z$  and  $w$  lie in  $\widehat{\mathcal{R}}_p$ , the lifting procedure follows the same recipe as before and provides an inverse operation to the projection.

$z \in \widehat{\mathcal{R}}_y, w \in \widehat{\mathcal{R}}_p$ : While thick disks with a positive corner at a minimum did not exist for the ordinary 2-copy, as dictated by Lemma 5.8, they are possible when the negative corner lies at a  $p$  chord. Similarly to the previous case, a disk in this case projects to a disk with a positive corner at  $\check{w}$  and a marked point in the position occupied by  $z$ . That is, the projection lies in  $\Delta^{r,s}(\underline{w}, \mathbf{b} t^{\pm 1} \mathbf{a})$ . Care must be taken with the enrichment. If the mixed enrichment is at  $t$ , then 0 is enriched at most once in  $\mathbf{w}_1$  and not enriched in  $\mathbf{w}_2$ . If the mixed enrichment is at  $t^{-1}$ , then 0 is not enriched in  $\mathbf{w}_1$  but may be enriched multiple times in  $\mathbf{w}_2$ . See Figure 18.

Again, once we specify that the lifts of  $z$  and  $w$  lie in  $\widehat{\mathcal{R}}_y$  and  $\widehat{\mathcal{R}}_p$  respectively, the lifting procedure follows the same recipe as before and provides an inverse operation to the projection.

*Remark 5.13.* We need not formally identify the remaining thick disks with  $z \in \widehat{\mathcal{R}}_q^{12|s,r}$  and  $w \in \widehat{\mathcal{R}}_p^{12|s,r}$ , though one can observe that they project to

disks with precisely *two* positive corners in  $\Lambda$ . By Lemma 5.12, there are no thick disks with  $z \in \widehat{\mathcal{R}}_x$  and  $w \in \widehat{\mathcal{R}}_p$ . Further, action considerations imply that there are no disks in  $\widehat{\Lambda}^{s,r}$  with  $z \in \widehat{\mathcal{R}}_p^{12|s,r}$  and  $w \in \widehat{\mathcal{R}}_q^{12|s,r}$ .

The descriptions of the projection and lifting operations above yield the following identification.

**Lemma 5.14** (Separated 2-Copy Thick Disk Identification). *Suppose the pair  $(\underline{z}, \mathbf{awb})$  is in  $(s, r)$ -copy form for  $\widehat{\Lambda}$  without any generator in  $\mathbf{awb}$  arising from a minimum of a perturbing function.*

- (1) *If  $z \in \widehat{\mathcal{R}}_q^{12|s,r}$  and  $w \in \widehat{\mathcal{R}}_q^{12|11}$ , there is a bijective correspondence between the disks in  $\Delta_{\widehat{\Lambda}^{s,r}}(\underline{z}, \mathbf{awb})$  and the doubly enriched disks in  $\Delta_{\Lambda}^{s-1,r-1}(\check{z}, \check{\mathbf{awb}})$ , where 0 has pure enrichments only if the mixed enrichment is at  $t^{-1}$ .*
- (2) *If  $z \in \widehat{\mathcal{R}}_p^{12|s,r}$  and  $w \in \widehat{\mathcal{R}}_p^{12|11}$ , there is a bijective correspondence between the disks in  $\Delta_{\Lambda^{s,r}}(\underline{z}, \mathbf{awb})$  and the doubly enriched disks in  $\Delta_{\Lambda}^{r-1,s-1}(\check{w}, \check{\mathbf{bz}}\check{\mathbf{a}})$ .*
- (3) *If  $y \in \widehat{\mathcal{R}}_q^{12|s,r}$  arises from a minimum and  $w \in \widehat{\mathcal{R}}_p^{12|11}$ , there is a bijective correspondence between the disks in  $\Delta_{\Lambda^{s,r}}(y, \mathbf{awb})$  and the doubly enriched disks in  $\Delta_{\Lambda}^{r-1,s-1}(\check{w}, \check{\mathbf{bt}}^{\pm 1}\check{\mathbf{a}})$ , where 0 is enriched at most once in  $\mathbf{w}_1$  and not enriched in  $\mathbf{w}_2$  if the mixed enrichment is at  $t$ , and 0 is not enriched in  $\mathbf{w}_1$  if the mixed enrichment is at  $t^{-1}$ .*

## 6. AUGMENTATION CATEGORIES, BIMODULES, AND ISOMORPHISMS

In this section, we define the central algebraic objects in the paper using the geometric models established in the previous section. We begin by reviewing the construction from [43] of the augmentation  $A_\infty$  categories  $\mathcal{A}\text{ug}_\pm(\Lambda)$  in Section 6.1; these constructions rely on the  $n$ -copy. Next, we define a variety of bimodules over  $\mathcal{A}\text{ug}_+(\Lambda)$  in Sections 6.2 and 6.3; these bimodules are constructed using the  $(s, r)$ -copy. Finally, we elucidate relationships between the augmentation bimodules using bimodules associated to the separated 2-copy in Section 6.4.

**6.1. Augmentation Categories.** We begin with a summary of the definition of the augmentation categories  $\mathcal{A}\text{ug}_\pm(\Lambda)$  associated to a Legendrian  $\Lambda$ , along with a third “circle category”  $\mathcal{C}$ . The first appearances of the categories  $\mathcal{A}\text{ug}_-(\Lambda)$  and  $\mathcal{A}\text{ug}_+(\Lambda)$  were in [2] and [43] respectively; see also the earlier paper [9]. All three categories are built on the geometric model of the  $n$ -copy  $\Lambda^n$ .

**6.1.1. Positive and Negative Augmentation Categories.** The objects of the  $A_\infty$  categories  $\mathcal{A}\text{ug}_\pm(\Lambda)$  are simply the augmentations of the Chekanov-Eliashberg DGA of  $\Lambda$ . We emphasize once again that we restrict ourselves to augmentations over  $\mathbb{F}_2$ .

To define the morphisms, differentials, and higher products, we generalize the algebraic structures presented in Section 2.2. Given an  $n$ -tuple of augmentations  $(\varepsilon_1, \dots, \varepsilon_n)$ , define the **diagonal augmentation**  $\hat{\varepsilon}$  on the  $n$ -copy  $\Lambda^n$  to equal  $\varepsilon_i$  on generators in  $\mathcal{S}^{ii}$  and to vanish on  $\mathcal{S}^{ij}$  for  $i \neq j$ . This augmentation respects the link grading on the  $n$ -copy by definition. Hence, using Proposition 3.2, we obtain the  $A_\infty$  algebra  $(A^\vee, \{m_{\hat{\varepsilon}}^k\})$  from the DGA of the  $n$ -copy  $\Lambda^n$ . Further, as noted in the discussion after Proposition 3.2, the vector space and products in the  $A_\infty$  algebra  $(A^\vee, \{m_{\hat{\varepsilon}}^k\})$  split, with the only non-vanishing products given by

$$(6.1) \quad m_{\hat{\varepsilon}}^k : A_{i_k i_{k+1}}^\vee \otimes \cdots \otimes A_{i_1 i_2}^\vee \rightarrow A_{i_1 i_{k+1}}^\vee.$$

We are now in position to define the morphism spaces and structure maps for the augmentation categories. First, given a pair of augmentations  $(\varepsilon_1, \varepsilon_2)$ , we define

$$\begin{aligned} \text{Hom}_+(\varepsilon_1, \varepsilon_2) &= A_{12}^\vee, \\ \text{Hom}_-(\varepsilon_2, \varepsilon_1) &= A_{21}^\vee. \end{aligned}$$

The morphism spaces depend neither on the augmentations  $\varepsilon_i$  nor on the number  $n$  of copies of  $\Lambda$  (so long as  $n \geq 2$ ). In the case of a simply perturbed Legendrian, we follow the conventions in Section 5.1.1 to denote the generators of  $A_{12}^\vee$  by  $a_k^+, x^+, y^+$  and those of  $A_{21}^\vee$  by  $a_k^-$ . Further, we may split the vector space  $A_{12}^\vee$  into  $A_{12,\Lambda}^\vee \oplus A_{12,f}^\vee$ , where  $A_{12,\Lambda}^\vee$  is generated by the  $a_k^+$  and  $A_{12,f}^\vee$  is generated by  $x^+$  and  $y^+$ .

To define the maps  $m_+^k : \text{Hom}_+(\varepsilon_{k+1}, \dots, \varepsilon_1) \rightarrow \text{Hom}_+(\varepsilon_1, \varepsilon_{k+1})$ , we first note that implicit in the translation of [43, Lemma 3.15] to the algebras of  $n$ -copies in [43, §4] is the fact that, for  $i < j$ , there is a chain isomorphism  $h_{ij} : A_{12}^\vee \rightarrow A_{ij}^\vee$  obtained by an identification of generators, and similarly for  $i > j$  using  $A_{21}^\vee$ . We then compose the structure map  $m_{\hat{\varepsilon}}^k$  with appropriate identifications  $h_{ij}$  to define  $m_+^k$ :

$$(6.2) \quad m_+^k = h_{1,k+1}^{-1} \circ m_{\hat{\varepsilon}}^k \circ (h_{k,k+1} \otimes \cdots \otimes h_{12}).$$

We will occasionally abuse notation for convenience and abbreviate  $h_{ij}$  by  $h$  and extend it to  $\mathcal{A}$ . As discussed in [43], the definition of  $m_k^+$  is independent of the number of knots in the  $n$ -copy, or even the choice of  $k+1$  components inside a given  $n$ -copy. The disks used in the definition of  $m_+^k(a_k^+, \dots, a_1^+)$  are those in  $\Delta_{\Lambda^{k+1}}(h(a), h(\mathbf{a}))$ , where the associated word is in positive  $(k+1)$ -copy form with  $a_{i_j} = a_j$  and  $\varepsilon_i(\mathbf{a}_i) = 1$ .

Similarly, the maps  $m_-^k : \text{Hom}_-(\varepsilon_1, \dots, \varepsilon_{k+1}) \rightarrow \text{Hom}_-(\varepsilon_{k+1}, \varepsilon_1)$  are defined as the composite

$$(6.3) \quad m_-^k = h_{k+1,1}^{-1} \circ m_{\hat{\varepsilon}}^k \circ (h_{21} \otimes \cdots \otimes h_{k+1,k}).$$

Note that since  $A_{ij}^\vee$  for  $i > j$  does not depend on the perturbation  $f$ , neither does  $m_-^k$ . The disks used in the definition of  $m_-^k(a_k^-, \dots, a_1^-)$  are those in

$\Delta_{\Lambda^{k+1}}(h(a), h(\mathbf{a}))$ , where  $(a, \mathbf{a})$  is in negative  $(k+1)$ -copy form with  $a_{ij} = a_j$  and  $\varepsilon_i(\mathbf{a}_i) = 1$ .

Summarizing, we state the following definition and its accompanying theorem.

**Definition 6.1.** The **positive and negative augmentation categories**  $\mathcal{A}\text{ug}_{\pm}(\Lambda)$  of a Legendrian knot  $\Lambda$  have augmentations of the associated Chekanov-Eliashberg DGA  $(\mathcal{A}, \partial)$  as objects,  $\text{Hom}_{\pm}$  as morphism spaces, and  $\{m_{\pm}^k\}$  as structure maps.

**Theorem 6.2** ([2, 43]). *The categories  $\mathcal{A}\text{ug}_{\pm}(\Lambda)$  are  $A_{\infty}$  categories. Up to  $A_{\infty}$  equivalence, the categories  $\mathcal{A}\text{ug}_{\pm}(\Lambda)$  do not depend on the perturbation  $f$  and are invariant under Legendrian isotopy.*

The reason we prefer  $\mathcal{A}\text{ug}_+$  to  $\mathcal{A}\text{ug}_-$  is that the former is a strictly unital category. The unit is straightforward to describe: the element  $y^+ \in \text{Hom}_+(\varepsilon, \varepsilon)$  is a strict unit [43]. Concretely, the disks that yield the action of the unit are the thin disks with positive corner at  $b^{13}$  (for  $b = a, x, y$ ) in Lemma 5.1.

It is useful to characterize the structure maps  $m_+^k$  in terms of thin disks and enriched disks in the original Lagrangian diagram of  $\Lambda$ , building on the ideas of [43, Proposition 4.26]. For our purpose, we consider the case when  $\Lambda^n$  is simply perturbed, though the model applies to any choice of perturbation function with changes to some details. The augmentation category defined in this manner is also termed **simply perturbed**.

Recall from Lemma 5.3 that there is a bijective correspondence between disks in the  $(k+1)$ -copy referenced above and  $k$ -enriched disks, with the correspondence given by projection from disks in the  $(k+1)$ -copy to enriched disks and geometric lifting of enriched disks to disks in the  $(k+1)$ -copy. To complement the geometric lifting process, we define the **algebraic lift**  $\hat{\alpha} : \Delta_{\Lambda}^k(a, \mathbf{a}) \rightarrow \mathcal{A}$  of a  $k$ -enriched disk  $(u, \mathbf{w})$  with  $\mathbf{w} = \{m_1 i_1, \dots, m_l i_l\}$  to be

$$\hat{\alpha}(u, \mathbf{w}) = \hat{a}_{i_1} \hat{a}_{i_2} \cdots \hat{a}_{i_l},$$

where  $\hat{a}_j = a_j$  if  $a_j \in \mathcal{R}_{\Lambda}$  and  $\hat{a}_j = x \cdots x$  for  $m_j$  number of  $x$  generators if  $a_j = t^{\pm 1}$ . It will also be convenient to define one more piece of notation. The augmentation of a word in  $(k+1)$ -copy form by taking the product of the augmentations of the pure generators:

$$(6.4) \quad \hat{\varepsilon}(\mathbf{a}) = \varepsilon_1(\mathbf{a}_1) \varepsilon_{1+m_1}(\mathbf{a}_2) \cdots \varepsilon_{k+1}(\mathbf{a}_{k+1}).$$

**Lemma 6.3.** *In the definition of  $m_+^k$  for a simply perturbed  $\mathcal{A}\text{ug}_+(\Lambda)$ , thin disks yield the terms dictated by the strict unitality of  $y^+$ , as well as the terms*

$$m_+^1(y^+) = (\varepsilon_1(a) + \varepsilon_2(a)) a^+.$$

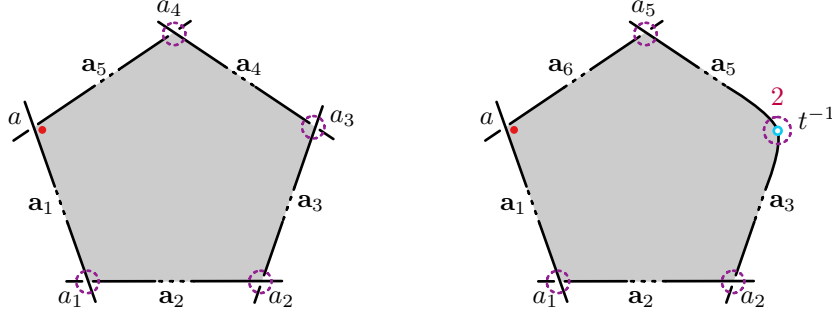


FIGURE 19. Enriched disks that contribute  $a^+$  to  $m_+^4(a_4^+, \dots, a_1^+)$  (left) and to  $m_+^5(a_5^+, x^+, x^+, a_2^+, a_1^+)$  (right). Enriched disks on the left, but not the right, side contribute to  $m_-^4(a_4^-, \dots, a_1^-)$ .

*Enriched disks yield additional terms*

$$m_+^k(a_k^+, \dots, a_1^+) = \sum_{\substack{(u, \mathbf{w}) \in \Delta_\Lambda^k(\check{a}, \check{\mathbf{a}}) \\ \hat{\alpha}(u, \mathbf{w}) = a_1 \cdots a_k}} \hat{\varepsilon}(\mathbf{a}) a^+.$$

The enriched disks involved in the definition of  $m_+$  appear in Figure 19.

*Proof.* The thin disk contributions follow directly from Lemma 5.1, while the thick disk contributions come from using Lemma 5.3 to identify the disks in the definition of  $m_+^k$  with enriched disks and their algebraic lifts.  $\square$

We may also characterize the structure maps  $m_-^k$  in terms of enriched disks. If  $(a, \mathbf{a})$  is in negative  $(k+1)$ -copy form, then all of the generators  $a_{ij}$  arise from genuine Reeb chords in  $\Lambda$ . Thus, any disk involved in the definition of  $m_-^k$  projects to an enriched disk with enrichments — which must have multiplicity 1 — only at Reeb chords.

**Lemma 6.4.** *In the definition of  $m_-^k$ , enriched disks with enrichments only at Reeb chords yield terms*

$$m_-^k(a_k^-, \dots, a_1^-) = \sum_{\substack{(u, \mathbf{w}) \in \Delta_\Lambda^k(\check{a}, \check{\mathbf{a}}) \\ \hat{\alpha}(u, \mathbf{w}) = a_1 \cdots a_k}} \hat{\varepsilon}(\mathbf{a}) a^-.$$

*Example 6.5.* Continuing the example of figure eight knot  $\Lambda$  presented in Figure 2, we note that its augmentation categories have two objects, namely  $\varepsilon_1$  and  $\varepsilon_2$  described in Example 2.5. The morphism spaces are

$$\text{Hom}_+(\varepsilon_i, \varepsilon_j) = \mathbb{F}_2 \langle a_1^+, \dots, a_7^+, x^+, y^+ \rangle,$$

$$\text{Hom}_-(\varepsilon_i, \varepsilon_j) = \mathbb{F}_2 \langle a_1^-, \dots, a_7^- \rangle,$$

where  $|a_k^+| = |a_k^-| = |a_k^\vee|$  as in Example 3.3 and  $|x^+| = 1$ ,  $|y^+| = 0$ .

The structure maps  $m_-^k$ , which only account for thick disks in  $\bar{\Lambda}$ , match the codifferential  $\delta_{\varepsilon_i}$  of the DGCA of  $\Lambda$  in Example 2.7 with suitable change of notation. As explained in Example 2.5, the maps  $m_-^k$  are independent of the choice of augmentations in this example.

The structure maps  $m_+^k$ , on the other hand, do depend on the choice of augmentations due to additional thin disk contributions. We shall describe the structure maps on  $\text{Hom}_+(\varepsilon_1, \varepsilon_1)$ , which happen to be the same as those on  $\text{Hom}_+(\varepsilon_2, \varepsilon_2)$ . For compactness of presentation, we do not list the 2-fold products that show that  $y^+$  acts as the identity.

$$\begin{aligned} m_+^1(a_2^+) &= a_4^+ & m_+^2(a_1^+, a_2^+) &= a_7^+ & m_+^3(a_3^+, a_1^+, a_2^+) &= a_4^+ \\ m_+^1(a_3^+) &= a_4^+ & m_+^2(a_3^+, a_1^+) &= a_6^+ & m_+^3(a_5^+, a_3^+, a_1^+) &= a_6^+ \\ m_+^1(a_5^+) &= a_6^+ + a_7^+ & & & m_+^3(a_1^+, a_2^+, a_5^+) &= a_7^+ \\ m_+^1(x^+) &= a_6^+ & & & & \end{aligned}$$

Unlike in the maps listed above, the  $m_+^1$  map on  $\text{Hom}_+(\varepsilon_1, \varepsilon_2)$  is non-vanishing on  $y^+$  with  $m_+^1(y^+) = a_4^+$ .

**6.1.2. The Circle Category.** We also define a third augmentation category that will prove essential in the upcoming duality structure. First, we need to define  $\mathcal{A}\text{ug}_+^{\text{Reeb}}(\Lambda)$  to be the wide subcategory of  $\mathcal{A}\text{ug}_+(\Lambda)$  whose morphisms are given by  $A_{12,\Lambda}^\vee$ . It follows from (the dual of) Lemma 2.3 and the fact that  $\mathcal{R}_\Lambda^{12}$  contains all of the Reeb chords above a certain length in  $\mathcal{R}^{12}$  that  $\mathcal{A}\text{ug}_+^{\text{Reeb}}(\Lambda)$  is indeed a subcategory. By Lemmas 6.3 and 6.4, we may identify  $\mathcal{A}\text{ug}_+^{\text{Reeb}}(\Lambda)$  with  $\mathcal{A}\text{ug}_-(\Lambda)$ .

**Definition 6.6.** The **circle category** is the quotient category  $\mathcal{C}(\Lambda) = \mathcal{A}\text{ug}_+(\Lambda)/\mathcal{A}\text{ug}_+^{\text{Reeb}}(\Lambda)$ .

In particular,  $\mathcal{C}$  is an  $A_\infty$  category with morphisms  $\text{Hom}_{\mathcal{C}}(\varepsilon_1, \varepsilon_2) = A_{12,f}^\vee$  and structure maps  $m_{\mathcal{C}}^k$  counting thin disks in  $\Lambda^{k+1}$ . When  $\Lambda^{k+1}$  is simply perturbed, Lemma 5.1 shows that the only nontrivial structure maps for the circle category are those that show that  $y^+$  is a strict unit.

On the linear level, the circle category reduces to the Morse complex for the perturbing function  $f$  of a circle, thus justifying its name. In fact, the category recovers the cohomology ring.

**6.2. Bimodules From Two-component Links.** The algebraic structures involved in the main theorem are  $A_\infty$  bimodules over  $\mathcal{A}\text{ug}_+(\Lambda)$  and morphisms between them. Thus, our next task is to define and understand the bimodule analogues of the augmentation categories in Section 6.1. To this end, we begin with a general construction of  $\mathcal{A}\text{ug}_+(\Lambda)$ -bimodules from an ordered two-component Legendrian link.

**Proposition 6.7.** *A Legendrian link  $\Lambda = \Lambda_1 \sqcup \Lambda_2$  induces an  $\mathcal{A}\text{ug}_+(\Lambda_2)$ - $\mathcal{A}\text{ug}_+(\Lambda_1)$  bimodule  $\mathcal{M}$  with the space  $\mathcal{M}(\varepsilon^2, \varepsilon^1)$  generated by  $\mathcal{R}^{12}$ .*

Intuitively, the induced bimodule  $\mathcal{M}$  repackages the information in the category  $\mathcal{A}\text{ug}_+(\Lambda)$  in a way that respects the 2-component structure of the link.

In the proof below and in subsequent sections, we adopt compact notation for arguments to bimodule structure maps. First, let  $\tilde{\varepsilon}^2 = (\varepsilon_{r+1}^2, \dots, \varepsilon_1^2)$  and  $\tilde{\varepsilon}^1 = (\varepsilon_1^1, \dots, \varepsilon_{s+1}^1)$ . Similarly, let  $\vec{a} = (a_1^+, \dots, a_s^+)$  and  $\tilde{b} = (b_r^+, \dots, b_1^+)$ .

*Proof.* To define the desired  $\mathcal{A}\text{ug}_+(\Lambda_2)$ - $\mathcal{A}\text{ug}_+(\Lambda_1)$  bimodule  $\mathcal{M}$ , let  $\varepsilon^i$  be an augmentation of  $\Lambda_i$ ,  $i = 1, 2$ . Set  $\mathcal{M}(\varepsilon^2, \varepsilon^1)$  to be the vector space generated by  $\mathcal{R}^{12}$ , with generators denoted  $w_i$ .

We next define the structure maps

$$(6.5) \quad n^{r|s} : \text{Hom}_{\mathcal{A}\text{ug}_+(\Lambda_2)}(\tilde{\varepsilon}^2) \otimes \mathcal{M}(\varepsilon_1^2, \varepsilon_1^1) \otimes \text{Hom}_{\mathcal{A}\text{ug}_+(\Lambda_1)}(\tilde{\varepsilon}^1) \rightarrow \mathcal{M}(\varepsilon_{r+1}^2, \varepsilon_{s+1}^1)$$

in terms of the structure maps of the category  $\mathcal{A}\text{ug}_+(\Lambda)$  or, more accurately, using its diagonal bimodule. In particular, we need to identify a tuple  $(\tilde{b}, \underline{w}, \vec{a})$  in the domain of  $n^{r|s}$  with a tuple in the domain of  $m_+^{r+s+1}$ .

The first step is to extend the augmentations  $\varepsilon_k^1$  on  $\Lambda_1$  to pure augmentations  $\hat{\varepsilon}_k^1$  on  $\Lambda$ . To effect this, for each  $k \in \{1, \dots, s+1\}$ , we define the extension  $\hat{\varepsilon}_k^1$  to equal  $\varepsilon_1^2$  on generators from  $\Lambda_2$ ; we make a similar definition for  $\hat{\varepsilon}_l^2$  for  $l \in \{1, \dots, r+1\}$ .

Next, consider a tuple  $\vec{a} \in \text{Hom}_{\mathcal{A}\text{ug}_+(\Lambda_1)}(\tilde{\varepsilon}^1)$ . Each  $a_k^+$  corresponds to a mixed Reeb chord of the 2-copy of the Legendrian link  $\Lambda_1$ , and hence a mixed Reeb chord of the 2-copy of the Legendrian link  $\Lambda$ . It follows that we may think of  $a_k^+$  as lying in  $\text{Hom}_{\mathcal{A}\text{ug}_+(\Lambda)}(\hat{\varepsilon}_{k+1}^1, \hat{\varepsilon}_k^1)$ ; notice the transposition of indices. Similarly, for a tuple  $\tilde{b} \in \text{Hom}_{\mathcal{A}\text{ug}_+(\Lambda_2)}(\tilde{\varepsilon}^2)$ , we may think of  $b_k^+$  as lying in  $\text{Hom}_{\mathcal{A}\text{ug}_+(\Lambda)}(\hat{\varepsilon}_{k+1}^2, \hat{\varepsilon}_k^2)$ . There is no transposition of indices in this case.

Finally, a generator  $w \in \mathcal{M}(\varepsilon^2, \varepsilon^1)$ , which corresponds to a Reeb chord of  $\Lambda$  from  $\Lambda_1$  to  $\Lambda_2$ , may be identified with the nearby mixed Reeb chord in the 2-copy  $\bar{\Lambda}$  that begins on the  $\Lambda_2$  component of the second copy and ends on the  $\Lambda_1$  component of the first copy. In particular,  $w$  may be thought of as lying in  $\text{Hom}_{\mathcal{A}\text{ug}_+(\Lambda)}(\hat{\varepsilon}_1^2, \hat{\varepsilon}_1^1)$ .

With the above identification of tuple  $(\tilde{b}, \underline{w}, \vec{a})$  in the domain of  $n^{r|s}$  as a tuple in the domain of  $m_+^{r+s+1}$  in hand, we define

$$n^{r|s}(\tilde{b}, \underline{w}, \vec{a}) = m_+^{r+s+1}(\tilde{b}, w, \vec{a}).$$

Since the structure maps of  $\mathcal{A}\text{ug}_+(\Lambda)_\Delta$  satisfy the defining  $A_\infty$  bimodule equations, so too will  $n^{r|s}$ .  $\square$

It will be useful to precisely specify the chords and disks involved in the definition of  $n^{r|s}$ . Recall that the structure map  $m_+^{r+s+1}$  is defined by counting disks in  $\Lambda^{r+s+2}$  whose first  $s$  negative mixed corners lie in the top  $(s+1)$ -copy of  $\Lambda_1^2$  and last  $r$  negative mixed corners lie in the bottom  $(r+1)$ -copy of  $\Lambda_2^2$ ; as before, there may be pure augmented corners as well. The

definition of  $n^{r|s}$  counts disks in a sublink of  $\Lambda^{r+s+2}$  identified with  $\Lambda^{s+1,r+1}$ . Thus, the  $(s+1, r+1)$ -copy is the correct geometric model for the bimodule  $\mathcal{M}$  as claimed.

Next, to identify the chords in the  $(s+1, r+1)$ -copy used in the definition of  $n^{r|s}$ , we refine the maps  $h_{ij}$  from Section 6.1.1 to maps  $h_{ij|kl}$  that identify a chord  $a^{ij}$  of  $\Lambda^{2,2}$  with the chord  $a^{ij|kl}$  of  $\Lambda^{s+1,r+1}$ .

Building on the remarks after Equation (6.2), we now identify the disks in  $\Lambda^{s+1,r+1}$  used to define  $n^{r|s}$ .

**Lemma 6.8.** *The disks used in the definition of  $n^{r|s}(\bar{b}, \underline{w}, \vec{a})$  are those in*

$$\Delta_{\Lambda^{s+1,r+1}}(h_{12|s+1,r+1}(z), h_{11|..}(\mathbf{a})h_{12|11}(w)h_{22|..}(\mathbf{b})),$$

where the associated word is in  $(s+1, r+1)$ -copy form with  $a_{ij} = a_j, b_{ij} = b_j$  and  $\varepsilon_i^1(\mathbf{a}_i) = \varepsilon_i^2(\mathbf{b}_i) = 1$ .

As in the construction of  $\text{Aug}_+^{\text{reeb}}(\Lambda)$  as wide subcategory of  $\text{Aug}_+(\Lambda)$ , we may use heights of Reeb chords to construct submodules of the bimodule  $\mathcal{M}$  of Proposition 6.7. Suppose  $\mathcal{R}_\lambda^{12} \subset \mathcal{R}^{12}$  consists of all Reeb chords with height greater than  $\lambda$ . For  $\varepsilon^i$  an augmentation of  $\Lambda_i$ ,  $i = 1, 2$ , let  $\mathcal{M}_\lambda(\varepsilon^2, \varepsilon^1) \subset \mathcal{M}(\varepsilon^2, \varepsilon^1)$  be the subspace generated by  $\mathcal{R}_\lambda^{12}$ . Combining Lemma 2.3 with Lemma 6.8 shows that  $\mathcal{M}_\lambda$  is an  $\text{Aug}_+(\Lambda_2)$ - $\text{Aug}_+(\Lambda_1)$  submodule of  $\mathcal{M}$ , which we call the **length filtration submodule at height  $\lambda$** .

**6.3. Augmentation Bimodules.** While one might be tempted to simply take diagonal bimodules of the three  $A_\infty$  categories defined in Section 6.1, we will need all three bimodules to have coefficients in the same category. This necessitates a more subtle approach using Proposition 6.7.

**Definition 6.9.** The **positive augmentation bimodule**  $\mathcal{M}_+$  of a Legendrian knot  $\Lambda$  is defined to be the result of applying Proposition 6.7 to the 2-copy  $\bar{\Lambda}$ .

The **negative augmentation bimodule**  $\mathcal{M}_-$  of a Legendrian knot  $\Lambda$  is defined to be the result of applying Proposition 6.7 to the opposite 2-copy  $\underline{\Lambda}$ .

An inspection of the proof of Proposition 6.7 shows that the augmentation bimodules defined above depend on the perturbation functions for both the (opposite) 2-copy and its  $(s+r+2)$ -copy. For our purposes, we only consider augmentation bimodules defined by a simply perturbed (opposite) 2-copy as well as its  $(s+r+2)$ -copy perturbed by a Morse function with the maxima and minima placed as shown in Figure 10. In this case, the combinatorics of the Lagrangian diagrams of  $\bar{\Lambda}^{s+r+2}$  and  $\underline{\Lambda}^{s+r+2}$  matches that of the diagrams of a simply perturbed  $\Lambda^{2s+2r+4}$  and  $\Lambda^{2s+2r+4}$ , up to relabeling. As a result, the base category  $\text{Aug}_+(\Lambda)$  is simply perturbed. An augmentation bimodule defined in this manner is also termed **simply perturbed**.

In this setting, we label the generators of the spaces  $\mathcal{M}_+(\varepsilon^2, \varepsilon^1)$  by  $a^+$ ,  $x^+$ , and  $y^+$ , and the generators of  $\mathcal{M}_-(\varepsilon^2, \varepsilon^1)$  by  $a^-$ , as the generators of  $\text{Hom}_\pm$  match those of  $\mathcal{M}_\pm$  in our chosen configuration. Following the discussion around Lemma 6.8, the sublink in  $\bar{\Lambda}^{s+r+2}$  used to define the structure maps  $n_{\mathcal{M}_+}^{r|s}$  can be identified with a simply perturbed  $(s+1, r+1)$ -copy of 2-copy.

*Remark 6.10.* It would be reasonable to expect that, using a consistent sequence of DGA maps as in [43, Proposition 4.21], any two perturbation schemes are conjecturally equivalent under an appropriate notion of equivalence of  $A_\infty$  bimodules over an equivalence of  $A_\infty$  categories.

In parallel to Lemma 6.3, we may use Lemmas 5.5 and 5.8 to characterize  $n_{\mathcal{M}_+}^{r|s}$  in terms of thin disks and doubly enriched disks in the original Lagrangian diagram of  $\Lambda$ . In order to do so, we define the **algebraic lift** of an  $(s, r)$ -enriched disk  $(u, \mathbf{w}_1, \mathbf{w}_2) \in \Delta_\Lambda^{s,r}(\underline{z}, \mathbf{a}\underline{w}\mathbf{b})$  with  $\mathbf{w}_1 = \{m_00, m_1i_1, \dots, m_ki_k\}$  and  $\mathbf{w}_2 = \{n_00, n_1j_1, \dots, n_lj_l\}$  to be

$$\hat{\alpha}(u, \mathbf{w}_1, \mathbf{w}_2) = \hat{a}_{i_k} \cdots \hat{a}_{i_1} \hat{w} \hat{b}_{j_1} \cdots \hat{b}_{j_l},$$

where  $\hat{a}$  and  $\hat{b}$  are defined as before, while  $\hat{w} = \underline{w}$  if  $w \in \mathcal{R}_\Lambda$  and  $\hat{w} = x \cdots x\underline{x}x \cdots x$  for  $m_0$  number of  $x$  generators preceding  $\underline{x}$  and  $n_0$  number of  $x$  generators following  $\underline{x}$ .

Using the notation defined after Proposition 6.7, we characterize the disks used in the definition of  $n_{\mathcal{M}_+}$  as follows.

**Lemma 6.11.** *In the definition of*

$$n_{\mathcal{M}_+}^{r|s} : \text{Hom}_+(\bar{\varepsilon}^2) \otimes \mathcal{M}_+(\varepsilon_1^2, \varepsilon_1^1) \otimes \text{Hom}_+(\bar{\varepsilon}^1) \rightarrow \mathcal{M}_+(\varepsilon_{r+1}^2, \varepsilon_{s+1}^1)$$

*(see discussion near Equation (6.5) for the notation) for a simply perturbed  $\mathcal{M}_+$ , thin disks yield the terms dictated by the strict unitality of  $y^+$ , as well as the terms*

$$\begin{aligned} n_{\mathcal{M}_+}^{0|0}(\underline{y}^+) &= (\varepsilon_1(a) + \varepsilon_2(a)) a^+, & n_{\mathcal{M}_+}^{1|0}(a^+, \underline{y}^+) &= n_{+}^{0|1}(\underline{y}^+, a^+) = a^+, \\ n_{\mathcal{M}_+}^{1|0}(x^+, \underline{y}^+) &= n_{+}^{0|1}(\underline{y}^+, x^+) = x^+. \end{aligned}$$

*Doubly enriched disks yield additional terms*

$$n_{\mathcal{M}_+}^{r|s}(\bar{b}, \underline{w}^+, \vec{a}) = \sum_{\substack{(u, \mathbf{w}_1, \mathbf{w}_2) \in \Delta_\Lambda^{s,r}(\underline{z}, \mathbf{a}\underline{w}\mathbf{b}) \\ \hat{\alpha}(u, \mathbf{w}_1, \mathbf{w}_2) = a_s \cdots a_1 \underline{w} b_1 \cdots b_r}} \hat{\varepsilon}^1(\mathbf{a}) \hat{\varepsilon}^2(\mathbf{b}) z^+$$

See Figure 20 for illustrations of the doubly enriched disks that contribute to  $n_{\mathcal{M}_+}$ .

*Proof.* The thin disk contributions follow directly from Lemma 5.5, while the thick disk contributions come from using Lemma 5.8 to identify the disks in the definition of  $n_{\mathcal{M}_+}^{r|s}$  with doubly enriched disks and their algebraic lifts.  $\square$

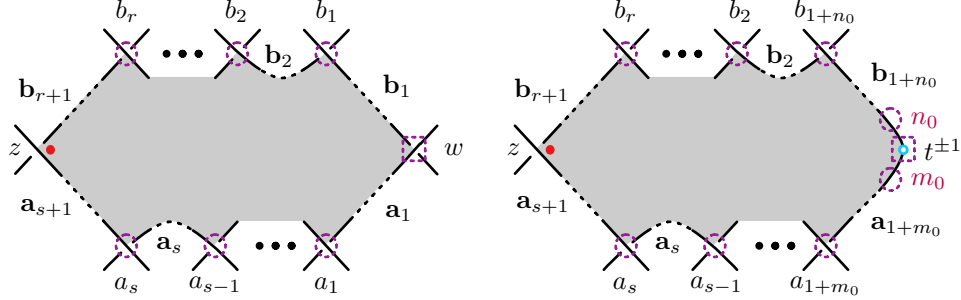


FIGURE 20. Doubly enriched disks that contribute  $z^+$  to  $n_{\mathcal{M}_+}^{r|s}(\bar{b}, \underline{w}^+, \vec{a})$  (left) and to  $n_{\mathcal{M}_+}^{r|s}(\bar{b}, \underline{t}^{\pm 1}, \vec{a})$ , with  $n_0$  and  $m_0$   $x^+$  generators before and after  $\underline{w}^+$  (right); recall that  $m_0 = 0 = n_0$  if  $w = t$ . Doubly enriched disks on the left side contribute  $z^-$  to  $n_{\mathcal{M}_-}^{r|s}(\bar{b}, \underline{w}^-, \vec{a})$  or  $w^\vee$  to  $n_{\mathcal{M}_-}^{s|r}(\vec{a}, \underline{z}^\vee, \bar{b})$ , while doubly enriched disks on the right side will contribute  $y^\vee$  to  $(\rho^\vee)^{s|r}(\vec{a}, \underline{z}^\vee, \bar{b})$  with  $m_0$   $x^+$  generators at the beginning and  $n_0$   $x^+$  generators at the end; again,  $m_0 = 0 = n_0$  if  $w = t$ . Finally, doubly enriched disks on the right side will contribute  $y^+$  to  $(\pi_{\mathcal{N}}\eta)^{s|r}$  with the same arguments, so long as  $m_0 = 0$  when  $w = t^{-1}$  or  $m_0 \leq 1$  and  $n_0 = 0$  when  $w = t$ .

Similarly, the structure maps  $n_{\mathcal{M}_-}^{r|s}$  of  $\mathcal{M}_-$  are defined using a simply perturbed  $(s+1, r+1)$ -copy of the opposite 2-copy. As above, we may characterize  $n_{\mathcal{M}_-}$  in terms of thin disks and doubly enriched disks using Lemma 5.5 and Lemma 5.8. In parallel to its category analogue  $\mathcal{A}\text{ug}_-(\Lambda)$ , note that a disk of the form  $(\underline{z}, \mathbf{a}\underline{w}\mathbf{b})$  involved in the definition of  $n_{\mathcal{M}_-}^{r|s}$  projects to an enriched disk with mixed enrichment only at a Reeb chord.

**Lemma 6.12.** *In the definition of*

$$n_{\mathcal{M}_-}^{r|s} : \text{Hom}_+(\bar{\varepsilon}^2) \otimes \mathcal{M}_-(\varepsilon_1^2, \varepsilon_1^1) \otimes \text{Hom}_+(\bar{\varepsilon}^1) \rightarrow \mathcal{M}_-(\varepsilon_{r+1}^2, \varepsilon_{s+1}^1),$$

*for a simply perturbed  $\mathcal{M}_-$ , thin disks yield the terms dictated by the strict unitality of  $y^+$ .*

*Doubly enriched disks with mixed enrichment at a Reeb chord yield additional terms*

$$n_{\mathcal{M}_-}^{s|r}(\bar{b}, \underline{w}^-, \vec{a}) = \sum_{\substack{(u, \mathbf{w}_1, \mathbf{w}_2) \in \Delta_\Lambda^{s,r}(\underline{z}, \check{\mathbf{a}}\check{\underline{w}}\check{\mathbf{b}}) \\ \hat{\alpha}(u, \mathbf{w}_1, \mathbf{w}_2) = a_s \cdots a_1 \underline{w} b_1 \cdots b_r}} \varepsilon^1(\mathbf{a}) \check{\varepsilon}^2(\mathbf{b}) z^-.$$

See Figure 20 once again.

It will also be useful to describe the structure maps of the linear dual  $\mathcal{M}^\vee$  of  $\mathcal{M}_-$  using thin and enriched disks. Following Section 3.3.2, we label the generators of the morphisms of  $\mathcal{M}^\vee$  by  $a^\vee$  with  $|a^\vee| = -|a^-|$ . We also define the **dual algebraic lift** of an  $(s, r)$ -enriched disk  $(u, \mathbf{w}_1, \mathbf{w}_2) \in \Delta_\Lambda^{s,r}(\underline{z}, \mathbf{a}\underline{w}\mathbf{b})$

to be

$$\hat{\alpha}^\vee(u, \mathbf{w}_1, \mathbf{w}_2) = x \cdots x \hat{a}_{i_1} \cdots \hat{a}_{i_k} \underline{\hat{z}} \hat{b}_{j_1} \cdots \hat{b}_{j_l} x \cdots x.$$

where  $\hat{a}$  and  $\hat{b}$  are defined as before and  $\underline{\hat{z}} = \underline{z}$  (recall that  $z \in \mathcal{R}_\Lambda$ ). Further, there are  $m_0$  number of  $x$  generators at the front and  $n_0$  number of  $x$  generators at the end.

**Lemma 6.13.** *In the definition of*

$$n_{\mathcal{M}_-^\vee}^{s|r} : \text{Hom}_+(\bar{\varepsilon}^1) \otimes \mathcal{M}_-^\vee(\varepsilon_{s+1}^1, \varepsilon_{r+1}^2) \otimes \text{Hom}_+(\bar{\varepsilon}^2) \rightarrow \mathcal{M}_-^\vee(\varepsilon_1^1, \varepsilon_1^2)$$

for a simply perturbed  $\mathcal{M}_-^\vee$ , thin disks yield the terms dictated by the strict unitality of  $y^+$ . Doubly enriched disks with mixed enrichment at a Reeb chord yield additional terms

$$n_{\mathcal{M}_-^\vee}^{s|r}(\vec{a}, \underline{\hat{z}}^\vee, \vec{b}) = \sum_{\substack{(u, \mathbf{w}_1, \mathbf{w}_2) \in \Delta_\Lambda^{s,r}(\underline{\hat{z}}, \underline{\hat{a}} \underline{\hat{w}} \underline{\hat{b}}) \\ \hat{\alpha}^\vee(u, \mathbf{w}_1, \mathbf{w}_2) = a_1 \cdots a_s z b_r \cdots b_1}} \bar{\varepsilon}^1(\mathbf{a}) \bar{\varepsilon}^2(\mathbf{b}) w^\vee.$$

Note the cyclic difference of the inputs in  $n_{\mathcal{M}_-}^{r|s}$  and  $n_{\mathcal{M}_-^\vee}^{s|r}$ , which arises from taking the adjoint as in Equation 3.4 in Section 3.3.2. See Figure 20 yet again.

In parallel to the construction of  $\mathcal{A}\text{ug}_+^{\text{Reeb}}(\Lambda)$  as a subcategory of  $\mathcal{A}\text{ug}_+(\Lambda)$ , let  $\mathcal{M}_+^{\text{Reeb}}$  be the length filtration submodule of  $\mathcal{M}_+$  generated by  $\mathcal{R}_\Lambda^{12}$ .

**Proposition 6.14.** *The submodule  $\mathcal{M}_+^{\text{Reeb}}$  is isomorphic to  $\mathcal{M}_-$ .*

*Proof.* Define a naïve morphism  $F : \mathcal{M}_- \rightarrow \mathcal{M}_+^{\text{Reeb}}$  on the generators of each morphism space  $\mathcal{M}_-(\varepsilon^2, \varepsilon^1)$  by  $F^{0|0}(\underline{a}^-) = a^+$ . To show that  $F$  is, indeed, an  $\mathcal{A}\text{ug}_+(\Lambda)$ -bimodule isomorphism, we note from Lemma 6.11 and 6.12 that the structure maps for both bimodules agree under  $F$  and its naïve inverse. In particular, we have that the only terms in  $n_{\mathcal{M}_+}^{r|s}$  arising from thin disks — besides those realizing  $y^+$  as a strict unit — take inputs that are not in  $\mathcal{M}_+^{\text{Reeb}}$ . Further, since  $\underline{x}$  cannot be an input for the structure map of  $\mathcal{M}_+^{\text{Reeb}}$ , the doubly enriched disks used in Lemmas 6.11 and 6.12 match.  $\square$

Finally, we define the bimodule associated to the circle category.

**Definition 6.15.** The **circle bimodule**  $\mathcal{N}$  is the quotient  $\mathcal{M}_+/\mathcal{M}_-$ .

To better understand these bimodules, we note that  $\mathcal{M}_+$  and  $\mathcal{N}$  arise from diagonal bimodules. We state this relationship more precisely, using  $\pi : \mathcal{A}\text{ug}_+(\Lambda) \rightarrow \mathcal{C}(\Lambda)$  to denote the canonical projection functor to the quotient category. Again, we assume that all constructions involved are simply perturbed.

**Proposition 6.16.** *Assuming all structures are simply perturbed, the positive augmentation bimodule  $\mathcal{M}_+$  is isomorphic to the diagonal bimodule  $\mathcal{A}\text{ug}_+(\Lambda)_\Delta$ , while the circle bimodule is isomorphic to the pullback module  $\pi^* \mathcal{C}(\Lambda)_\Delta$ .*

*Proof.* Define a naïve morphism  $F : \mathcal{M}_+ \rightarrow \mathcal{A}\text{ug}_+(\Lambda)_\Delta$  on the generators of each morphism space  $\mathcal{M}_+(\varepsilon^2, \varepsilon^1)$  by  $F^{0|0}(\underline{a}^+) = a^+$ . That  $F$  is, indeed, an  $\mathcal{A}\text{ug}_+(\Lambda)$ -bimodule isomorphism follows from the observation made after the proof of Proposition 6.7 that by identifying  $\Lambda^{s+r+2}$  with  $\Lambda^{s+1,r+1}$ , the structure maps of  $\mathcal{A}\text{ug}_+(\Lambda)_\Delta$  are the same as those in Lemma 6.11.

The proof that  $\mathcal{N} \simeq \pi^*\mathcal{C}(\Lambda)_\Delta$  follows the same observation with appropriate quotients of the domains and codomains of the structure maps taken into account.  $\square$

The proposition above implies that the morphism spaces  $\mathcal{N}(\varepsilon^2, \varepsilon^1)$  are generated by  $x^+$  and  $y^+$ . Besides those dictated by strict unitality of  $y^+$ , the only nontrivial maps are

$$(6.6) \quad n_{\mathcal{N}}^{1|0}(x^+, y^+) = n_{\mathcal{N}}^{0|1}(y^+, x^+) = x^+.$$

We end this section with the following useful structural result that follows immediately from Lemma 3.15.

**Proposition 6.17.**  $\mathcal{M}_+$  is the mapping cone of a bimodule morphism  $\rho : \mathcal{N}[-1] \rightarrow \mathcal{M}_-$ .

The adjoint  $\rho^\vee : \mathcal{M}_-^\vee \rightarrow \mathcal{N}^\vee[1]$  of the morphism in the mapping cone above will be important in the proof of the main theorem in Section 7. As above, we may describe the map in terms of thin disks and doubly enriched disks in  $\Lambda$ . Note the cyclic permutation arising from taking the adjoint as in Lemma 6.13.

**Lemma 6.18.** In the definition of  $\rho^\vee : \mathcal{M}_-^\vee \rightarrow \mathcal{N}^\vee[1]$  between simply perturbed bimodules, thin disks yield the terms

$$(\rho^\vee)^{0|0}(\underline{a}^\vee) = (\varepsilon_1^1(a) + \varepsilon_1^2(a))y^\vee, \quad (\rho^\vee)^{1|0}(a^+, \underline{a}^\vee) = (\rho^\vee)^{0|1}(\underline{a}^\vee, a^+) = y^\vee.$$

Doubly enriched disks with mixed enrichment at a base point yield additional terms

$$(\rho^\vee)^{s|r}(\vec{a}, \underline{z}^\vee, \vec{b}) = \sum_{\substack{(u, \mathbf{w}_1, \mathbf{w}_2) \in \Delta_\Lambda^{s,r}(\underline{z}, \underline{\mathbf{a}}t^{\pm 1}\underline{\mathbf{b}}) \\ \hat{\alpha}^\vee(u, \mathbf{w}_1, \mathbf{w}_2) = a_1 \cdots a_s z b_r \cdots b_1}} \hat{\varepsilon}^1(\mathbf{a}) \hat{\varepsilon}^2(\mathbf{b}) x^\vee.$$

See the doubly enriched disks on the right side of Figure 20.

*Proof.* The construction of the map  $\rho$  in Lemma 3.15 shows that, for  $w = x^+$  or  $y^+$ ,  $\rho^{r|s}(b_r^+, \dots, b_1^+, \underline{w}, a_1^+, \dots, a_s^+)$  outputs the same terms as  $n_{\mathcal{M}_+}^{r|s}$  except for contributions of other  $x^+$  and  $y^+$  terms. Thus, the enumeration of the terms arising from thin disks follows from Lemma 6.11 after taking the adjoint as in Equation (3.4) in Section 3.3.2.

Similarly, the terms from the doubly enriched disks follow from recognizing that the only possible input into a thick disk for  $\rho$  is a maximum. Hence, once again, the enumeration of the terms arising from thick disks follows from Lemma 6.11 after taking the adjoint as in Equation (3.4).  $\square$

*Example 6.19.* We use Example 6.5 to illustrate the map  $\rho^\vee : \mathcal{M}_-^\vee \rightarrow \mathcal{N}^\vee[1]$  when both augmentations are  $\varepsilon_1$  (or  $\varepsilon_2$ ). The non-vanishing components are

$$\begin{aligned} (\rho^\vee)^{0|0}(\underline{a}_6^\vee) &= x^\vee, \\ (\rho^\vee)^{1|0}(a_i^+, \underline{a}_i^\vee) &= y^\vee, \\ (\rho^\vee)^{0|1}(\underline{a}_i^\vee, a_i^+) &= y^\vee. \end{aligned}$$

**6.4. The Separated Bimodule.** Our second application of Proposition 6.7 associates an  $\mathcal{A}\text{ug}_+(\Lambda)$ -bimodule to the separated 2-copy of  $\Lambda$ . As we shall see in this section, this bimodule encodes the augmentation bimodules  $\mathcal{M}_+$  and  $\mathcal{M}_-^\vee$  as parts of an acyclic mapping cone. The resulting quasi-isomorphism will be a key input into the algebraic machinery of Section 4 in the proof of the main theorem.

**Definition 6.20.** The **separated 2-copy bimodule**  $\widehat{\mathcal{M}}$  is defined to be the result of applying Proposition 6.7 to the separated 2-copy  $\widehat{\Lambda}$ .

As above, we only consider separated 2-copy bimodules defined by simply perturbed copies of  $\Lambda$ . In particular, the base category  $\mathcal{A}\text{ug}_+(\Lambda)$  is simply perturbed and the morphisms of  $\widehat{\mathcal{M}}$  are generated by Reeb chords of a simply perturbed separated 2-copy  $\widehat{\Lambda}$ . The structure maps  $n_{\widehat{\mathcal{M}}}^{r|s}$  count disks in a simply perturbed  $(s, r)$ -copy of  $\widehat{\Lambda}$ . Again,  $\widehat{\mathcal{M}}$  defined in this manner is termed **simply perturbed**.

In order to find the augmentation bimodules inside  $\widehat{\mathcal{M}}$ , we use Proposition 5.9 and the discussion afterwards to obtain, for all  $\varepsilon^1, \varepsilon^2 \in \text{ob}(\mathcal{A}\text{ug}_+(\Lambda))$ ,

$$(6.7) \quad \widehat{\mathcal{M}}(\varepsilon^2, \varepsilon^1) \simeq \text{Hom}_+(\varepsilon^2, \varepsilon^1) \oplus \text{Hom}_-^\vee(\varepsilon^2, \varepsilon^1)[-1].$$

Recall that, in the decomposition above, Reeb chords that generate  $\text{Hom}_+$  are denoted by  $q^+$ ,  $x^+$ , or  $y^+$ , while chords that generate  $\text{Hom}_-^\vee$  are denoted by  $p^-$ .

With respect to this decomposition, we find a submodule  $\mathcal{Q}$  of  $\widehat{\mathcal{M}}$  using the length filtration bimodule construction at length  $Z$ .

**Lemma 6.21.** *There exists a submodule  $\mathcal{Q}$  of  $\widehat{\mathcal{M}}$  so that, for all  $\varepsilon^1, \varepsilon^2 \in \text{ob}(\mathcal{A}\text{ug}_+(\Lambda))$ ,  $\mathcal{Q}(\varepsilon^2, \varepsilon^1) \simeq \text{Hom}_+(\varepsilon^2, \varepsilon^1)$ . Further, there is a quotient module  $\mathcal{P} = \widehat{\mathcal{M}}/\mathcal{Q}$  whose underlying vector spaces are generated by equivalence classes of generators of  $\text{Hom}_-^\vee(\varepsilon^2, \varepsilon^1)[-1]$ .*

We proceed to explicitly characterize the structure maps of  $\mathcal{Q}$  and  $\mathcal{P}$  in terms of thin disks and doubly enriched disks in  $\Lambda$ . In more detail, using Lemma 6.8 with Lemma 5.10 for thin disk contributions and Lemma 5.14(1) for enriched disk contributions yields the following lemma.

**Lemma 6.22.** *In the definition of*

$$n_{\mathcal{Q}}^{r|s} : \text{Hom}_+(\varepsilon^2) \otimes \mathcal{Q}(\varepsilon_1^2, \varepsilon_1^1) \otimes \text{Hom}_+(\varepsilon^1) \rightarrow \mathcal{Q}(\varepsilon_{r+1}^2, \varepsilon_{s+1}^1)$$

for a simply perturbed  $\mathcal{Q}$ , thin disks yield the terms dictated by the strict unitality of  $y^+$ , as well as the terms

$$\begin{aligned} n_{\mathcal{Q}}^{0|0}(\underline{y}^+) &= (\varepsilon_1(a) + \varepsilon_2(a)) q^+ & n_{\mathcal{Q}}^{1|0}(q^+, \underline{y}^+) &= n_+^{0|1}(\underline{y}^+, q^+) = q^+ \\ & & n_{\mathcal{Q}}^{1|0}(x^+, \underline{y}^+) &= n_+^{0|1}(\underline{y}^+, x^+) = x^+ \end{aligned}$$

Doubly enriched disks yield additional terms

$$n_{\mathcal{Q}}^{r|s}(\tilde{b}, \underline{w}^+, \vec{a}) = \sum_{\substack{(u, \mathbf{w}_1, \mathbf{w}_2) \in \Delta_{\Lambda}^{s,r}(\underline{z}, \check{\mathbf{a}}\underline{w}\check{\mathbf{b}}) \\ \hat{\alpha}(u, \mathbf{w}_1, \mathbf{w}_2) = a_s \cdots a_1 \underline{w} b_1 \cdots b_r}} \hat{\varepsilon}^1(\mathbf{a}) \hat{\varepsilon}^2(\mathbf{b}) z^+.$$

Next, the characterization of the structure maps  $n_{\mathcal{P}}$  of  $\mathcal{P}$  follows from Lemma 5.11 for thin disk contributions and Lemma 5.14(2) for enriched disk contributions. To explain this characterization, we first emphasize the cyclic permutation in the correspondence between enriched and lifted disks in Lemma 5.14(2). Second, the mixed enrichment for the enriched disks in Lemma 5.14(2) must lie at a Reeb chord in  $\Lambda$ . To match the enriched disks in the characterization of  $n_{\mathcal{P}}$  with those in the characterization of  $n_{\mathcal{M}_{-}^{\vee}}$  in Lemma 6.13, we apply Lemma 5.14(2) to enriched disks in  $\Delta_{\Lambda}^{s,r}(\underline{z}, \mathbf{a}\underline{w}\mathbf{b})$  in place of the enriched disks in  $\Delta_{\Lambda}^{r,s}(\underline{w}, \mathbf{b}\underline{w}\mathbf{a})$  that are referred to in the statement of the lemma.

**Lemma 6.23.** *In the definition of*

$$n_{\mathcal{P}}^{s|r} : \text{Hom}_+(\tilde{\varepsilon}^1) \otimes \mathcal{P}(\varepsilon_{s+1}^1, \varepsilon_{r+1}^2) \otimes \text{Hom}_+(\tilde{\varepsilon}^2) \rightarrow \mathcal{P}(\varepsilon_1^1, \varepsilon_1^2)$$

for a simply perturbed  $\mathcal{P}$ , thin disks yield the terms dictated by the strict unitality of  $y^+$ .

Doubly enriched disks with mixed enrichment at a Reeb chord yield additional terms

$$n_{\mathcal{P}}^{s|r}(\vec{a}, \underline{z}^-, \tilde{b}) = \sum_{\substack{(u, \mathbf{w}_1, \mathbf{w}_2) \in \Delta_{\Lambda}^{s,r}(\underline{z}, \check{\mathbf{a}}\underline{w}\check{\mathbf{b}}) \\ \hat{\alpha}^{\vee}(u, \mathbf{w}_1, \mathbf{w}_2) = a_1 \cdots a_s \underline{z} b_r \cdots b_1}} \hat{\varepsilon}^1(\mathbf{a}) \hat{\varepsilon}^2(\mathbf{b}) w^-.$$

A comparison of the characterizations of the structure maps for  $\mathcal{M}_{\pm}$ ,  $\mathcal{Q}$ , and  $\mathcal{P}$  leads to the following identification.

**Proposition 6.24.** *There are  $\text{Aug}_+(\Lambda)$ -bimodule isomorphisms  $\mathcal{M}_+ \simeq \mathcal{Q}$  and  $\mathcal{M}_{-}^{\vee}[-1] \simeq \mathcal{P}$ .*

*Proof.* Define a naïve morphism  $F : \mathcal{M}_+ \rightarrow \mathcal{Q}$  by  $F^{0|0}(\underline{a}_k^+) = q_k^+$ ,  $F^{0|0}(x^+) = x^+$ ,  $F^{0|0}(y^+) = y^+$ . We see from Lemmas 6.11 and 6.22 that the structure maps of  $\mathcal{M}_+$  and  $\mathcal{Q}$  agree under this identification, yielding  $\mathcal{M}_+ \simeq \mathcal{Q}$ .

Similarly, the naïve morphism  $G : \mathcal{M}_{-}^{\vee} \rightarrow \mathcal{P}$  defined on the generators by  $G^{0|0}(a^{\vee}) = p^-$ , combined with Lemmas 6.13 and 6.23, shows that  $\mathcal{M}_{-}^{\vee}[-1] \simeq \mathcal{P}$ .  $\square$

Finally, an application of Lemma 3.15 to  $(\widehat{\mathcal{M}}, \mathcal{Q})$  yields a bimodule morphism  $\eta : \mathcal{P}[-1] \rightarrow \mathcal{Q}$  with  $\widehat{\mathcal{M}} \simeq \text{Cone}(\eta)$ . The map  $\eta$  extends the linear duality map in [47] to the  $A_\infty$  bimodule setting.

**Proposition 6.25.** *The map  $\eta : \mathcal{P}[-1] \rightarrow \mathcal{Q}$  is a quasi-isomorphism. Thus, by a slight abuse of notation, there exists a bimodule quasi-isomorphism  $\eta : \mathcal{M}_-^\vee[-2] \rightarrow \mathcal{M}_+$ .*

*Proof.* There is a Legendrian isotopy of  $\widehat{\Lambda}$  that shifts  $\Lambda_1$  horizontally, e.g. in the  $x$  direction, so that the resulting link has no mixed chords. Thus, by the invariance of (bi-)linearized Legendrian contact homology, we see that  $\widehat{\mathcal{M}}$  is acyclic as a chain-level mapping cone and hence that  $\eta$  is a quasi-isomorphism.  $\square$

*Example 6.26.* Referring back to Example 6.5, we describe the thick disk contribution to the duality morphism  $\eta : \mathcal{M}_-^\vee[-1] \rightarrow \mathcal{M}_+$ . By Lemma 5.14 and Remark 5.13, such disks correspond to disks with either two positive punctures or with one positive puncture and a base point on the boundary in Figure 2. Different inputs of augmentations produce different maps in  $\eta$ . For instance, the thick disks yield the following terms to the collection of maps on  $\text{Hom}_+(\varepsilon_1, \dots, \varepsilon_1) \otimes \mathcal{M}_-^\vee(\varepsilon_1, \varepsilon_1) \otimes \text{Hom}_+(\varepsilon_1, \dots, \varepsilon_1)$ :

$$\begin{aligned} \eta^{0|0}(\underline{a}_1^\vee) &= a_2^+ + a_3^+ & \eta^{1|0}(a_4^+, \underline{a}_2^\vee) &= a_6^+ & \eta^{2|0}(a_5^+, a_4^+, \underline{a}_2^\vee) &= a_6^+ \\ \eta^{0|0}(\underline{a}_2^\vee) &= a_1^+ + a_6^+ & \eta^{1|0}(a_4^+, \underline{a}_7^\vee) &= a_3^+ & \eta^{2|0}(a_5^+, a_4^+, \underline{a}_7^\vee) &= a_3^+ \\ \eta^{0|0}(\underline{a}_3^\vee) &= a_1^+ + a_7^+ & \eta^{0|1}(\underline{a}_6^\vee, a_4^+) &= a_2^+ & \eta^{0|2}(\underline{a}_6^\vee, a_4^+, a_5^+) &= a_2^+ \\ \eta^{0|0}(\underline{a}_4^\vee) &= a_5^+ & \eta^{0|1}(\underline{a}_3^\vee, a_4^+) &= a_7^+ & \eta^{0|2}(\underline{a}_3^\vee, a_4^+, a_5^+) &= a_7^+ \\ \eta^{0|0}(\underline{a}_5^\vee) &= a_4^+ \\ \eta^{0|0}(\underline{a}_6^\vee) &= a_2^+ + y^+ \\ \eta^{0|0}(\underline{a}_7^\vee) &= a_3^+ \end{aligned}$$

A direct computation shows that the cohomology ring  $H^* \mathcal{M}_-^\vee(\varepsilon_1, \varepsilon_1)$  is generated by  $\{[a_1^\vee], [a_2^\vee], [a_6^\vee + a_7^\vee]\}$  and  $H^* \mathcal{M}_+(\varepsilon_1, \varepsilon_1)$  is generated by  $\{[a_2^+ + a_3^+], [a_1^+], [y^+]\}$ . Thus,  $\eta$  is, indeed, a quasi-isomorphism on  $\mathcal{M}_-^\vee(\varepsilon_1, \varepsilon_1)$ .

In the proof of the main theorem, we will need to identify disks in the definition of  $\pi_{\mathcal{N}}\eta : \mathcal{M}_-^\vee[-2] \rightarrow \mathcal{N}$  in a manner similar to that in Lemma 6.18.

**Lemma 6.27.** *In the definition of  $\pi_{\mathcal{N}}\eta : \mathcal{M}_-^\vee[-2] \rightarrow \mathcal{N}$  between simply perturbed bimodules, thin disks yield the following terms to  $\pi_{\mathcal{N}}\eta$ :*

$$(6.8) \quad \begin{aligned} (\pi_{\mathcal{N}}\eta)^{0|0}(\underline{a}^\vee) &= (\varepsilon_1^1(a) + \varepsilon_1^2(a))x^+ & (\pi_{\mathcal{N}}\eta)^{1|1}(x^+, \underline{a}^\vee, a^+) &= x^+ \\ (\pi_{\mathcal{N}}\eta)^{1|0}(a^+, \underline{a}^\vee) &= x^+ & (\pi_{\mathcal{N}}\eta)^{2|0}(x^+, a^+, \underline{a}^\vee) &= x^+ \\ (\pi_{\mathcal{N}}\eta)^{1|0}(x^+, \underline{a}^\vee) &= (\varepsilon_1^1(a) + \varepsilon_1^2(a))x^+ \\ (\pi_{\mathcal{N}}\eta)^{0|1}(\underline{a}^\vee, a^+) &= x^+ \end{aligned}$$

*Doubly enriched disks with mixed enrichment at a base point yield additional terms*

$$(6.9) \quad (\pi_{\mathcal{N}}\eta)^{s|r}(\vec{a}, \underline{z}^\vee, \bar{b}) = \sum_{\substack{(u, \mathbf{w}_1, \mathbf{w}_2) \in \Delta_\Lambda^{s,r}(\underline{z}, \check{\mathbf{a}}\underline{t}^{\pm 1}\check{\mathbf{b}}) \\ \hat{\alpha}^\vee(u, \mathbf{w}_1, \mathbf{w}_2) = a_1 \cdots a_s \underline{w} b_r \cdots b_1}} \hat{\varepsilon}^1(\mathbf{a}) \hat{\varepsilon}^2(\mathbf{b}) y^+,$$

where  $m_0 \leq 1$  and  $n_0 = 0$  if the mixed enrichment is at  $t$ , and  $m_0 = 0$  if the mixed enrichment is at  $t^{-1}$ .

Once again, see the doubly enriched disks on the right side of Figure 20, though care should be taken with  $m_0$  and  $n_0$  as in the statement of the lemma.

*Proof.* The formulae for the thin disks follows from Lemma 5.12, while the formula for the doubly enriched disks follows from Lemma 5.14(3). Once again, we apply Lemma 5.14(3) to enriched disks in  $\Delta_\Lambda^{s,r}(\underline{z}, \check{\mathbf{a}}\underline{t}^{\pm 1}\check{\mathbf{b}})$  in place of the enriched disks in  $\Delta_\Lambda^{r,s}(\underline{w}, \check{\mathbf{b}}\underline{t}^{\pm 1}\check{\mathbf{a}})$  that are referred to in the statement of the lemma.  $\square$

*Example 6.28.* From Example 6.26, we see that when all augmentations are  $\varepsilon_1$ , the only non-vanishing term in  $\pi_{\mathcal{N}}\eta$  arising from a thick disk is

$$(\pi_{\mathcal{N}}\eta)^{0|0}(a_6^\vee) = y^+.$$

## 7. PROOF OF THE MAIN THEOREM

With the algebraic tools of Section 4 and the geometric structures of Sections 5 and 6 in hand, we are ready to prove Theorem 1.1. The first step is to prove that when the augmentation category of a Legendrian knot is simply perturbed, there is a very weak relative Calabi-Yau structure of dimension  $-2$  on the morphism  $\rho^\vee : \mathcal{M}_-^\vee[-1] \rightarrow \mathcal{N}^\vee$ , which was defined in Proposition 6.17. This is accomplished in Sections 7.1 and 7.2.

After noting that  $(\mathcal{A}\text{ug}_+(\Lambda) \xrightarrow{\pi} \mathcal{C}(\Lambda), \mathcal{N}[-1] \xrightarrow{\rho} \mathcal{M}_-)$  is a conical pair, we then apply Proposition 4.4 to obtain a weak right relative Calabi-Yau structure of dimension 2 on  $\pi : \mathcal{A}\text{ug}_+(\Lambda) \rightarrow \mathcal{C}(\Lambda)$ , which completes the proof of Theorem 1.1. This is accomplished in Section 7.3.

**7.1. The Poincaré Duality Morphism.** We start by describing a weak Calabi-Yau structure of dimension 1 on  $\mathcal{N}$ . That is, we specify a bimodule quasi-isomorphism  $\theta : \mathcal{N}^\vee[-1] \rightarrow \mathcal{N}$ . Given that the generators of the underlying vector spaces of  $\mathcal{N}$  are  $x^+, y^+$ , we denote the dual basis for the underlying vector spaces of  $\mathcal{N}^\vee$  by  $x^\vee, y^\vee$ . We then have the following proposition.

**Proposition 7.1.** *The bimodule pre-morphism  $\theta : \mathcal{N}^\vee[-1] \rightarrow \mathcal{N}$  defined by*

$$(7.1) \quad \begin{aligned} \theta^{0|0}(y^\vee) &= x^+, & \theta^{0|1}(y^\vee, x^+) &= x^+, \\ \theta^{0|0}(\underline{x}^\vee) &= y^+, & \theta^{0|1}(\underline{x}^\vee, x^+) &= y^+, \end{aligned}$$

*with all other components vanishing, is an  $A_\infty$  bimodule quasi-isomorphism.*

The proof follows from a direct calculation using strict unitality, the formulae in Equation (6.6), and their adjoints.

The motivation for this construction is a Morse-theoretic proof of Poincaré Duality for  $S^1$ . Given a Morse function  $f : S^1 \rightarrow \mathbb{R}$ , swap the maximum and minimum by trading  $f$  for  $-f$ , and then compose with the continuation map for a homotopy of  $-f$  back to  $f$ . In the  $A_\infty$  setting, the swap of  $-f$  for  $f$  extends naïvely to a bimodule quasi-isomorphism from  $\mathcal{N}^\vee[-1]$  to  $\mathcal{N}$ . The map  $\theta$  above is then the composition of this quasi-isomorphism with an extension of the continuation map  $\Psi : \mathcal{N} \rightarrow \mathcal{N}$ . See Remark 7.3 for further discussion.

**7.2. Very Weak Calabi-Yau Structures.** At this point, we have obtained morphisms that fit into the following diagram, where the vertical morphisms are quasi-isomorphisms by Propositions 6.25 and 7.1.

$$(7.2) \quad \begin{array}{ccccccc} \cdots & \longrightarrow & \mathcal{M}_-^\vee[-2] & \xrightarrow{\rho^\vee} & \mathcal{N}^\vee[-1] & \xrightarrow{\pi_{\mathcal{N}}^\vee} & \mathcal{M}_+^\vee[-1] \longrightarrow \cdots \\ & & \downarrow \eta & & \downarrow \theta & & \downarrow \eta' \\ \cdots & \longrightarrow & \mathcal{M}_+ & \xrightarrow{\pi_{\mathcal{N}}} & \mathcal{N} & \xrightarrow{\rho} & \mathcal{M}_-[-1] \longrightarrow \cdots \end{array}$$

Once we show that the left square of the diagram commutes up to homotopy, we will be licensed to use Lemma 4.3 to complete the construction of the very weak Calabi-Yau structure on  $\rho^\vee : \mathcal{M}_-^\vee[-1] \rightarrow \mathcal{N}^\vee$ .

**Lemma 7.2.**  $\theta\rho^\vee \sim \pi_{\mathcal{N}}\eta$ .

We begin the proof of the lemma by characterizing the morphism  $\theta\rho^\vee$  in terms of thin disks and doubly enriched disks in  $\Lambda$ ; such a characterization for  $\pi_{\mathcal{N}}\eta$  already appeared in Lemma 6.27. We will then write down a homotopy  $H$  between the two morphisms, and finally verify that  $H$  is, indeed, a homotopy.

First, we use Lemma 6.18 and Proposition 7.1 to write down formulae for  $\theta\rho^\vee : \mathcal{M}_-^\vee[-2] \rightarrow \mathcal{N}$ . Fix augmentations  $\varepsilon_1^1, \dots, \varepsilon_{r+1}^1$  and  $\varepsilon_1^2, \dots, \varepsilon_{s+1}^2$ . A composition of the formula in Lemma 6.18 with Equation (7.1) shows that thin disks yield the following terms for  $\theta\rho^\vee$ :

$$(7.3) \quad \begin{aligned} (\theta\rho^\vee)^{0|0}(\underline{a}^\vee) &= (\varepsilon_1^1(a) + \varepsilon_1^2(a))x^+ & (\theta\rho^\vee)^{1|1}(a^+, \underline{a}^\vee, x^+) &= x^+ \\ (\theta\rho^\vee)^{1|0}(a^+, \underline{a}^\vee) &= x^+ & (\theta\rho^\vee)^{0|2}(\underline{a}^\vee, a^+, x^+) &= x^+ \\ (\theta\rho^\vee)^{0|1}(\underline{a}^\vee, a^+) &= x^+ \\ (\theta\rho^\vee)^{0|1}(\underline{a}^\vee, x^+) &= (\varepsilon_1^1(a) + \varepsilon_1^2(a))x^+ \end{aligned}$$

The composition of the formulae in Lemma 6.18 and Equation (7.1) shows that doubly enriched disks with mixed enrichment at a base point yield

additional terms

$$(7.4) \quad \theta^{0|0}(\rho^\vee)^{s|r}(\vec{a}, \underline{z}^\vee, \tilde{\vec{b}}) = \sum_{\substack{(u, \mathbf{w}_1, \mathbf{w}_2) \in \Delta_\Lambda^{s,r}(\underline{z}, \check{\mathbf{b}} \underline{t}^{\pm 1} \check{\mathbf{a}}) \\ \hat{\alpha}^\vee(u, \mathbf{w}_1, \mathbf{w}_2) = a_1 \cdots a_s \underline{z} b_r \cdots b_1}} \hat{\varepsilon}^1(\mathbf{a}) \hat{\varepsilon}^2(\mathbf{b}) y^+.$$

and

$$(7.5) \quad \theta^{0|1}((\rho^\vee)^{s|r-1}(\vec{a}, \underline{z}^\vee, \tilde{\vec{b}}), x^+) = \sum_{\substack{(u, \mathbf{w}_1, \mathbf{w}_2) \in \Delta_\Lambda^{s,r-1}(\underline{z}, \check{\mathbf{b}} \underline{t}^{\pm 1} \check{\mathbf{a}}) \\ \hat{\alpha}^\vee(u, \mathbf{w}_1, \mathbf{w}_2) = a_1 \cdots a_s \underline{z} b_r \cdots b_2}} \hat{\varepsilon}^1(\mathbf{a}) \hat{\varepsilon}^2(\mathbf{b}) y^+,$$

where  $\tilde{\vec{b}} = (b_r^+, \dots, b_2^+)$  in this case. All other components of  $\theta\rho^\vee$  vanish.

We claim that the pre-morphism  $H : \mathcal{M}_-^\vee[-2] \rightarrow \mathcal{N}$  defined by its non-vanishing components

$$(7.6) \quad \begin{aligned} H^{0|0}(\underline{a}^\vee) &= (\varepsilon_1^1(a) + \varepsilon_1^2(a)) y^+, \\ H^{1|0}(a^+, \underline{a}^\vee) &= y^+, \\ H^{0|1}(\underline{a}^\vee, a^+) &= y^+, \end{aligned}$$

is an  $A_\infty$  homotopy between  $\pi_N \eta$  and  $\theta\rho^\vee$ . Since we have explicit formulae for all of the maps, the proof will be a direct verification using the definition of homotopy (cf. Definition 3.11).

*Remark 7.3.* The continuation morphism  $\Psi : \mathcal{N} \rightarrow \mathcal{N}$  discussed after Proposition 7.1 and the homotopy  $H : \mathcal{M}_-^\vee[-2] \rightarrow \mathcal{N}$  used in the proof of Lemma 7.2 can both be interpreted geometrically. In our setup, the  $(s, r)$ -copy of the separated 2-copy is obtained via a triple of Morse functions  $(f, f, f)$ , where the second entry is used to perturb the separated 2-copy, while the first and third entries are used to perturb the  $s$ - and  $r$ -copy. We may also use  $(-f, f, -f)$  for the perturbation; see Figure 21 for a comparison. There is a Legendrian isotopy from  $\widehat{\Lambda}_{f,f,f}^{s,r}$  to  $\widehat{\Lambda}_{-f,f,-f}^{s,r}$  induced by a sequence of Reidemeister III that moves the  $y$  chords for the  $s$ - and  $r$ -copies around the knot. The corresponding components of the induced DGA map yield  $\Psi$  and  $H$ .

Consider an input of the form  $(\tilde{\vec{b}}, \underline{a}^\vee, \vec{a})$ . The verification that  $H$  is a homotopy breaks down to what type of generators the input begins and ends with. In particular, we consider the following three cases:

**Case 1:** Both  $a_s$  and  $b_r$  are in  $\mathcal{R}_\Lambda$  (or are empty),

**Case 2:** One of  $a_s$  and  $b_r$  is in  $\mathcal{R}_f$  and the other is in  $\mathcal{R}_\Lambda$  (or is empty),

**Case 3:** Both  $a_s$  and  $b_r$  are in  $\mathcal{R}_f$ .

**7.2.1. Case 1.** We begin by considering Case 1, detailing two special cases in Claims 7.4 and 7.5. The verification of the general case follows the same ideas as in the second claim. The proofs of these and subsequent claims are all structured in the same way: terms in the homotopy equation arising from thin disks cancel by direct computation using the explicit characterizations of  $\theta\rho^\vee$ ,  $\pi\eta$ , and  $H$ , while one class of terms arising from thick disks form

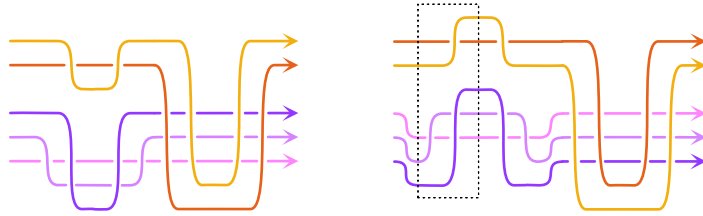


FIGURE 21. A comparison of the perturbation functions  $(f, f, f)$  at left and  $(-f, f, -f)$  at right for the separated 2-copy. By isotoping the boxed  $y$  chords for the  $s$ - and  $r$ -copies in the  $(-f, f, -f)$  perturbation leftwards around the knot, we recover the  $(f, f, f)$  perturbation.

telescoping sums whose “ends” cancel with other terms that also arise from thick disks. The differences lie in which thick disks are involved and in how the “ends” of the telescoping sums are canceled.

**Claim 7.4.** *Definition 3.11 holds for a single input  $a^\vee$ .*

*Proof.* In this case, the homotopy equation from Definition 3.11 reads as follows:

$$(7.7) \quad (\pi_{\mathcal{N}}\eta)^{0|0}(\underline{a}^\vee) + (\theta\rho^\vee)^{0|0}(\underline{a}^\vee) = H^{0|0}n_{\mathcal{M}_-^\vee}^{0|0}(\underline{a}^\vee) + n_{\mathcal{N}}^{0|0}H^{0|0}(\underline{a}^\vee).$$

The formulae (6.8) and (7.3) show that terms arising from thin disks that contribute to  $(\pi_{\mathcal{N}}\eta)^{0|0}(\underline{a}^\vee)$  and  $(\theta\rho^\vee)^{0|0}(\underline{a}^\vee)$  cancel. On the other side, we know that  $n_{\mathcal{N}}^{0|0} = 0$  by the discussion after Proposition 6.16, and that no thin disks contribute to  $n_{\mathcal{M}_-^\vee}^{0|0}$  by Lemma 6.13.

Turning to thick disks, we first note that contributions to  $(\pi_{\mathcal{N}}\eta)^{0|0}(\underline{a}^\vee)$  and  $(\theta\rho^\vee)^{0|0}(\underline{a}^\vee)$  cancel since the formulae in Equations (6.9) and (7.4) match precisely when  $r = s = 0$ . In particular, thick disk contributions to these terms arise from the same doubly enriched disks.

For the final term in Equation (7.7), we need only verify that

$$(7.8) \quad H^{0|0}n_{\mathcal{M}_-^\vee}^{0|0}(\underline{a}^\vee) = 0.$$

Lemma 6.13 shows that  $n_{\mathcal{M}_-^\vee}^{0|0}(\underline{a}^\vee)$  counts doubly enriched disks with no enrichments other than the mixed enrichment at a Reeb chord. Rewriting the contributions to  $n_{\mathcal{M}_-^\vee}^{0|0}(\underline{a}^\vee)$  in terms of the collection of all disks in  $\Lambda$  with a positive corner at  $a$  (which we denote  $\Delta(a, \mathbf{a})$  for notational compactness) yields the following formula, illustrated in Figure 22:

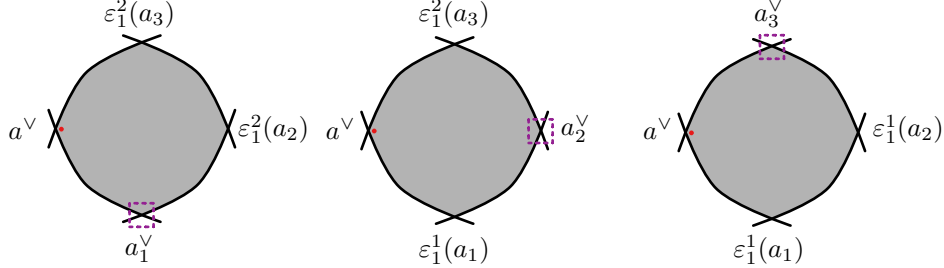


FIGURE 22. The disk in  $\Lambda$  pictured has multiple possible mixed enrichments, each of which could contribute to  $n_{\mathcal{M}_-}^{0|0}(\underline{a}^\vee)$ , depending on the value the augmentations  $\varepsilon_1^1$  and  $\varepsilon_1^2$  take on the non-enriched negative corners. The corners are labeled with these augmentation values and the potential output that appear in Equation (7.9).

$$(7.9) \quad n_{\mathcal{M}_-}^{0|0}(\underline{a}^\vee) = \sum_{\Delta(a, \mathbf{a})} \sum_{k=1}^n \varepsilon_1^2(a_1) \cdots \varepsilon_1^2(a_{k-1}) \varepsilon_1^1(a_{k+1}) \cdots \varepsilon_1^1(a_n) a_k^\vee.$$

It follows that

$$\begin{aligned} H^{0|0} n_{\mathcal{M}_-}^{0|0}(\underline{a}^\vee) &= \sum_{\Delta(a, \mathbf{a})} \sum_{k=1}^n (\varepsilon_1^2(a_1) \cdots \varepsilon_1^2(a_{k-1}) \varepsilon_1^1(a_k) \varepsilon_1^1(a_{k+1}) \cdots \varepsilon_1^1(a_n)) \\ &\quad + \varepsilon_1^2(a_1) \cdots \varepsilon_1^2(a_{k-1}) \varepsilon_1^2(a_k) \varepsilon_1^1(a_{k+1}) \cdots \varepsilon_1^1(a_n)) y^+. \end{aligned}$$

This is a telescoping sum, and hence we obtain

$$\begin{aligned} H^{0|0} n_{\mathcal{M}_-}^{0|0}(\underline{a}^\vee) &= \sum_{\Delta(a, \mathbf{a})} (\varepsilon_1^2(a_1) \cdots \varepsilon_1^2(a_n) + \varepsilon_1^1(a_1) \cdots \varepsilon_1^1(a_n)) y^+ \\ &= (\varepsilon_1^2 \circ \partial(a) + \varepsilon_1^1 \circ \partial(a)) y^+ \\ &= 0, \end{aligned}$$

where  $\partial$  is the differential of the Chekanov-Eliashberg DGA of  $\Lambda$ , and hence has the property that  $\varepsilon_1^2 \circ \partial = \varepsilon_1^1 \circ \partial = 0$ . In all, we have shown that Equation (7.8) holds, and the claim follows.  $\square$

**Claim 7.5.** *Definition 3.11 holds for inputs of the form  $(\underline{a}^\vee, a_j^+)$ , where  $a_j \in \mathcal{R}_\Lambda$ .*

*Proof.* In this case, the homotopy equation from Definition 3.11 reads as follows:

$$\begin{aligned} (7.10) \quad &(\pi_{\mathcal{N}} \eta)^{0|1}(\underline{a}^\vee, a_j^+) + (\theta \rho^\vee)^{0|1}(\underline{a}^\vee, a_j^+) = \\ &H^{0|0} n_{\mathcal{M}_-}^{0|1}(\underline{a}^\vee, a_j^+) + H^{0|1}(n_{\mathcal{M}_-}^{0|0}(\underline{a}^\vee), a_j^+) + H^{0|1}(\underline{a}^\vee, m_+^1(a_j^+)) \\ &\quad + n_{\mathcal{N}}^{0|1}(H^{0|0}(\underline{a}^\vee), a_j^+) + n_{\mathcal{N}}^{0|0}(H^{0|1}(\underline{a}^\vee, a_j^+)). \end{aligned}$$

Both  $n_{\mathcal{N}}^{0|1}(H^{0|0}(\underline{a}^{\vee}), a_j^+)$  and  $n_{\mathcal{N}}^{0|0}(H^{0|1}(\underline{a}^{\vee}, a_j^+))$  vanish according to the definition of  $n_{\mathcal{N}}$ . For the remaining terms, we follow a similar analysis of thin and thick disks as in the previous proof..

First, the formulae (6.8) and (7.3) show that terms arising from thin disks that contribute to  $(\pi_{\mathcal{N}}\eta)^{0|1}(\underline{a}^{\vee}, a_j^+)$  and  $(\theta\rho^{\vee})^{0|1}(\underline{a}^{\vee}, a_j^+)$  cancel. Lemma 6.13 shows that no thin disks contribute to other terms in the equation.

Turning to thick disks, we see that contributions to  $(\pi_{\mathcal{N}}\eta)^{0|1}(\underline{a}^{\vee}, a_j^+)$  and  $(\theta\rho^{\vee})^{0|1}(\underline{a}^{\vee}, a_j^+)$  cancel since formulae in Equations (6.9) and (7.4) match precisely when  $r = 0$  and  $s = 1$ . Thus, we need only verify that, for thick disk contributions, we have

$$(7.11) \quad H^{0|0}n_{\mathcal{M}_{\underline{\mathbf{a}}}^{\vee}}^{0|1}(\underline{a}^{\vee}, a_j^+) + H^{0|1}(n_{\mathcal{M}_{\underline{\mathbf{a}}}^{\vee}}^{0|0}(\underline{a}^{\vee}), a_j^+) + H^{0|1}(\underline{a}^{\vee}, m_+^1(a_j^+)) = 0.$$

Lemma 6.13 shows that  $n_{\mathcal{M}_{\underline{\mathbf{a}}}^{\vee}}^{0|1}(\underline{a}^{\vee}, a_j^+)$  counts doubly enriched disks with a pure enrichment in  $\mathbf{w}_1$  at  $a_j$  and a mixed enrichment at a Reeb chord counterclockwise between  $a$  and  $a_j$ . Rewriting these contributions in terms of disks in  $\Lambda$  with a positive corner at  $a$  and negative corners counterclockwise at  $a_{i_1}, \dots, a_{i_m}, a_j, a_{j_n}, \dots, a_{j_1}$  yields the following formula, illustrated in Figure 23:

$$(7.12) \quad n_{\mathcal{M}_{\underline{\mathbf{a}}}^{\vee}}^{0|1}(\underline{a}^{\vee}, a_j^+) = \sum_{\Delta(a, \mathbf{a})} \sum_{k=1}^m \varepsilon_1^2(a_{i_1}) \cdots \varepsilon_1^2(a_{i_{k-1}}) \varepsilon_2^1(a_{i_{k+1}}) \cdots \varepsilon_2^1(a_{i_m}) \varepsilon_1^1(a_{j_1}) \cdots \varepsilon_1^1(a_{j_n}) a_{i_k}^{\vee}.$$

As above, the telescoping nature of the sum yields the following:

$$(7.13) \quad H^{0|0}n_{\mathcal{M}_{\underline{\mathbf{a}}}^{\vee}}^{0|1}(\underline{a}^{\vee}, a_j^+) = \sum_{\Delta(a, \mathbf{a})} (\varepsilon_1^2(a_{i_1}) \cdots \varepsilon_1^2(a_{i_m}) \varepsilon_1^1(a_{j_1}) \cdots \varepsilon_1^1(a_{j_n}) + \varepsilon_2^1(a_{i_1}) \cdots \varepsilon_2^1(a_{i_m}) \varepsilon_1^1(a_{j_1}) \cdots \varepsilon_1^1(a_{j_n})) y^+.$$

Next, we consider  $H^{0|1}(n_{\mathcal{M}_{\underline{\mathbf{a}}}^{\vee}}^{0|0}(\underline{a}^{\vee}), a_j^+)$ . This term can only be nonzero when  $n_{\mathcal{M}_{\underline{\mathbf{a}}}^{\vee}}^{0|0}(\underline{a}^{\vee}) = a_j^{\vee}$ , and Lemma 6.13 shows that such contributions arise from the same underlying disks as above, but with no enrichment other than the mixed enrichment at  $a_j$ . The result is the following:

$$(7.14) \quad H^{0|1}(n_{\mathcal{M}_{\underline{\mathbf{a}}}^{\vee}}^{0|0}(\underline{a}^{\vee}), a_j^+) = \sum_{\Delta(a, \mathbf{a})} \varepsilon_1^2(a_{i_1}) \cdots \varepsilon_1^2(a_{i_m}) \varepsilon_1^1(a_{j_1}) \cdots \varepsilon_1^1(a_{j_n}) y^+.$$

Finally,  $H^{0|1}(\underline{a}^{\vee}, m_+^1(a_j^+))$  is non-vanishing only if  $m_+^1(a_j^+) = a^+$ , and Lemma 6.3 shows that such contributions arise from the same disks as above with a single enrichment at  $a_j$ . This yields a similar formula as above, but with a different set of augmentations involved due to the difference of the

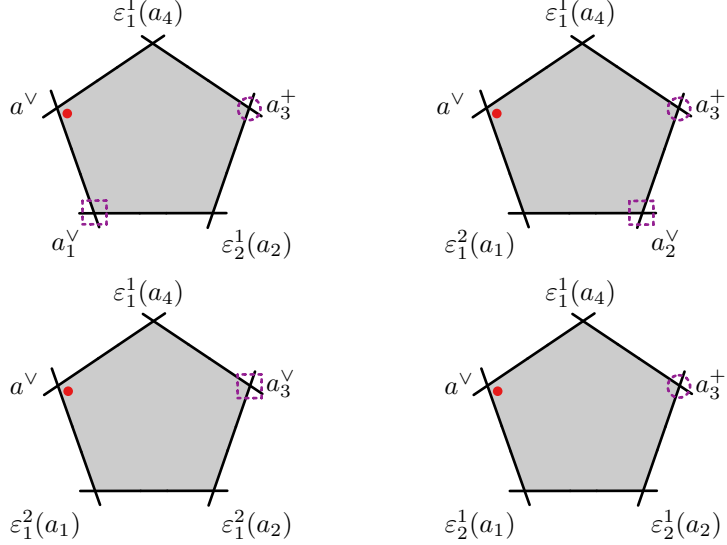


FIGURE 23. The disk in  $\Lambda$  pictured has multiple possible enrichments. The disks in the top row could contribute to  $n_{\mathcal{M}^-}^{0|1}(\underline{a}^\vee, a_j^+)$ , depending on the value the augmentations take on the non-enriched negative corners; here,  $j = 3$ . The disk at bottom left could contribute to  $H^{0|1}(n_{\mathcal{M}^-}^{0|0}(\underline{a}^\vee), a_j^+)$ , while the disk at bottom right could contribute to  $H^{0|1}(\underline{a}^\vee, m_+^1(a_j^+))$ .

domains:

$$(7.15) \quad H^{0|1}(\underline{a}^\vee, m_+^1(a_j^+)) = \sum_{\Delta(a, \mathbf{a})} \varepsilon_2^1(a_{i_1}) \cdots \varepsilon_2^1(a_{i_m}) \varepsilon_1^1(a_{j_1}) \cdots \varepsilon_1^1(a_{j_n}) y^+.$$

Putting the formulae (7.13), (7.14), and (7.15) together, we see that the desired Equation (7.11) holds.  $\square$

As mentioned above, a similar argument using disks with more pure enrichments works for longer inputs that begin and end with generators in  $\mathcal{R}_\Lambda$ .

**7.2.2. Case 2.** Next, we verify the homotopy equation when one of  $a_s$  and  $b_r$  is in  $\mathcal{R}_f$  or the other is in  $\mathcal{R}_\Lambda$  (or is empty). As above, we detail three special cases in Claims 7.6, 7.7, and 7.8. The remaining cases either follow from symmetric or slightly generalized arguments with no new ideas necessary.

We first examine a case with a  $y^+$  as part of the input.

**Claim 7.6.** *Definition 3.11 holds for inputs of the form  $(\underline{a}^\vee, y^+)$ .*

*Proof.* Having  $y^+$  as one of the input variables implies that only thin disks are involved in the verification of the homotopy equation, which is of the

same form as Equation (7.10) with  $y^+$  in place of  $a_j^+$ . The formulae in Equations (6.8) and (7.3) show that the terms in  $(\pi_N \eta)^{0|1}$  and  $(\theta \rho^\vee)^{0|1}$  vanish. Of the remaining terms,  $n_N^{0|0}(H^{0|1}(\underline{a}^\vee, y^+))$  and  $H^{0|1}(n_{M_-}^{0|0}(\underline{a}^\vee), y^+)$  vanish by the definition of  $H$ , while  $H^{0|1}(\underline{a}^\vee, m_+^1(y^+))$  vanishes since  $m_+^1(y^+) = 0$  for simply perturbed augmentation categories. Finally, both  $H^{0|0}n_{M_-}^{0|1}(\underline{a}^\vee, y^+)$  and  $n_N^{0|1}(H^{0|0}(\underline{a}^\vee), y^+)$  are equal to  $(\varepsilon_1^1(a) + \varepsilon_1^2(a))y^+$ , and hence cancel.  $\square$

A similar computation holds for any inputs in Case 2 that begin or end with  $y^+$ . Inputs that begin or end with  $x^+$  are more subtle, as they involve thick disks as well as thin ones.

**Claim 7.7.** *Definition 3.11 holds for inputs of the form  $(\underline{a}^\vee, x^+)$ .*

*Proof.* In parallel to Equation (7.10), we want to verify that

$$(7.16) \quad \begin{aligned} & (\pi_N \eta)^{0|1}(\underline{a}^\vee, x^+) + \theta^{0|0}(\rho^\vee)^{0|1}(\underline{a}^\vee, x^+) + \theta^{0|1}((\rho^\vee)^{0|0}(\underline{a}^\vee), x^+) = \\ & H^{0|0}n_{M_-}^{0|1}(\underline{a}^\vee, x^+) + H^{0|1}(n_{M_-}^{0|0}(\underline{a}^\vee), x^+) + H^{0|1}(\underline{a}^\vee, m_+^1(x^+)) \\ & + n_N^{0|0}H^{0|1}(\underline{a}^\vee, x^+) + n_N^{0|1}(H^{0|0}(\underline{a}^\vee), x^+). \end{aligned}$$

By definition of  $H$  and of  $n_N$ , observe that the terms  $H^{0|1}(n_{M_-}^{0|0}(\underline{a}^\vee), x^+)$  and  $n_N^{0|0}(H^{0|1}(\underline{a}^\vee, x^+))$  both vanish. As in previous claims, terms coming from the thin disks cancel by direct computation using Equations (6.8), (7.3) and (7.6). Further, the thick disks that contribute terms to  $H^{0|0}n_{M_-}^{0|1}(\underline{a}^\vee, x^+)$ ,  $H^{0|1}(\underline{a}^\vee, m_+^1(x^+))$ , and  $\theta^{0|1}(\rho^\vee)^{0|0}(\underline{a}^\vee), x^+$  cancel using a telescoping sum argument similar to that in the proof of Claim 7.5.

The thick disks beyond those that appear in the telescoping sum contribute to  $(\pi_N \eta)^{0|1}(\underline{a}^\vee, x^+)$  and  $\theta^{0|0}\rho^{0|1}(\underline{a}^\vee, x^+)$ . Equations (6.9) and (7.4) show that contributions come from doubly enriched disks with a positive corner at  $a$ , a pure enrichment in  $\mathbf{w}_2$  at  $t^{\pm 1}$ , and the mixed enrichment at  $t^{\pm 1}$ . There are two possibilities for the underlying disks. First, the  $x^+$  could correspond to a pure enrichment at index 0 (i.e.  $n_0 = 1$ , which is possible for both  $\theta \rho^\vee$  and  $\pi_N \eta$ ). Second, the  $x^+$  could correspond to a pure enrichment at a nonzero index, which arises when the disk passes through the base point at least twice. In either case, the terms in  $\theta \rho^\vee$  and  $\pi_N \eta$  cancel.  $\square$

In fact, a similar computation holds for any inputs in Case 2 that end with  $x^+$  because enrichments at index 0 for the  $t^{-1}$  markings in Lemma 6.27 and in (7.4) and (7.5) are handled similarly when the  $x^+$  coefficients come after  $\underline{a}^\vee$ . For inputs that begin with  $x^+$ , the argument can be more subtle because of the asymmetry in how basepoints are handled in Lemma 6.27. We detail the case with inputs of the form  $(x^+, \underline{a}^\vee, a_j^+)$ ; other cases beginning with  $x^+$  follow the same pattern with no new ideas.

**Claim 7.8.** *Definition 3.11 holds for inputs of the form  $(x^+, \underline{a}^\vee, a_j^+)$ , where  $a_j \in \mathcal{R}_\Lambda$ .*

*Proof.* In this case, we want to verify that

$$(7.17) \quad \begin{aligned} & (\pi_N \eta)^{1|1}(x^+, \underline{a}^\vee, a_j^+) + \theta^{0|0}(\rho^\vee)^{1|1}(x^+, \underline{a}^\vee, a_j^+) \\ &= H^{0|0} n_{\mathcal{M}_-^\vee}^{1|1}(x^+, \underline{a}^\vee, a_j^+) + H^{0|1}(n_{\mathcal{M}_-^\vee}^{1|0}(x^+, \underline{a}^\vee), a_j^+) \\ & \quad + n_N^{0|1}(x^+, H^{0|1}(\underline{a}^\vee, a_j^+)), \end{aligned}$$

where we only display terms that do not vanish a priori. The analysis is similar to the previous proof with one new ingredient. Again, terms coming from the thin disks cancel by direct computation.

Turning to thick disks, a similar analysis to that in the proof of Claim 7.5 will show that the thick disk contributions to  $H^{0|0} n_{\mathcal{M}_-^\vee}^{1|1}(x^+, \underline{a}^\vee, a_j^+)$  and  $H^{0|1}(n_{\mathcal{M}_-^\vee}^{1|0}(x^+, \underline{a}^\vee), a_j^+)$  will cancel with *some* of the thick disk contributions to either  $\theta^{0|0}(\rho^\vee)^{1|1}(x^+, \underline{a}^\vee, a_j^+)$  or  $\pi_N^{0|0} \eta^{1|1}(x^+, \underline{a}^\vee, a_j^+)$ . In more detail, Lemma 6.13 shows that thick disk contributions to  $n_{\mathcal{M}_-^\vee}^{1|1}(x^+, \underline{a}^\vee, a_j^+)$  arise from doubly enriched disks with a positive corner at the Reeb chord  $a$ , a pure enrichment in  $\mathbf{w}_1$  at  $t^{\pm 1}$ , a pure enrichment in  $\mathbf{w}_2$  at  $a_j$ , and mixed enrichment at a Reeb chord that lies counterclockwise between  $t^{\pm 1}$  and  $a_j$ . As in the proof of Claim 7.5, for each of the underlying disks,  $H^{0|0} n_{\mathcal{M}_-^\vee}^{1|1}(x^+, \underline{a}^\vee, a_j^+)$  is a telescoping sum. One end of this sum cancels with a term in  $H^{0|1}(n_{\mathcal{M}_-^\vee}^{1|0}(x^+, \underline{a}^\vee), a_j^+)$ , which comes from doubly enriching the disk involved with a pure enrichment in  $\mathbf{w}_1$  at  $t^{\pm 1}$  and mixed enrichment at  $a_j$  that lies counterclockwise between  $t^{\pm 1}$  and  $a$ .

The other end of the telescoping sum is more subtle to cancel. Equations (6.9) and (7.4) show that the other end of the telescoping sum cancels with a term in either  $\pi_N^{0|0} \eta^{1|1}(x^+, \underline{a}^\vee, a_j^+)$  or  $\theta^{0|0}(\rho^\vee)^{1|1}(x^+, \underline{a}^\vee, a_j^+)$ , depending on whether the disk involved has a pure enrichment at  $t$  or  $t^{-1}$  for its contribution to  $n_{\mathcal{M}_-^\vee}^{1|1}(x^+, \underline{a}^\vee, a_j^+)$ . Specifically, if the enrichment is at  $t$ , the sum cancels with a term in  $\pi_N^{0|0} \eta^{1|1}(x^+, \underline{a}^\vee, a_j^+)$  that comes from doubly enriching the disk involved with a pure enrichment  $0 \in \mathbf{w}_1$  at  $t$ , a pure enrichment in  $\mathbf{w}_2$  at  $a_j$ , and the mixed enrichment at  $t$  again; the disk does not contribute to  $\theta^{0|0}(\rho^\vee)^{1|1}(x^+, \underline{a}^\vee, a_j^+)$  since the index 0 cannot be purely enriched if the mixed enrichment is a  $t$ . Otherwise, the sum cancels with a term in  $\theta^{0|0}(\rho^\vee)^{1|1}(x^+, \underline{a}^\vee, a_j^+)$  that comes from doubly enriching the disk involved with a pure enrichment  $0 \in \mathbf{w}_1$  at  $t^{-1}$ , a pure enrichment in  $\mathbf{w}_2$  at  $a_j$ , and the mixed enrichment at  $t^{-1}$  again; the disk does not contribute to  $\pi_N^{0|0} \eta^{1|1}(x^+, \underline{a}^\vee, a_j^+)$  according to Lemma 6.27.

Finally, Equation (6.9) and Equation (7.4) show that the remaining thick disk contributions to  $\pi_{\mathcal{N}}^{0|0}\eta^{1|1}(x^+, \underline{a}^\vee, a_j^+)$  and  $\theta^{0|0}(\rho^\vee)^{1|1}(x^+, \underline{a}^\vee, a_j^+)$  both arise from doubly enriched disks with a positive corner at  $a$ , a pure enrichment in  $\mathbf{w}_1$  at  $t^{\pm 1}$ , a pure enrichment in  $\mathbf{w}_2$  at  $a_j$ , and mixed enrichment at  $t^{\pm 1}$  that lies *strictly* between the pure enrichments  $t^{\pm 1}$  and  $a_j$  counterclockwise. Thus, they cancel out.  $\square$

**7.2.3. Case 3.** It remains to consider inputs in Case 3. If either  $a_r$  or  $b_s$  is  $y$ , only thin disks may be involved and it is a direct check that all terms in the homotopy equation vanish. Thus, we are led to the case  $a_r = b_s = x$ . As above, we detail the case when the input is  $(x^+, \underline{a}^\vee, x^+)$ . The remaining cases follow similar arguments with no new ideas necessary.

**Claim 7.9.** *Definition 3.11 holds for inputs of the form  $(x^+, \underline{a}^\vee, x^+)$ .*

*Proof.* In parallel to Equation (7.17), we want to verify that

$$(7.18) \quad \begin{aligned} (\pi_{\mathcal{N}}\eta)^{1|1}(x^+, \underline{a}^\vee, x^+) + \theta^{0|0}(\rho^\vee)^{1|1}(x^+, \underline{a}^\vee, x^+) + \theta^{0|1}((\rho^\vee)^{1|0}(x^+, \underline{a}^\vee), x^+) \\ = H^{0|0}n_{\mathcal{M}_-}^{1|1}(x^+, \underline{a}^\vee, x^+), \end{aligned}$$

where, as above, we only present terms that do not vanish a priori. Observe that there is no thin disk contribution to the equation. Turning to thick disks, first, the thick disks that contribute terms to  $H^{0|0}n_{\mathcal{M}_-}^{1|1}(x^+, \underline{a}^\vee, x^+)$  cancel with *some* of the thick disk contributions to  $\theta^{0|1}((\rho^\vee)^{1|0}(x^+, \underline{a}^\vee), x^+)$  and either to  $\theta^{0|0}(\rho^\vee)^{1|1}(x^+, \underline{a}^\vee, x^+)$  or  $(\pi_{\mathcal{N}}\eta)^{1|1}(x^+, \underline{a}^\vee, x^+)$  using a telescoping sum argument as in Claim 7.8.

The only new feature in this case is that Equation (7.5) shows that there is thick disk contribution to the term  $\theta^{0|1}((\rho^\vee)^{1|0}(x^+, \underline{a}^\vee), x^+)$  that comes from doubly enriched disks with a pure enrichment  $0 \in \mathbf{w}_1$  at  $t^{-1}$  and the mixed enrichment at  $t^{-1}$  again. The same underlying disks contribute to  $\theta^{0|0}(\rho^\vee)^{1|1}(x^+, \underline{a}^\vee, x^+)$  by pure enrichments  $0 \in \mathbf{w}_1, \mathbf{w}_2$  at  $t^{-1}$  and the mixed enrichment at  $t^{-1}$  again. Thus, they cancel out.

Finally, Equation (6.9) and Equation (7.4) show that the remaining thick disk contributions to  $\pi_{\mathcal{N}}^{0|0}\eta^{1|1}(x^+, \underline{a}^\vee, x^+)$  and  $\theta^{0|0}(\rho^\vee)^{1|1}(x^+, \underline{a}^\vee, x^+)$  cancel as before.  $\square$

**7.3. Weak Relative Calabi-Yau Structures.** In summary, using Lemma 4.3, we obtain by Proposition 6.24, Proposition 7.1, and Lemma 7.2 the promised very weak relative Calabi-Yau structure on  $\rho : \mathcal{N}[-1] \rightarrow \mathcal{M}_-$ . In sum, we obtain:

**Proposition 7.10.** *Suppose  $\text{Aug}_+(\Lambda)$  is simply perturbed. There is a very weak relative Calabi-Yau structure of dimension  $-2$  on the morphism  $\rho : \mathcal{N}[-1] \rightarrow \mathcal{M}_-$  defined in Proposition 6.17.*

By Proposition 6.17, observe that  $(\mathcal{A}\text{ug}_+(\Lambda) \xrightarrow{\pi} \mathcal{C}(\Lambda), \mathcal{N}[-1] \xrightarrow{\rho} \mathcal{M}_-)$  is a conical pair. The main theorem of the paper, Theorem 1.1, then follows from Propositions 4.4 and 7.10.

*Remark 7.11.* We return to Remark 1.2 now that all of the categories and bimodules have been defined and the commutative diagrams underlying the main theorem have been explained. To see that Theorem 1.1 truly is a generalization of the duality long exact sequence of [15], fix an augmentation  $\varepsilon$  and consider Diagram (1.1) at the linear level. Use Proposition 6.14, Definition 6.15, and Proposition 6.16 to translate the bimodule vector spaces to the morphism spaces of  $\mathcal{A}\text{ug}_\pm(\Lambda)$  and  $\mathcal{C}$ . In the derived category, the top line of the diagram thus becomes

$$\cdots \longrightarrow H^k \text{Hom}_+(\varepsilon, \varepsilon) \longrightarrow H^k(\Lambda) \longrightarrow H^{k+1} \text{Hom}_-(\varepsilon, \varepsilon) \longrightarrow \cdots$$

Use the leftmost vertical quasi-isomorphism in Diagram (1.1) — that is, the quasi-isomorphism from Proposition 6.25 — to replace  $H^k \text{Hom}_+(\varepsilon, \varepsilon)$  with  $H^{k-2} \text{Hom}_-^\vee(\varepsilon, \varepsilon)$ . Finally, as noted in [43, §5.2], we may translate  $H^k \text{Hom}_-(\varepsilon, \varepsilon)$  to  $LCH^{k-1}(\varepsilon)$  and  $H^{k-2} \text{Hom}_-^\vee(\varepsilon, \varepsilon)$  to  $LCH_{-k+1}(\varepsilon)$ . Thus, we obtain the original duality long exact sequence described in Theorem 2.8.

## REFERENCES

1. Johan Asplund, *Singular Legendrian unknot links and relative Ginzburg algebras*, Available as arXiv:2311.03330, 2023.
2. Frédéric Bourgeois and Baptiste Chantraine, *Bilinearized Legendrian contact homology and the augmentation category*, J. Symplectic Geom. **12** (2014), no. 3, 553–583. MR 3248668
3. Christopher Brav and Tobias Dyckerhoff, *Relative Calabi-Yau structures*, Compos. Math. **155** (2019), no. 2, 372–412. MR 3911626
4. Emily E. Casey and Michael B. Henry, *Computing homology invariants of Legendrian knots*, J. Knot Theory Ramifications **23** (2014), no. 11, 1450056, 18. MR 3293043
5. Baptiste Chantraine, Georgios Dimitroglou Rizell, Paolo Ghiggini, and Roman Golovko, *Floer theory for Lagrangian cobordisms*, J. Differential Geom. **114** (2020), no. 3, 393–465. MR 4072203
6. Yuri Chekanov, *Differential algebra of Legendrian links*, Invent. Math. **150** (2002), 441–483.
7. Zhenyi Chen,  *$A_\infty$  Sabloff duality via the LSFT algebra*, Preprint available as arXiv:2410.20523, 2024.
8. Cheol-Hyun Cho, *Strong homotopy inner product of an  $A_\infty$ -algebra*, Int. Math. Res. Not. IMRN (2008), no. 13, Art. ID rnm041, 35. MR 2436560
9. Gokhan Civan, John B. Etnyre, Paul Koprowski, Joshua M. Sabloff, and Alden Walker, *Product structures for Legendrian contact homology*, Math. Proc. Camb. Phil. Soc. **150** (2011), no. 2, 291–311.
10. Georgios Dimitroglou Rizell, *Lifting pseudo-holomorphic polygons to the symplectisation of  $P \times \mathbb{R}$  and applications*, Quantum Topol. **7** (2016), no. 1, 29–105.
11. Georgios Dimitroglou Rizell and Noémie Legout, *Relative Calabi–Yau structure from acyclic Rabinowitz–Floer complexes of Legendrians*, Mini-Workshop: Flavors of Rabinowitz Floer and Tate Homology (Kai Cieliebak, Alexandru Oancea, and Nathalie Wahl, eds.), vol. 20, Oberwolfach Rep., no. 4, 2023, pp. 3168–3169.

12. Tobias Ekholm, *Rational symplectic field theory over  $\mathbb{Z}_2$  for exact Lagrangian cobordisms*, J. Eur. Math. Soc. (JEMS) **10** (2008), no. 3, 641–704.
13. ———, *Rational SFT, linearized Legendrian contact homology, and Lagrangian Floer cohomology*, Perspectives in analysis, geometry, and topology, Progr. Math., vol. 296, Birkhäuser/Springer, New York, 2012, pp. 109–145.
14. Tobias Ekholm, John Etnyre, and Michael Sullivan, *The contact homology of Legendrian submanifolds in  $\mathbb{R}^{2n+1}$* , J. Differential Geom. **71** (2005), no. 2, 177–305. MR 2197142
15. Tobias Ekholm, John B. Etnyre, and Joshua M. Sabloff, *A duality exact sequence for Legendrian contact homology*, Duke Math. J. **150** (2009), no. 1, 1–75.
16. Tobias Ekholm, Ko Honda, and Tamas Kálmán, *Legendrian knots and exact Lagrangian cobordisms*, J. Eur. Math. Soc. (JEMS) **18** (2016), no. 11, 2627–2689.
17. Yakov Eliashberg, *Invariants in contact topology*, Proceedings of the International Congress of Mathematicians, Vol. II (Berlin, 1998), 1998, pp. 327–338. MR 1648083
18. Yakov Eliashberg, Alexander Givental, and Helmut Hofer, *Introduction to symplectic field theory*, 2000, GAFA 2000 (Tel Aviv, 1999), pp. 560–673. MR 1826267
19. John B. Etnyre and Lenhard L. Ng, *Legendrian contact homology in  $\mathbb{R}^3$* , Surveys in differential geometry 2020., Surv. Differ. Geom., vol. 25, Int. Press, Boston, MA, 2022, pp. 103–161. MR 4479751
20. John B. Etnyre, Lenhard L. Ng, and Joshua M. Sabloff, *Invariants of Legendrian knots and coherent orientations*, J. Symplectic Geom. **1** (2002), no. 2, 321–367.
21. Dmitry Fuchs, *Chekanov-Eliashberg invariant of Legendrian knots: existence of augmentations*, J. Geom. Phys. **47** (2003), no. 1, 43–65. MR 1985483
22. Dmitry Fuchs and Tigran Ishkhanov, *Invariants of Legendrian knots and decompositions of front diagrams*, Mosc. Math. J. **4** (2004), no. 3, 707–717.
23. Kenji Fukaya, Yong-Geun Oh, Hiroshi Ohta, and Kaoru Ono, *Lagrangian intersection Floer theory: anomaly and obstruction. Part I*, AMS/IP Studies in Advanced Mathematics, vol. 46.1, American Mathematical Society, Providence, RI; International Press, Somerville, MA, 2009. MR 2553465
24. Sheel Ganatra, *Symplectic Cohomology and Duality for the Wrapped Fukaya Category*, ProQuest LLC, Ann Arbor, MI, 2012, Thesis (Ph.D.)—Massachusetts Institute of Technology. MR 3121862
25. ———, *Cyclic homology,  $S^1$ -equivariant Floer cohomology and Calabi-Yau structures*, Geom. Topol. **27** (2023), no. 9, 3461–3584. MR 4674834
26. Sheel Ganatra, John Pardon, and Vivek Shende, *Sectorial descent for wrapped Fukaya categories*, J. Amer. Math. Soc. **37** (2024), no. 2, 499–635. MR 4695507
27. Sheel Ganatra, Timothy Perutz, and Nick Sheridan, *Mirror symmetry: from categories to curve counts*, Preprint available as arXiv:1510.03839, 2015.
28. Ezra Getzler and John D. S. Jones,  *$A_\infty$ -algebras and the cyclic bar complex*, Illinois J. Math. **34** (1990), no. 2, 256–283. MR 1046565
29. Mikhail Gorsky and Fabian Haiden, *Counting in Calabi-Yau categories, with applications to Hall algebras and knot polynomials*, Preprint available as arXiv:2409.10154, 2024.
30. Michael B. Henry and Dan Rutherford, *Ruling polynomials and augmentations over finite fields*, J. Topol. **8** (2015), no. 1, 1–37. MR 3335247
31. Tornike Kadeišvili, *On the theory of homology of fiber spaces*, Uspekhi Mat. Nauk **35** (1980), no. 3(213), 183–188, International Topology Conference (Moscow State Univ., Moscow, 1979).
32. Bernhard Keller, *Introduction to A-infinity algebras and modules*, Homology Homotopy Appl. **3** (2001), no. 1, 1–35. MR 1854636
33. Maxim Kontsevich and Yan Soibelman, *Homological mirror symmetry and torus fibrations*, Symplectic geometry and mirror symmetry (Seoul, 2000), World Sci. Publ., River Edge, NJ, 2001, pp. 203–263. MR 1882331

34. Christopher Kuo and Wenyuan Li, *Relative calabi-yau structure on microlocalization*, Preprint available as arXiv:2408.04085, 2024.
35. Noémie Legout, *Calabi-Yau structure on the Chekanov-Eliashberg algebra of a Legendrian sphere*, Preprint available as arXiv:2304.03014, 2023.
36. Wenyuan Li, *Estimating Reeb chords using microlocal sheaf theory*, Preprint available as arXiv:2106.04079, 2021.
37. Hanming Liu, *Augmentation categories in higher dimensions*, Available as arXiv:2508.06822, 2025.
38. Paul Melvin and Sumana Shrestha, *The nonuniqueness of Chekanov polynomials of Legendrian knots*, Geom. Topol. **9** (2005), 1221–1252.
39. Kirill Mishachev, *The  $n$ -copy of a topologically trivial Legendrian knot*, J. Symplectic Geom. **1** (2003), no. 4, 659–682.
40. Lenhard L. Ng, *Computable Legendrian invariants*, Topology **42** (2003), no. 1, 55–82. MR 1928645
41. ———, *Rational symplectic field theory for Legendrian knots*, Invent. Math. **182** (2010), no. 3, 451–512.
42. Lenhard L. Ng, Dan Rutherford, Vivek Shende, and Steven Sivek, *The cardinality of the augmentation category of a Legendrian link*, Math. Res. Lett. **24** (2017), no. 6, 1845–1874. MR 3762698
43. Lenhard L. Ng, Dan Rutherford, Vivek Shende, Steven Sivek, and Eric Zaslow, *Augmentations are sheaves*, Geom. Topol. **24** (2020), no. 5, 2149–2286. MR 4194293
44. Lenhard L. Ng and Joshua M. Sabloff, *The correspondence between augmentations and rulings for Legendrian knots*, Pacific J. Math. **224** (2006), no. 1, 141–150.
45. Joshua M. Sabloff, *Invariants of Legendrian knots in circle bundles*, Comm. Contemp. Math. **5** (2003), no. 4, 569–627.
46. ———, *Augmentations and rulings of Legendrian knots*, Int. Math. Res. Not. (2005), no. 19, 1157–1180.
47. ———, *Duality for Legendrian contact homology*, Geom. Topol. **10** (2006), 2351–2381 (electronic).
48. Joshua M. Sabloff and Lisa Traynor, *Obstructions to Lagrangian cobordisms between Legendrian submanifolds*, Algebr. Geom. Topol. **13** (2013), 2733–2797.
49. ———, *The minimal length of a Lagrangian cobordism between Legendrians*, Selecta Math. (N.S.) **23** (2017), no. 2, 1419–1448.
50. ———, *The relative Gromov width of Lagrangian cobordisms between Legendrians*, J. Symplectic Geom. **18** (2020), no. 1, 217–250. MR 4088752
51. Paul Seidel,  *$A_\infty$ -subalgebras and natural transformations*, Homology Homotopy Appl. **10** (2008), no. 2, 83–114. MR 2426130
52. ———, *Fukaya categories and Picard-Lefschetz theory*, Zurich Lectures in Advanced Mathematics, European Mathematical Society (EMS), Zürich, 2008. MR 2441780 (2009f:53143)
53. ———, *Fukaya  $A_\infty$ -structures associated to Lefschetz fibrations. I*, J. Symplectic Geom. **10** (2012), no. 3, 325–388. MR 2983434
54. Nick Sheridan, *On the Fukaya category of a Fano hypersurface in projective space*, Publ. Math. Inst. Hautes Études Sci. **124** (2016), 165–317. MR 3578916
55. James Dillon Stasheff, *Homotopy associativity of  $H$ -spaces. I, II*, Trans. Amer. Math. Soc. **108** (1963), 293–312, **108** (1963), 275–292; ibid. MR 158400
56. Wai-Kit Yeung, *Relative Calabi-Yau completions*, Available as arXiv:1612.06352, v2, 2022.

DUKE UNIVERSITY, DURHAM, NC 27708  
*Email address:* jason.ma@duke.edu

HAVERFORD COLLEGE, HAVERFORD, PA 19041  
*Email address:* jsabloff@haverford.edu